FLOODING ANALYSIS AND SLOPE STABILITY ASSESSMENT DUE TO A CONFINED AQUIFER IN THE ELBİSTAN-ÇÖLLOLAR OPEN CAST MINE

A THESIS SUBMITTED TO
THE GRADUATE SCHOOL OF APPLIED AND NATURAL SCIENCES
OF
MIDDLE EAST TECHNICAL UNIVERSITY

BY

SELİN YONCACI

IN PARTIAL FULFILLMENT OF THE REQUIREMENTS
FOR
THE DEGREE OF MASTER OF SCIENCE
IN
MINING ENGINEERING

DECEMBER 2009

Approval of the thesis:

FLOODING ANALYSIS AND SLOPE STABILITY ASSESSMENT DUE TO A CONFINED AQUIFER IN THE ELBİSTAN-ÇÖLLOLAR OPEN CAST MINE

submitted by **SELİN YONCACI** in partial fulfillment of the requirements for the degree of **Master of Science in Mining Engineering Department, Middle East Technical University** by,

Prof. Dr. Canan Özgen _____
Dean, Graduate School of **Natural and Applied Sciences**

Prof. Dr. Ali İhsan Arol _____
Head of Department, **Mining Engineering**

Assoc. Prof. Dr. Levent Tutluoğlu
Supervisor, **Mining Engineering Dept., METU** _____

Examining Committee Members:

Prof. Dr. Celal Karpuz _____
Mining Engineering Dept., METU

Assoc. Prof. Dr. Levent Tutluoğlu _____
Mining Engineering Dept., METU

Assoc. Prof. Dr. Sadık Bakır _____
Civil Engineering Dept., METU

Assoc. Prof. Dr. H. Aydın Bilgin _____
Mining Engineering Dept., METU

Dr. Nuray Demirel _____
Mining Engineering Dept., METU

Date:

I hereby declare that all information in this document has been obtained and presented in accordance with academic rules and ethical conduct. I also declare that, as required by these rules and conduct, I have fully cited and referenced all material and results that are not original to this work.

Name, Last name: Selin YONCACI

Signature :

ABSTRACT

FLOODING ANALYSIS AND SLOPE STABILITY ASSESSMENT DUE TO A CONFINED AQUIFER IN THE ELBİSTAN-ÇÖLLOLAR OPEN CAST MINE

Yoncacı, Selin
M.Sc., Department of Mining Engineering
Supervisor: Assoc. Prof. Dr. Levent Tutluoğlu

December 2009, 106 pages

Groundwater can be a critical issue to be considered in civil engineering, mining engineering and interdisciplinary fields. Karstic structures and aquifers enclosing groundwater are potential risks in case they are not studied in detail. Enclosed groundwater can result in floods at pit bottom or can cause instabilities of permanent pit slopes.

This study is about analyses of flooding possibility at the pit bottom and possible instabilities of pit slopes in the Elbistan-Çöllolar open cast coal mine due to the presence of a karstic aquifer under the lignite formation.

Thickness and permeability of the bottom clay formation under the lignite bed are necessary critical parameters for investigating a possible water rush from a confined aquifer in limestone formation underneath the bottom clay. These parameters were changed, and water flow quantities towards the pit bottom were determined by finite element models. Critical values of these parameters were investigated considering the lack of accurate site investigation information regarding the

thickness and permeability of bottom clay. Possible strength loss, fracturing, and thus permeability increase in bottom clay due to a confined aquifer were studied. In flooding and slope stability analyses Phase^2 software based on finite element method is used.

Results of analyses showed that as reported thickness of bottom clay is around 120 m at the pit bottom and permeability values are in orders of magnitudes of 10^{-8} m/s, no serious flooding problems are expected to occur unless the thickness of bottom clay layer drops down to around 20 m, and the permeability of this layer reaches an order of magnitude of 10^{-5} m/s.

Mechanical effects of confined aquifer on slopes and bottom clay displacements were investigated, and thus fracturing and failure possibilities of bottom clay and permanent slope were assessed. Slope and pit bottom displacements increased to meter levels for less than 60 m bottom clay thicknesses. Whereas 50-60 m bottom clay thickness can be critical for cracking, 20 m bottom clay thickness was found to be critical for water rush to the pit bottom.

With reported bottom clay thickness of 120 m and with 25^o slope angle permanent slope factor of safety was found to be 1.2, and this value was not effected unless clay layer thickness drops below 70 m levels. Higher than 32^o overall slope angle there will be a risk of slope failure for permanent and production slopes, reflected by safety factors less than one, in the stability analyses.

Keywords: Elbistan-Çöllolar, karstic aquifer, groundwater flow, slope stability, sensitivity analysis

ÖZ

ELBİSTAN-ÇÖLLOLAR AÇIK LİNYİT OCAĞINDA BASINÇLI AKİFERE BAĞLI SU BASMASI ANALİZİ VE ŞEV DURAYLILIĞI DEĞERLENDİRMESİ

Yoncacı, Selin
Y. Lisans, Maden Mühendisliği Bölümü
Tez Danışmanı: Doç. Dr. Levent Tutluoğlu

Aralık 2009, 106 sayfa

Yer altı suyu inşaat mühendisliği ve maden mühendisliği gibi yer bilimleriyle ortak yürütülen dallar için kritik bir konu olabilir. Karstik yapılar ve içlerinde yer altı suyu barındıran akiferler detaylı araştırılmazlarsa potansiyel risk teşkil ederler. Barındırılan yer altı suyu ocak tabanında su basmasına veya kalıcı şevlerin duraysızlığına neden olabilir.

Bu çalışma, Elbistan-Çöllolar açık ocak linyit madeninde linyit formasyonunun altındaki karstik akiferin varlığının ocak tabanına su basması durumu ve kalıcı şevlerin olası duraysızlığının analizi hakkındadır.

Linyit yatağının altında yer alan taban kilinin kalınlığı ve geçirgenliği, taban kilinin altında olan kireçtaşı formasyonundaki basınçlı akiferinden olası su basması durumunu incelemek için gerekli kritik parametrelerdir. Bu parametreler değiştirilmiş ve ocak tabanına akan su miktarı sonlu elemanlar modelleriyle kararlaştırılmıştır. Taban kilinin kalınlık ve geçirgenlik özellikleri hakkında yetersiz saha çalışmaları nedeniyle eksik bilgilerin bulunmasına rağmen bu parametrelerin

kritik değerleri gözden geçirilmiştir. Taban kilinde basınçlı akifer etkisiyle meydana gelen olası dayanım kaybı, çatlama ve geçirgenlik artışı incelenmiştir. Su basması ve şev duraylılığı analizlerinde sonlu elemanlar metoduna dayalı olan Phase^2 programı kullanılmıştır.

Analizlerin sonuçları gösteriyor ki; taban kili kalınlığı 20 m civarına düşmedikçe ve bu katmanın geçirgenliği 10^{-5} m/s değerlerine ulaşmadıkça, rapor edilen taban kili kalınlığı ocak tabanında yaklaşık 120 m ve geçirgenlik değerleri de 10^{-8} m/s değerlerinde olursa ciddi bir sel problemi oluşması beklenmemektedir.

Basınçlı akiferin, şev ve taban kili yer değiştirmeleri üzerindeki mekanik etkileri incelenmiş ve bunun sonucunda da taban kili ve kalıcı şevlerin çatlama ve yenilme olasılıkları değerlendirilmiştir. Taban kili kalınlığının 60 m altına düştüğü durumlarda şev ve ocak tabanındaki yer değiştirme değerleri metre düzeyine yükselmektedir. Bunun yanı sıra, 50-60 m taban kili kalınlığı çatlama için, 20 m taban kil kalınlığı da ocak tabanında su basması açısından kritik değerlerdir.

Bildirilen 120 m taban kili kalınlığı ve 25° kalıcı şev açısı için bulunan güvenlik katsayısı 1,2 olup, bu değer kil kalınlığı 70 m altına düşmediği sürece etkilenmemektedir. Genel şev açısı 32° olduğu durumda ise kalıcı şev ve üretim şevlerinde kayma riski oluştuğu, güvenlik katsayılarının birden küçük bulunmasıyla duraylılık analizlerinde de yansıtılmıştır.

Anahtar Kelimeler: Elbistan-Çöllolar, karstik akifer, yer altı suyu akımı, şev duraylılığı, duyarlılık analizi.

To My Family and Friends

ACKNOWLEDGEMENTS

I highly express my sincere appreciation to Assoc. Prof. Dr. Levent Tutluoğlu for his kind supervision, encouragements, support and guidance in preparation of this thesis.

I would also like to thank Prof. Dr. Celal Karpuz for his suggestions and comments.

I offer my thanks to the examining committee members Assoc. Prof. Dr. H. Aydın Bilgin, Assoc. Prof. Dr. Sadık Bakır and Dr. Nuray Demirel for accepting to serve in my committee and for their participation.

I would like to thank my friend research assistant Mustafa Erkayaoğlu for his help and sharing his valuable knowledge for my research study. Also I am grateful to my friends İ. Ferit Öge, Nazlı Demirtaş, Gökhan Tuncay, İpek Sabah, Dünya Başol, Esin Pekpak and Levent İlkay for their continuous support and moral boost during the various stages of the thesis.

I finally want to thank to my family, who have been supporting me all through my life.

TABLE OF CONTENTS

LIST OF TABLES

Tables

LIST OF FIGURES

Figures

LIST OF SYMBOLS

$\mathbf{n}$	:	Porosity
$\mathbf{V_v}$	:	Volume of Void Space
$\mathbf{V_T}$	:	Total Bulk Volume of Material
$\mathbf{n_e}$	:	Effective Porosity
$\mathbf{V_a}$	:	Aggregate Volume of Water Draining from Rock
$\mathbf{K}$	:	Hydraulic Conductivity
$\mathbf{k}$	:	Permeability Constant
$\mathbf{Q}$	:	Flow Rate
$\mathbf{A}$	:	Cross Section Area
$\mathbf{i}$	:	Hydraulic Gradient
$\mathbf{h_l}$	:	Hydraulic Loss in the Flow Direction
$\mathbf{l}$	:	Spacing of the Flow Monitoring Points for Darcy's Law
$\mathbf{v}$	:	Darcy Velocity
$\mathbf{v_s}$	:	Linear Seepage Velocity
$\mathbf{w_n}$	:	Water Content
γ_n	:	Unit Weight
$\mathbf{c'_p}$	:	Effective Peak Cohesion
$\mathbf{c'_r}$	:	Effective Residual Cohesion
φ'_p	:	Effective Peak Internal Friction Angle
φ'_r	:	Effective Residual Internal Friction Angle
$\mathbf{t}$	:	Thickness
$\mathbf{H}$	:	Slope Height
$\mathbf{L_v}$	:	Flooding Area Extension Section
$\mathbf{t_d}$	:	Thickness of Discharge Section
$\mathbf{Q_c}$	:	Critical Flooding Value
$\mathbf{H_u}$	:	Hydrostatic Water Pressure Coefficient
$\mathbf{u}$	:	Pore Pressure
γ_w	:	The Pore Fluid Unit Weight
$\mathbf{h}$	:	The Vertical Distance From a Point to a Piezometric Line

CHAPTER 1

INTRODUCTION

Groundwater analysis is a critical aspect to be studied in detail both in mining and civil engineering fields. In case the behavior of groundwater is not understood correctly, serious problems may occur in the mining area. Simply, these problems are listed as profit loss, production delay, machine loss and even loss of lives.

In surface mining activities the effect of groundwater is observed as either flooding or slope failures (e.g. landslides). After planning the mine, if any groundwater activities or aquifer behaviors are determined anywhere in the site, the whole analyses especially slope design should be done again to be sure that the design and slope parameters are safe enough. In addition a detailed dewatering plan should be planned for both investment and production stages.

Turkey has 8.3 billion ton lignite reserve and 46% of this reserve is located in Afşin-Elbistan Lignite Coal Basin. In Elbistan, there are two thermal power plants, namely as A and B power plants. Power plants produce 2795 MW energy totally whereas their potential energy is 4000 MW. In spite of its low quality (average calorific value 1070 kcal/kg, ash content 17%, water content 55%, and sulphur value 1.46%) Afşin-Elbistan lignite is the most essential material resource for the plants. At present for thermal power plants A and B, lignite is supplied from Kışlaköy open pit mine, the current operating mine in the basin. However, for power plant B, starting from year 2010 to year 2035 lignite will be supplied from Çöllolar open pit mine, which is the second largest size mine in the basin and is operated by a Ciner Group Firm, Park Teknik Inc. The coal production of Turkey will increase when Çöllolar open pit mine is operated in full capacity. Çöllolar lignite basin is going to be operated totally 28 years, as 3 years in development and

25 years in production. According to the statements of the EÜAŞ (Electricity Generation Inc.) the Çöllolar basin will produce 9 billion KWh energy in consideration of 17 million ton/year lignite coal.

The planning stage, slope stability and groundwater analysis should be done carefully as Elbistan lignite basin is the most essential coal and energy supply of Turkey. In Çöllolar basin, during the investment stage a karstic aquifer is detected under the lignite horizon, and therefore the critical hydrological and mechanical analyses should be reconsidered to prevent the mining area from hazardous consequences. In this study, the hydrological and mechanical effects of karstic aquifers are investigated, and slope stability analyses are performed in presence of a karstic confined aquifer under lignite beds.

1.1 Statement of the Problem

Elbistan-Çöllolar coal basin is very important for Turkey's energy resources. Therefore, the whole technical analysis related to the mining activities should be done properly. The progressive slope stability analyses and parallel dewatering planning of Elbistan-Çöllolar basin are from the stability point of view.

After the site investigation of Elbistan-Çöllolar area was done, it was found that there is a possible karstic confined aquifer lying underneath the coal beds. Recently discovered aquifer and its effects on mining activities should be analyzed, and also checked from the slope stability point.

The slope stability is important in the design of excavations such as open pits, quarries, and foundations, and in natural slopes forming cliffs, valley sides, and reservoirs, where movement may have serious consequences. Slopes, especially permanent slopes in surface mines have to be studied in detail including their design stage as miscalculations cause severe hazards. In open pit mines, there is an obvious

risk of flooding in case there is groundwater present, and this makes the slope stability analysis even a more critical issue. Flooding can be considered as a crucial concept in surface mining that can result in catastrophic accidents. To sum up, effect of groundwater presence on mining activities must be analyzed especially for open pit/cast mines elaborately.

1.2 Objective of the Study

The aim of this thesis is to investigate the possible negative effects of a confined aquifer on mining activities and stability of permanent pit slope in Elbistan-Çöllolar surface mine, considering the presence of water under high pressure in a confined karstic aquifer in limestone formation under the lignite seam and bottom clay underneath.

1.3 Methodology of the Study

The effects of the confined aquifer on the stability of south-west permanent slope are studied by numerical models. Flooding and slope stability problems are explained in detail under two main headlines under which details of the numerical models are explained. The first headline is about flooding scenarios and the second one is related to the mechanical effects of confined aquifers.

The worst case scenarios with the aquifer models of different dimensions and locations are simulated because dimensions, exact location and distribution of the aquifer in the region are not well known. Dewatering activity in the region is behind the excavation and overburden removal program. Therefore, according to the updated groundwater levels combined with the possible karstic aquifer models, stability of slopes is analyzed for different stages of mining progress. Flooding and

slope stability problems are handled by numerical models. A finite element method software Phase^2 is used in solutions.

1.4 Organization of the Thesis

This thesis is composed of eight chapters. In the first chapter, general information is supplied about the thesis and problem.

In Chapter 2, the concept of groundwater, its basic terms, definition and types of aquifers, an introductory knowledge about groundwater modeling equations, Darcy's Law, and effects of groundwater on mining activities are included.

Afşin-Elbistan Coal basin is explained in detail in terms of location, dimension, formation, rock characterization and history in Chapter 3. Based on the previous studies geology and hydrology are reviewed. Previous important work related to Afşin-Elbistan basin is presented. In the end of this chapter, mining activities in Kışlaköy and Çöllolar are described and dewatering activities of Çöllolar are summarized.

In Chapter 4, geotechnical borehole and laboratory test data are presented and also related to this work detection of aquifer and field dewatering operations in the area are covered.

The finite element software Phase^2, modeling work, related cross sections and used models, the finite element are explained in Chapter 5 in detail. Input parameters used in modeling and design of permanent pit slope are given and discussed in this part.

In Chapter 6 modeling studies for possible flooding into the pit bottom from confined aquifer are presented. By changing some important parameters like clay thickness and permeability, related sensitivity analyses are conducted.

Finite element analyses of the stability of the permanent slope due to a confined aquifer are conducted in Chapter 7. Safety factors for the permanent slope are determined for different bottom clay thickness and different overall slope angles for the permanent slope.

The last Chapter 8 summarizes the results with conclusion and recommendations given in this chapter.

CHAPTER 2

BASIC CONCEPTS ABOUT GROUNDWATER AND CONFINED AQUIFERS

Groundwater is a crucial source of fresh water throughout the world. Groundwater is an essential part of the hydrologic cycle and is important in sustaining streams, lakes, wetlands, and aquatic communities (Alley et al., 2002). In a hydraulic water cycle, groundwater comes from surface waters (river, sea, precipitation lake, reservoir, etc.) and percolates into the ground beneath the water table. The groundwater table is the surface of the groundwater exposed to an atmospheric pressure beneath the ground surface (Lee and Lin, 2000). The study of the distribution and movement of groundwater is as hydrogeology and/or groundwater hydrology.

On the earth, approximately 3% of the total water is fresh water. Of this, groundwater comprises 95%, surface water 3.5%, and soil moisture 1.5% out of all the freshwater on earth, only 0.36% is readily available to use (Lee and Lin, 2000). Groundwater is the largest source of fresh water on the planet excluding the polar icecaps and glaciers. The amount of ground water within 800 m from the ground surface is over 30 times the amount in all fresh water lakes and reservoirs, and about 3000 times the amount in stream channels, at any one time (Raghunath, 2007).

Groundwater is an important source of water supply. It is also a major source of industrial uses (cooling, water supply, etc.) and agricultural uses (irrigation and livestock). The quantity of groundwater available is an important issue (Lee and Lin, 2000).

The groundwater plays important roles in mining, civil engineering, and geological engineering activities to understand the groundwater and hydrological concepts better some basic terms and laws related to groundwater should be introduced and explained briefly.

2.1 Basic Terms about Groundwater

The basic terms related to groundwater and hydrological issues are explained below.

2.1.1 Porosity

Water within the rock occurs in pore spaces of various size, shape, and origin. Used in geology, hydrogeology, soil science, and building science, the porosity of a porous medium (such as rock or sediment) describes the fraction of void space in the material, where the void may contain, for example, air or water to the total bulk volume (Misstear et al., 2006). As seen in Equation 2.1 it is defined by the ratio:

$$n = \frac{V_v}{V_T} \tag{2.1}$$

where V_V is the volume of void-space (such as fluids) and V_T is the total or bulk volume of material, including the solid and void components. The symbols n is used to denote porosity (Ford and William, 2007).

Porosity is a fraction between 0 and 1, typically ranging from less than 0.01 for solid granite to more than 0.5 for peat and clay, although it may also be represented in percent terms by multiplying the fraction by 100.

According to Ford and Williams (2007) a distinction is made between the porosity n of a rock and its effective porosity n_e. Whereas porosity is defined as the ratio of the volume of void spaces (or pores) to the total bulk volume of the rock, effective porosity refers only to those voids that are hydrologically interconnected.

For a fully saturated rock, it can be expressed as the ratio of the aggregate volume of gravitation water that will drain from the rock V_a to the total bulk volume of the rock V_T (Equation 2.2).

$$n = \frac{V_a}{V_T} \tag{2.2}$$

Porosities of some rocks are shown in Figure 2.1 below.

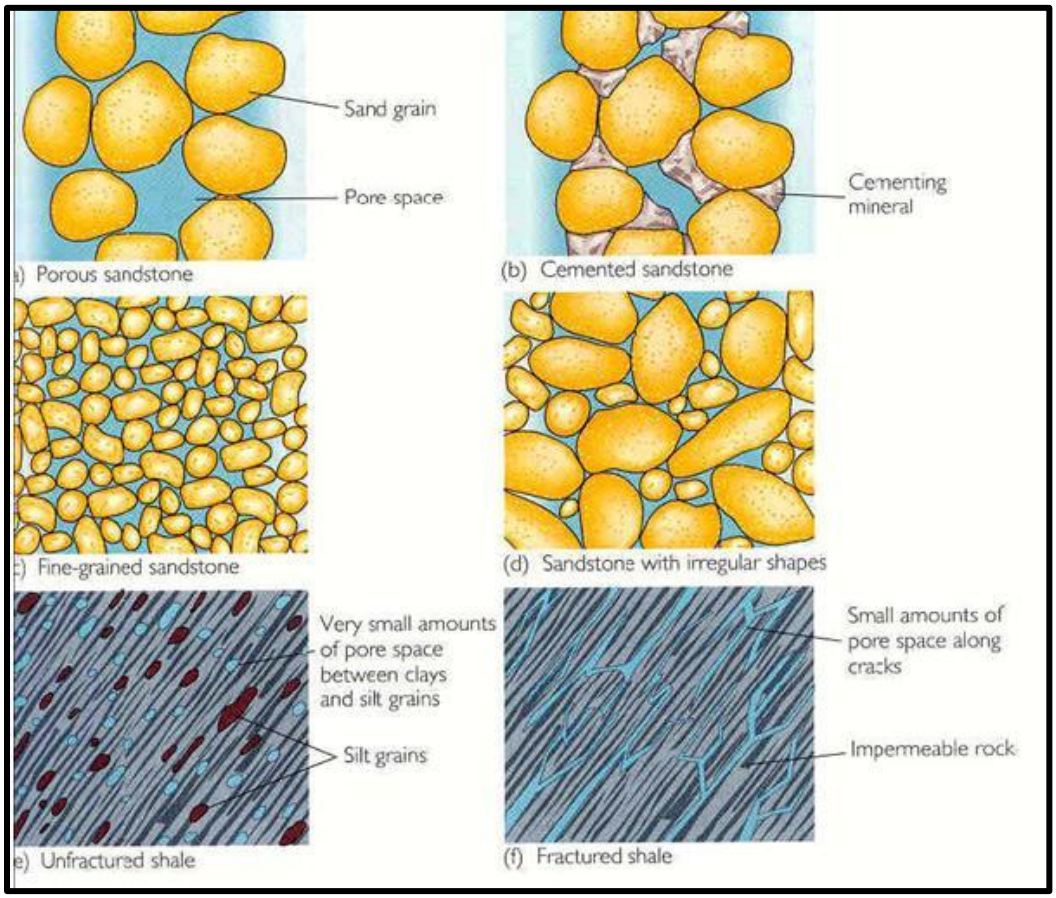

Figure 2.1 Porosity of some rocks (Dirik, 2006)

2.1.2 Hydraulic Conductivity

Symbolically represented as K, is a property of vascular plants, soil or rock that describes the ease with which water can move through pore spaces or fractures. It has dimensions of velocity (m/s) and it depends on the inherent permeability of the material and on the degree of saturation. The terms hydraulic conductivity and coefficient of permeability are often used interchangeably, especially in engineering texts. The term hydraulic conductivity assumes that the fluid under consideration is water (or groundwater). The hydraulic conductivity of an intergranular aquifer depends on the grain size and sorting of the aquifer material and the degree of cementation. Saturated hydraulic conductivity, K_{sat}, describes water movement through saturated media (Misstear et al., 2006).

2.1.3 Permeability

Permeability in the earth sciences, commonly symbolized as κ, or k, is a measure of the ability of a material (typically, a rock or unconsolidated material) to transmit fluids and its unit is m/s for water flow. However, permeability constant is independent of the properties of the fluid and it has dimension of area (m^2 or cm^2). Also, a common permeability unit is darcy: 1 darcy equals 9.86 x 10^{-9} cm^2 (Goodman, 1989).

Permeability is a measure of the rate at which fluid passes through a porous medium. The permeability has a dimension of velocity. So the permeability depends on the soil type and the conditions in the soil will be different if the soil is of coarse or fine grained (Obrer, 2006).

It is of great importance in determining the flow characteristics of hydrocarbons in oil and gas reservoirs, and of groundwater in aquifers. It is typically measured in the laboratory by application of Darcy's law under steady state conditions or more

generally, by application of various solutions to the diffusion equation for unsteady flow conditions (Ford and William, 2007). The scaled range of values of hydraulic conductivity and permeability constant for some rock and soil units is shown in Figure 2.2.

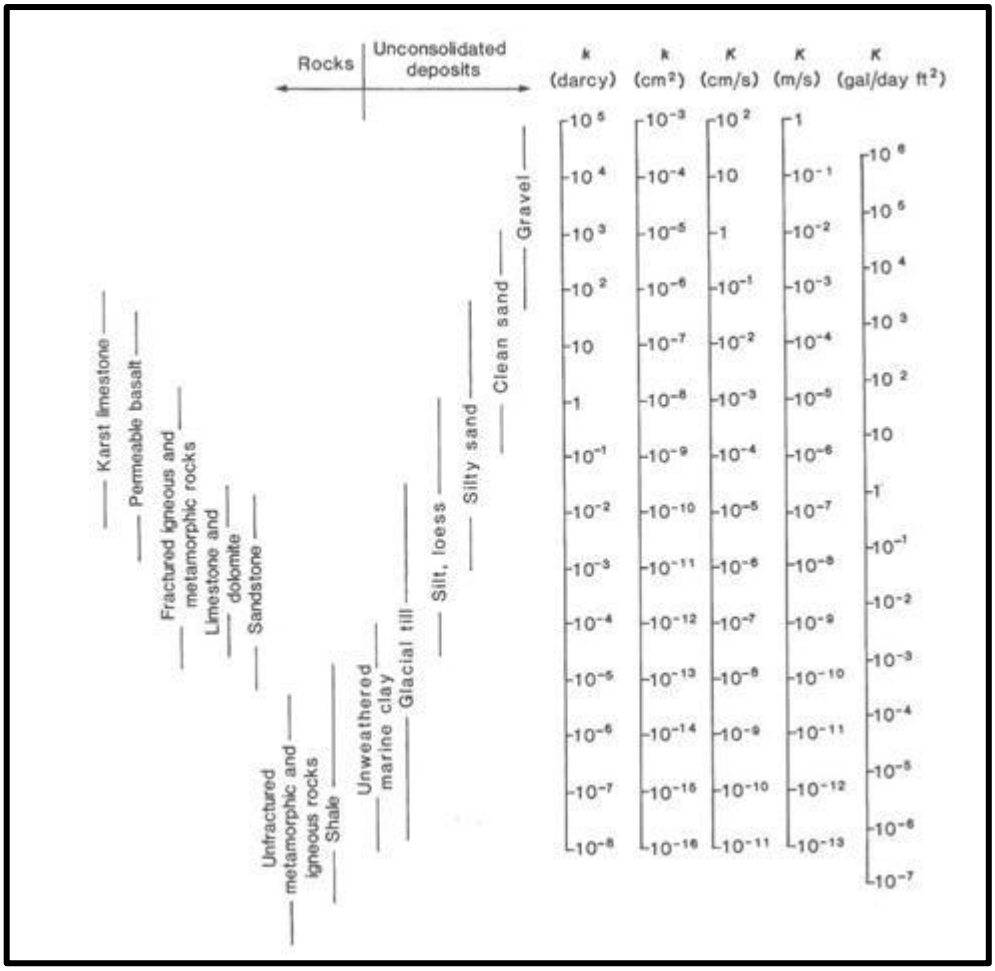

Figure 2.2 Range of values of hydraulic conductivity and permeability constant (Ford and William, 2007)

2.2 Groundwater Flow Calculation

The process of groundwater flow is generally assumed to be governed by the relations expressed in Darcy's law and the conservation of mass (Konikow and Reilly, 1991).

In 1856, French hydraulic engineer Henry Darcy (1803-1858) published a report on the water supply of the city of Dijon, France. In that report, Darcy described the results of an experiment designed to study the flow of water through a porous medium. Darcy's experiment resulted in the formulation of a mathematical law that describes fluid motion in porous media. Darcy's Law states that the rate of fluid flow through a porous medium is proportional to the potential energy gradient within that fluid. It also forms the scientific basis of the fluid permeability used in the earth sciences (Thusyanthan & Madabhushi, 2003).

One application of Darcy's law is to flow of water through an aquifer. Darcy's law along with the equation of the conservation of mass is equivalent to the groundwater flow equation, one of the basic relationships of hydrogeology. Darcy's law is also used to describe oil, water, and gas flows through petroleum reservoirs.

Darcy's law summarizes much of the physics of groundwater flow by relating the velocity vector to the gradient of potential. Continuity or conservation is the second important law. For steady-state conditions, continuity requires that the amount of water flowing into a representative elemental volume be equal to the amount flowing out. The existence of steady-state conditions implies that head is independent of time (Wang and Anderson, 1982).

Darcy's law is formulated as below

$$Q = - A K i \qquad (2.3)$$

In equation 2.3,

Q = Groundwater flow rate (or total discharge (m^3/s))

K = Hydraulic conductivity or permeability constant (m/s)

A = Cross section area perpendicular to flow direction (m^2)

i = Hydraulic gradient = h_l/l (m/m)

h_l = Hydraulic loss in the flow direction (m)

l = Spacing of the monitoring points on which hydraulic loss is measured (m)

The negative sign indicates that flow takes place in the direction of negative (i.e. decreasing) hydraulic gradient, although in subsequent equations in here it will be omitted as usually only the magnitude of flow is concerned (Doyuran, 2006).

The flow rate per unit cross sectional area of saturated aquifer is given in equation 2.4 by the Darcy velocity (v), also known as the specific discharge:

$$v = \frac{Q}{A} = Ki \tag{2.4}$$

where v is in m/s.

It is seen that v, which determines the flow rate of groundwater, is proportional with hydraulic gradient. According to this when the hydraulic gradient is increasing the flow rate is also increasing.

To obtain an estimate of the flow velocity through the pores, it is necessary to divide the Darcy velocity by the effective porosity; n_e. Equation 2.5 gives the linear seepage velocity v_s:

$$v_s = \frac{Ki}{n_e} \tag{2.5}$$

Darcy's, law shown basically in Figure 2.3 is not applicable for aquifers formed in magmatic formations because generally in this type of aquifers turbulent flow is the dominant flow type (Misstear et al., 2006).

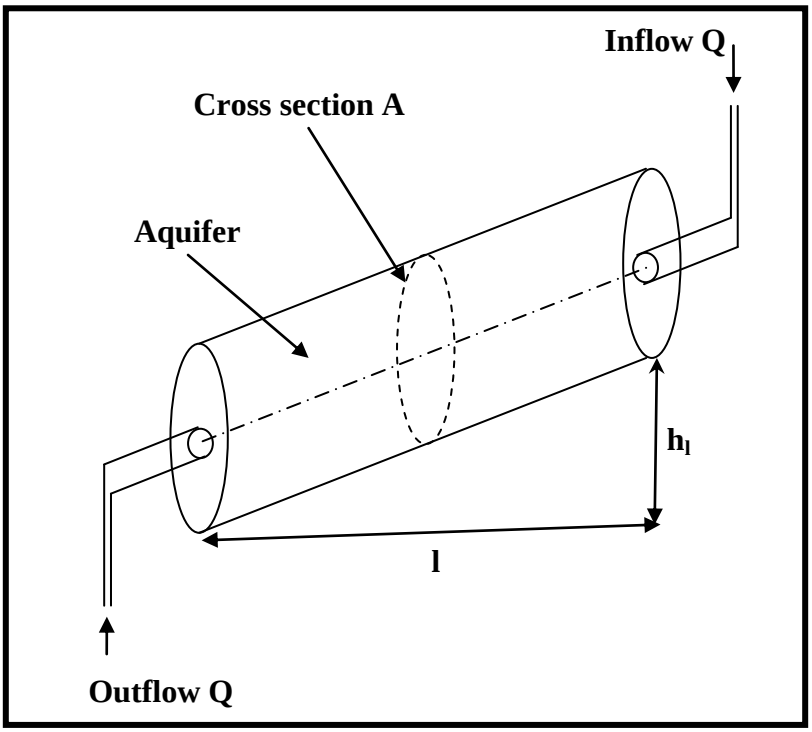

Figure 2.3 Figure of Darcy's law (Rushton, 2003)

Darcy's law is a simple mathematical statement which summarizes several familiar properties that groundwater flowing in aquifers exhibits, including:

- if there is no pressure gradient over a distance, no flow occurs (this is hydrostatic conditions),

- if there is a pressure gradient, flow will occur from high pressure towards low pressure (opposite the direction of increasing gradient),

- the greater the pressure gradient (through the same formation material), the greater the discharge rate, and

- the discharge rate of fluid will often be different — through different formation materials (or even through the same material, in a different direction) — even if the same pressure gradient exists in both cases (Doyuran, 2006).

An implication of accepting the Darcian approach is that the rock is considered as a continuum of voids and soil matter for which certain generalized macroscopic parameters (such as K) can be defined, that represent and in some sense describe the true microscopic behavior. In karst this means that the fractured rock penetrated by solution conduits would be replaced by a conceptual representative continuum for which it is assumed possible to determine hydrologically meaningful macroscopic parameters (Ford and William, 2007).

Numerical flow models are important tools for effective management of groundwater resources. Representing groundwater flow through karst aquifers is challenging because of the highly heterogeneous nature of groundwater flow through a medium with multiple interacting flow systems (i.e. flow through the matrix, fractures, and conduits). The finite element method is better suited to represent complex geometries (Painter, et al., 2006).

The application of the finite element method to groundwater problems is a relatively recent development compared with the finite difference method. The finite difference method is usually implemented with rectangular cells. The finite element method is implemented with a variety of element types, but the triangular element is a good beginning point for describing the method. Triangular elements are defined by three nodes one at each corner. These nodes serve the purpose of locating unknown heads; that is, they are the points within the problem domain at which the heads are computed. However, the flexibility of the finite element method is useful in solving coupled problems, such as contaminant transport, or in solving moving boundary problems, such as a moving water table (Wang and Anderson, 1982).

2.3 Description of Aquifers

An aquifer is a layer of relatively porous substrate that contains and transmits groundwater. Aquifer is a geologic formation, group of formation or part of a formation that contains sufficient saturated permeable material to yield significant quantities of water to wells and springs. The Great Artesian Basin in central and eastern Australia is one of the largest aquifer systems in the world, extending for almost 2 million km^2 (Kasenow, 2000).

Substrate with relatively low porosity that permits limited transmission of groundwater is known as an aquitard. An aquiclude (or aquifuge) is a substrate with porosity so low that it is virtually impermeable to groundwater (Misstear et al., 2006).

Some examples of these are as follows;
Aquifers: gravel, sandstone, breccias, limestone, etc.
Aquicludes: claystone, tuff like material, etc.
Aquitards: siltstone, clayed sand, etc. (JF409, COMU).

Aquifers can occur at various depths. Those closer to the surface are not only more likely to be exploited for water supply and irrigation, but are also more likely to be topped up by the local rainfall. Many desert areas have limestone hills or mountains within them or close to them which can be exploited as groundwater resources (Misstear et al., 2006).

The characteristics of aquifers vary with the geology and structure of the substrate and topography in which they occur. Limestone aquifers can yield large amounts of groundwater because of extensive porous space created by solution. The Floridian Aquifer in Florida is an excellent example of a high water-yielding limestone aquifer (Cech, 2009).

If a rock unit of low porosity is highly fractured, it can also make a good aquifer (via fissure flow), provided the rock has an appreciable hydraulic conductivity to facilitate movement of water. Porosity is important, but alone, it does not determine a rock's ability of being an aquifer (Hiscock, 2005).

Aquifers can range in size from very small formations of a few feet (1 m) thick that extend less than 1 mile (1600 m) to massive systems that extend hundreds of miles (hundreds of kilometers) across multiple state, provincial, or international borders. Aquifers can vary greatly in depth from the land surface. In some locations, the top of an aquifer may extend to the land surface and then tilt gradually downward for hundreds of feet (over 100 m). Regional geology provides the setting for groundwater and aquifers (Cech, 2009).

A perched aquifer, for example, is often found in formations of glacial outwash where clay layers form impermeable layers above a primary aquifer. This upper and perched groundwater usually covers a small area but allows groundwater to exist above the saturated zone of a lower aquifer system. A perched aquifer is often located relatively close to streams.

A fractured aquifer it found in rocks, such as granite and basalt, which contain usable amounts of groundwater in cracks, fissures, or joints. Limestone formations arc sometimes found in fractured aquifers but often contain cracks or other openings enlarged by solution (dissolving of rock) (Cech, 2009).

Groundwater exists in an aquifer under two different conditions: confined (also called artesian) or unconfined (sometimes called water tables or phreatic surface).
An unconfined aquifer, shown in Figure 2.4, is generally located near the land surface and is recharged directly by surface water. The term "perched" refers to ground water accumulating above a low-permeability unit or strata, such as a clay layer. The difference between perched and unconfined aquifers is their size (perched is smaller) (Usul, 2008).

Alluvial aquifers arc excellent examples of unconfined aquifers. Recharge can occur from the downward seepage of surface water through the unsaturated zone or from lateral movement or upward seepage of groundwater from underlying geologic strata (Cech, 2009).

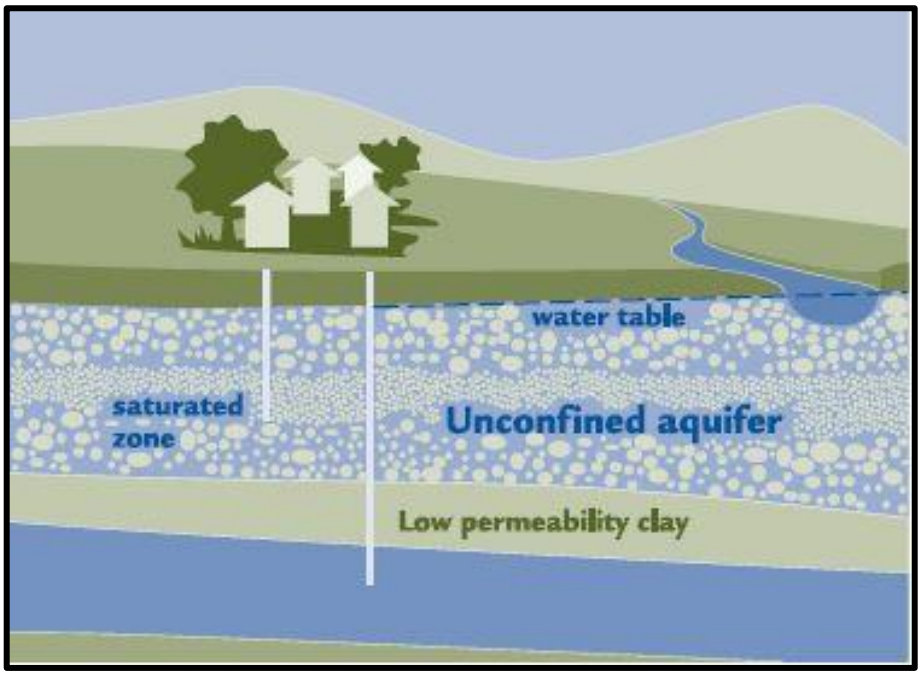

Figure 2.4 Unconfined aquifer (www.tol.ca, last visited on 28.08.2009)

Confined (shown in Figure 2.5), or artesian, conditions occur when an inclined water-bearing formation is located at depth below an impermeable layer of geologic material such as rock, clay, or shale. This geologic barrier "confines" groundwater and causes it to be under pressure. If the pressure is great enough, groundwater can emerge at the land surface as an artesian spring. A spring can also occur if groundwater in an unconfined aquifer moves from a higher to a lower elevation and emerges on the land surface. If a confined aquifer follows a downward grade from its recharge zone, groundwater can become pressurized as it flows (Cech, 2009).

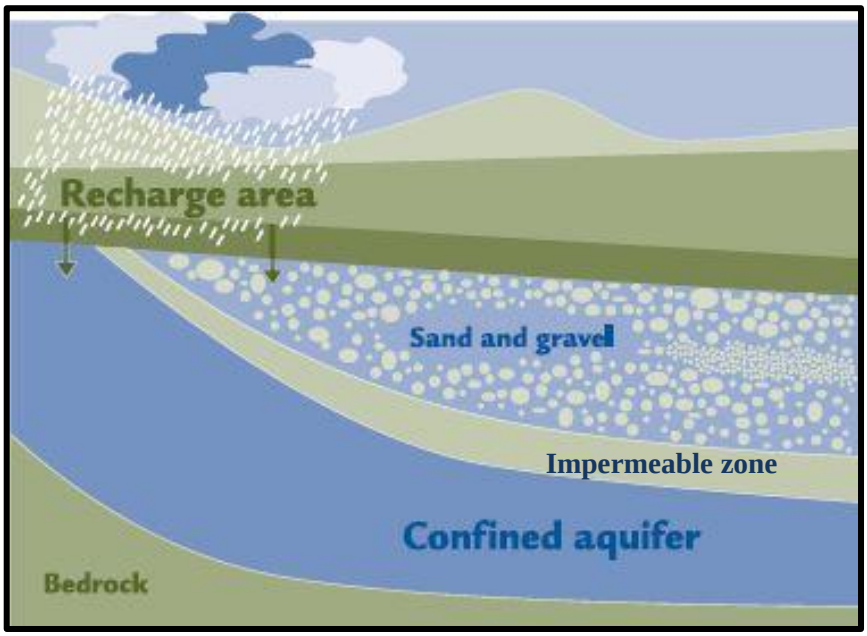

Figure 2.5 Confined aquifer (www.tol.ca, last visited on 28.08.2009)

In a confined aquifer, the water in a bore tapping the water-bearing formation usually rises up the borehole under pressure to a level that is above the top of the aquifer. The theoretical surface fitted to the water levels in such bores is termed the potentiometric surface (Ford and Williams, 2007).

In confined aquifers groundwater flow equation is obtained by combining Darcy's law and steady-state equations (Usul, 2008).

The term karst is used widely to describe the distinctive landforms that develop on rock types such as limestone, gypsum, and halite that are readily dissolved by water. Karst areas are typically characterized by a lack of permanent surface streams and the presence of swallow holes and enclosed depressions. Rainfall runoff usually occurs underground in solutionally enlarged channels, some of which are large enough to form caves (Hiscock, 2005).

Karstic aquifers are those that contain solution-generated cavities that permit rapid transport of groundwater, often in turbulent flow, and often carrying a sediment load. Such aquifers are found in gypsum, limestone, and dolomite rocks. In most aquifers there is a mismatch of many orders of magnitude between groundwater flow rates within the aquifer and stream flow rates on the land surface above. In karstic aquifers, there is a continuum of flow rates such that the groundwater system in karstic aquifers takes on the characteristics of both surface water and groundwater. There is also a rapid interchange of surface water and groundwater (White, 2000).

Nowadays, the basic knowledge about the properties of karst aquifers, about the hydrodynamics of the flow through it, and about the dissolution kinetics of the soluble rocks can be known. Together with the computational power, building numerical models of karst aquifers and studying them becomes easier (Romanov, 2003).

2.4 General Effects of Groundwater in Mining Activities

Traditionally, in mining activities the problems that can be caused by groundwater can be categorized in two ways;

a. Sudden flood situation
b. Seepage situation

Sudden flood situation is seen generally in saturated dissolution pores on karstic region, in magmatic rocks intersected by joints and fractures or in fault zones formed by tensile forces. Sudden flood is very important for mining activities and can cause dangerous problems about time and money which are very valuable aspects in mining.

Seepage is discharge of water stored in primary pores on rocks according to permeability or conductivity properties of rocks. Seepage causes usually negligible problems, because it can easily be drained during mining activities (Doyuran, 2006).

According to Loofbourow (1973) the effects of groundwater are categorized in two different parts which are direct effects and indirect effects namely.

Direct effects are:

- cost of pumping and/or drainage,
- the loss of personnel and equipment caused by sudden flood situation,
- being closed of management temporarily or permanently, and
- effects on mining methods selection.

Indirect effects

- Working conditions would be harder.
- Cost of equipment maintenance would be higher.
- Soft rocks would be dragged on to the working area.
- Because of increase in decomposing on rocks subsidence would occur.
- Efficiency of blasting material would be affected.

In mining industry, for the effective and realistic solution of the groundwater problems it is recommended to be prepared to handle these kinds of difficulties. Thus, in planning stage hydrologic investigations should be done carefully.

Especially in the working area hydrologic studies would be necessary when some signs related to groundwater (e.g. surface water, seepage, wells, and springs) are found during the geological investigations (Doyuran, 2006).

2.5 Effects of a Confined Aquifer on Surface Mining Activities

Possible effects to be considered here include;

1. Presence of a confined aquifer with water under high pressure can lead to flooding at the pit bottom unless the impermeable layer confining the aquifer is not thick enough.

2. High water pressure in the confined aquifer can crack or fracture the impermeable layer, and thus increase its permeability which may again cause high water income to the pit bottom.

3. Permanent slope adjacent to the pit bottom may be affected from the water pressure applied to the upper boundary and slope stability issues may arise for high overall slope angles.

CHAPTER 3

AFŞİN-ELBİSTAN LIGNITE BASIN AND MINING ACTIVITIES

Afşin-Elbistan Lignite basin, shown in Figure 3.1, has 46% of Turkey Lignite reserve therefore this basin has a major role in energy production of Turkey. Elbistan Coal basin is divided as A (Kışlaköy), B (Çöllolar), C (Afşin), D (Kuşkayası), E (Çobanbey) and F sectors namely because of its big extent. There is the Hurman River in the middle of basin, and sectors are sketched in Figure 3.2. At the western side of the basin, C and E sectors are located, and at the east side of it A, B, D and F sectors are located.

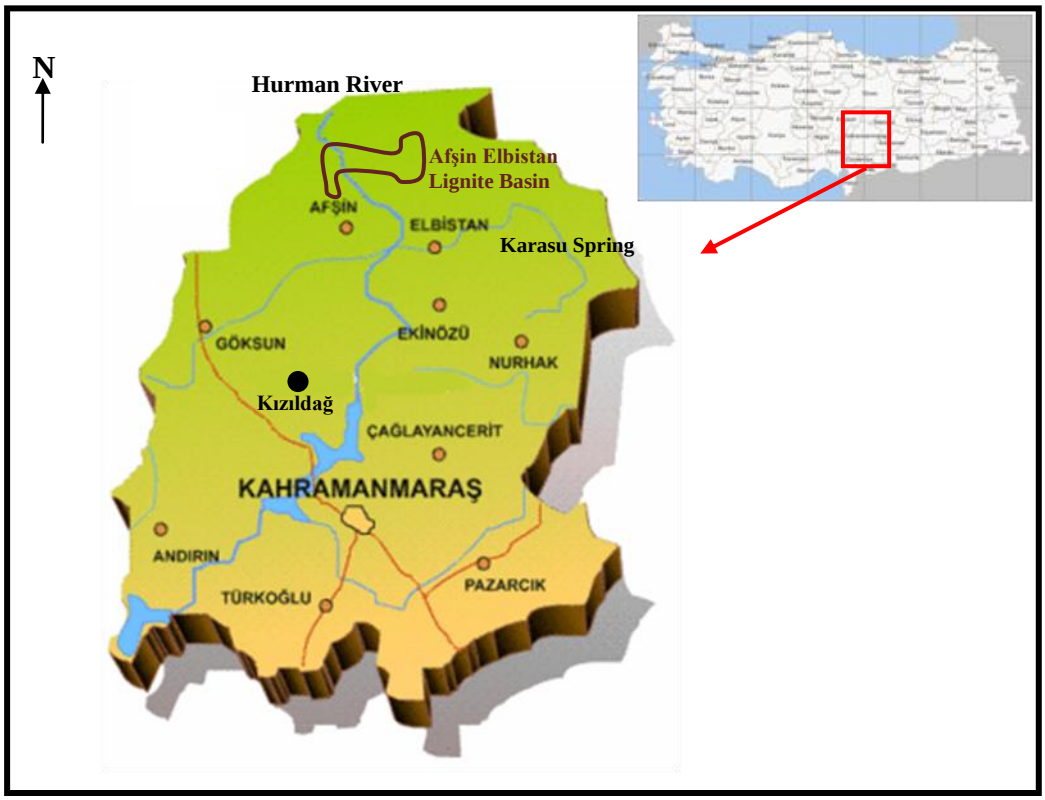

Figure 3.1 The orientation of the Afşin-Elbistan Lignite basin

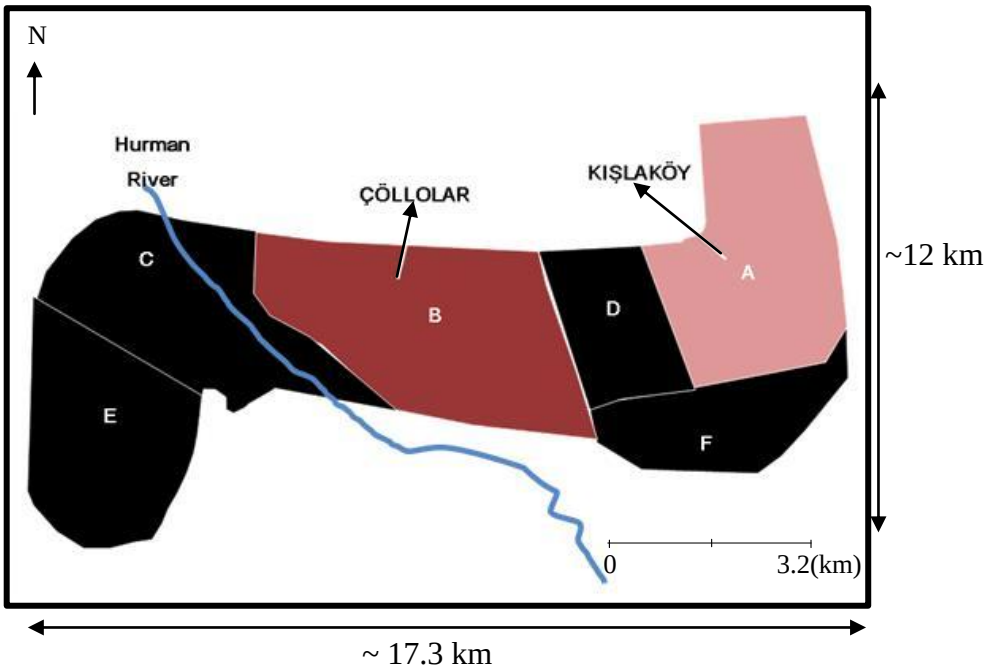

Figure 3.2 The orientation of the Afşin-Elbistan Lignite basin sectors (Bulut, 2008)

3.1 Description of the Study Area

Afşin-Elbistan Lignite basin is in Afşin and Elbistan districts which are bound to Kahramanmaraş, Turkey. This lignite basin is approximately 120 km^2. Specifically, the Afşin sector is 12.6 km^2, the Kışlaköy Sector is 18.7 km^2, and the Çöllolar sector is 18.7 km^2 approximately. Topography is rising to the north with a little inclination (Koçak et al., 2003).

The first exploration drilling was initiated by West Germany technical support with General Directorate of Mineral Research and Exploration (MTA) in 1966. After that lignite formation was detected in 1967. Feasibility study of the basin was prepared in 1969.

A detailed feasibility study of Kışlaköy sector including power plant was conducted in 1971 by three foreign and two Turkish firms and in that sense planning and design works were done by a West Germany firm. 20 million tons of lignite was

planned to be produced and 18.6 million tons of it was planned to be sent to the power plants for electricity production (Yörükoğlu, 1991). Extraction work of lignite coal started in Kışlaköy sector because upper coal was at the lowest depth in that sector. Koçak et al. (2001) stated that in Afşin-Elbistan basin the proven reserve amount is around 4.3 billion ton however 3.8 billion ton of lignite can be operated. Çöllolar open cast mine will be the second largest mining activity in the basin after active Kışlaköy open cast mine. A Ciner Group firm, Park Teknik Inc. signed a contract in 04.04.2007 for 25 years production of lignite in Çöllolar sector.

In Elbistan, there are two thermal power plants namely as A and B power plants. Both power plants produce 2795 MW energy totally. It is planned that Çöllolar basin will provide 17 million tons of lignite yearly for Afşin-Elbistan thermal power plant B. In Figure 3.3 Afşin-Elbistan Lignite Basin, thermal power plants A and B, Kışlaköy and Çöllolar mining areas are shown.

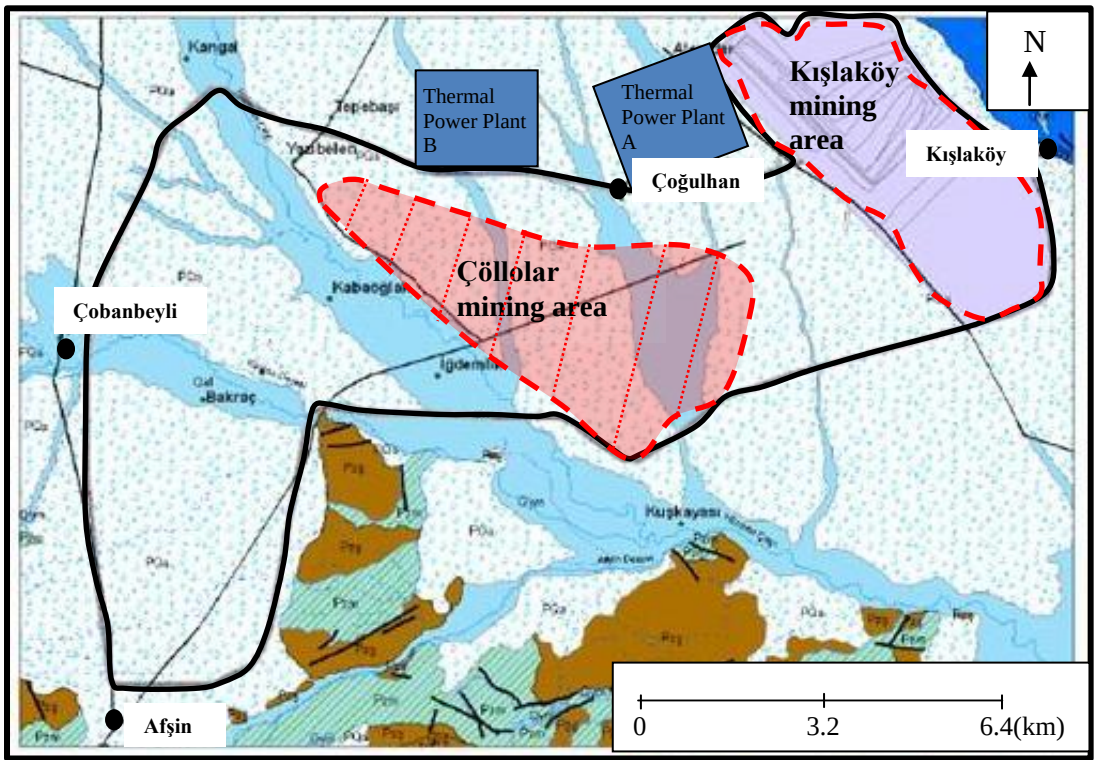

Figure 3.3 The Afşin-Elbistan Lignite Basin, thermal power plants A and B, Kışlaköy and Çöllolar mining areas (Akbulut, 2006)

3.2 General Geology and Hydrology of the Area

In general, Çöllolar open cast mine is located in the Afşin-Elbistan lignite basin which is surrounded by the Binboğa, Nurhak and Engizek mountains. The major water stream is the Ceyhan River with the Hurman River which is a minor part of Ceyhan River. In addition, Afşin-Elbistan lignite bed is in a closed basin which is formed during the rise of the Toros Mountains after Alpine Orogeny. Region base is formed by Permo-Carboniferious old limestone (Yörükoğlu, 1991).

In upper clay and gyttja series one or two lignite layers are located with depths ranging between 50-100 m. A combination of humus and coal is present in this soft lignite series. This situation in the bedding zone occurs vertically as well as horizontally (Koçak, et al. 2003).

On the south of Kızıldağ, outcrops of Neogene formations are observed, and in other places, the formations are covered by Quaternary old precipitations. The thickness of the whole sedimentary deposition is about 300-500 m. Neogene lithologies are listed from bottom to top as:

- Limestone formation (containing possible confined aquifer): Red, brown coarse grained clastic precipitations, sandy, marl sedimentations,
- Bottom clay (green clay): Greenish, bluish-plastic clay and marls of lignite bottom,
- Lignite zone with transitive layers of coal and gyttja,
- Gyttja,
- Greenish, bluish, plastic clay, loam and marls of lignite top.

Typical formations and their thicknesses are illustrated in Figure 3.4.

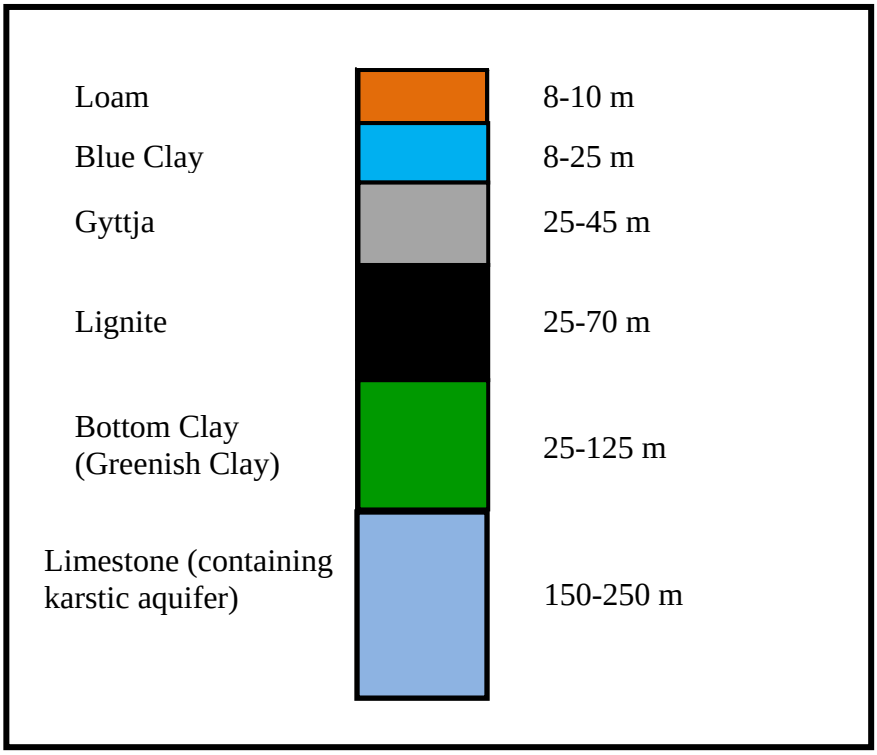

Figure 3.4 Typical Formations and their thicknesses in the Çöllolar mine

There are successive layers of coal and gyttja in overburden. Lignite which is formed in Pliocene age is just beneath the gyttja, having a thickness of 10-80 m. From east to west and north to south the thickness of the coal increases. Additionally, faults are observed on the south of Kışlaköy sector (Yörükoğlu, 1991).

Hydrology of the study area is as important as geology for mining activities. According to Yörükoğlu (1991) the Ceyhan River and its branches the Hurman River, Söğütlü and Sarsap Streams are important water streams in Elbistan basin to be considered in hydrological investigations.

Groundwater conditions are critical that not only a static water table but also a confined aquifer with water under high pressure exist in the area. Yörükoğlu (1991) indicated that five types of aquifers are present in the mining area of Elbistan lignite

basin. These are Quaternary aquifer, Gyttja aquifer, Artesian aquifer, Paleozoic and karstic limestone aquifer.

3.2.1 Quaternary aquifer

This layered formation with its coarse grains has high permeability values such as 10^{-6}. Especially, in rainy seasons, these permeable layers ease the circulation of groundwater. Because of blue clay existence, groundwater trapped in blue clay zones acts like aquifers. Flow direction in these aquifers is from the north to the south.

3.2.2 Gyttja aquifer

Some parts of gyttja, located above the lignite zone have a thickness of 40-50 m, and have high water content. Because of this high amount of water content this is important from the aspect of mining activities. Water trapped locally in the pockets of gyttja shows a kind of pressurized aquifer behavior and these local aquifers may be exposed and cause small water rushes into the pit during the excavation of the pit slopes. Gyttja has low permeability such as 10^{-9} and water does not dissipate easily.

3.2.3 Artesian aquifer

This thin aquifer formation is located under the lignite zone and hence it is not important for mining in the area.

3.2.4 Paleozoic and karstic limestone aquifer

The Paleozoic and karstic limestone aquifer may have reach the pit slopes and pit bottom through tectonic and permeable zones. Kızıldağ limestone had contact with

lignite layer during tectonic movements and this limestone created permeable zones. Karstic aquifer is very important from the point of mining activities as Kızıldağ water, called as “karstic area”, finds access to mining area. This karstic aquifer in the limestone formation acts as a confined aquifer and contains pressurized water.

Limestone located in the coal bottom has an obvious characteristic of a good aquifer (Akbulut, 2006). According to the MTA Report (Akbulut, 2006) these properties can lead to problems in production because of the high hydrostatic pressure of water in the aquifer and possible leaking of this pressurized water through tectonic structures like local faults. Moreover Akbulut referred to Özbek and Güçlüer’s study done in 1977, and according to this study, in limestone zone there are some regions having karstic properties and with the help of faults there may a massive water flow into the coal production area.

First studies related to the Elbistan Coal Basin were about investigating coal properties and coal reserves. After 1980, feasibility, geophysical and geotechnical studies were carried out in detail. Based on the reserve studies in 1981, Elbistan Basin has 466 million tons of lignite (Akbulut et al., 2007). Besides determining the planning criteria, coal production amount, machinery and equipment used, Yörükoğlu (1991) also studied the geological and hydrological properties of the area.

3.3 Previous Stability Studies Related To The Area

Slope stability of permanent slope of neighboring Kışlaköy open cast mine was studied by Akbulut et al. (2007) aiming to design a new safe permanent slope. Core drilling, sampling and laboratory analysis were carried out for geotechnical investigations. In order to determine Mohr-Coulomb parameters, 2D Limit equilibrium back-analysis of a major slide in Kışlaköy sector was conducted. As Kışlaköy is neighboring Çöllolar mining area within the same lignite basin, this

investigation constitutes a significant background for the slope stability studies in this thesis. Çöllolar sector of the basin is studied by Karpuz et al. (2008) concentrating mainly on stability of major slopes in the mine.

3.4 Mining Activities in Kışlaköy

Lignite in Kışlaköy open cast mine lies almost horizontal in the middle part of the basin whereas an inclination of 5-20 degrees is present at the edges of the basin. Overburden in operating benches is loosened by blasting, excavated by a shovel and transported to the backfill site with trucks by the contractor. The company transports all of the lignite and a certain portion of the overburden for backfilling to the stock area by a Bucket Wheel Excavator (BWE) shown in the Figure 3.5.

Figure 3.5 Bucket wheel excavator in Kışlaköy open cast mine (Akbulut et al., 2007)

In Kışlaköy, belts are used as conveying equipment with 1800 mm belt width and 5.2 m/sec conveying speed. Kışlaköy open pit mine is operated on six benches with one BWE on each bench. These bucket wheel excavators have an approximate capacity of 3000 m^3/hr. Site used for backfilling is organized by five spreaders of 5600 m^3/hr capacity. Bucket wheel excavators are able to excavate benches up to 30 m height with 4 m depth from their operating location. It is also possible to operate BWE's in levels on the same bench.

3.5 Mining Activities in Çöllolar

First three years of the operation in Çöllolar sector is dedicated to the overburden removal to reach the coal reserve. Hydraulic excavators will be used for both overburden removal and loading of material on trucks. Stripped overburden will be transported to the dump site outside the field of operations. A rectangular geometry based box-cut will be excavated to initiate mining operations on the south-west border of the mine field. Mining is planned to advance to southern region of this box-cut in future.

Initial box-cut will reach a depth of approximately 100 m and expand over an area of approximately 2.6 km^2 (260 ha) at the end of the third year. The operation will reach a depth of about 145 m and the operation area covered will be 3.8 km^2 (380 ha) at the end of the 5^{th} year. Development work in pit geometry for bucket wheel excavators will start after three years (Oge, 2008).

3.6 Dewatering Activities

In Kışlaköy open cast mine, a permanent slope failure occurred in 2006 affecting the mining activities. Dewatering was not effective in Kışlaköy mine groundwater level being as close as 15 m to the ground surface at the top of the slope. This high

groundwater level and high overall slope angles, and some local tectonic features like faults and weak clay layers above and below the lignite zone were believed to trigger the major slope failure of 2006.

Kışlaköy sector was close to the edge of the basin where lignite zone and associated weak layer inclinations are as high as 10-20^{o} and a number of local faults exists around the edge of the basin related to the origin of sedimentary deposition close to the bedrock. Çöllolar sector being more close to the center of the basin is believed to be in a more favourable condition against slides along composite surfaces that can be triggered by weak layer and fault combinations.

The only problem remaining in Çöllolar sector is a good slope design with proper overall slope angle for the critical permanent slope. This design effort must be supported by an efficient dewatering plan to reduce the groundwater levels and preferably try to keep groundwater levels parallel to the downward advancement of the pit bottom in the initial 3 years of mining.

Therefore, in Çöllolar sector Park Teknik scheduled and applied an extensive dewatering program. Park Teknik with the consulting firm MBEG firm plans to lower the water table 100 m below the surface within the 5th year targets. In another word, when the mine reaches a depth of 145 m at the end of the 5th year, groundwater level will be at a depth of 100 m from the surface.

In Çöllolar, in order to pump out the water from upper aquifer and gyttja aquifer together, wells were opened prior to stripping operation and dewatering in the region was sustained. Five new wells were opened in December 2008. Until January 01, 2009 a total of 392 dewatering wells (Table 3.1) and 49 wells for measurements were drilled and a total borehole advance of 35,118 meters was reached (Neuhaus & Özdemir, 2008).

Table 3.1 Water wells (Neuhaus & Özdemir, 2008)

	Date		
	30.11.2008	1-30.12.2008	01.01.2009
Total number of drilled water wells	387	5	392
Number of wells from which pumps were detached	92	4	96
Number of operating wells	286	2	284
Number of wells not operating due to maintenance or defect	9	2	7
Total amount of water pumped out (m^3)	5,721,387	533,207	6,471,331
Total advance (m)	0	35,118	531

Three wells that were not used due to defects and stripping operation joined dewatering process in December 2008 so that a total amount of 749,944 m^3 groundwater was pumped from recent and old wells. Together with the former operating wells, 284 boreholes drained 6,471,331 m^3 groundwater until 01.12.2008.

Drainage channels were opened at the north, west and eastern borders of the mine excavation and connected to the Hurman River in order to prevent any flow into the region from surface waters and agricultural irrigation channels (Figure 3.6).

Figure 3.6 Drainage channels for surface water (Neuhaus & Özdemir, 2008)

Water drained from wells is also directed to these channels. Moreover, water flowing into the pit is accumulated in pools and pumped up into these channels (Figure 3.7). Flygt pumps are used to pump out the accumulated water from the pool.

Figure 3.7 Pumping well in water accumulation pool (Neuhaus & Özdemir, 2008)

Two 12” diameter steel pipes were laid to construct a pipeline of approximately 1500 m to redirect and force Karasu spring to flow into the Hurman River at the dump site. Three submersible Flygt pumps with 70 l/sec capacity are used to pump and force the water along the pipes. A mud pump with 80 l/sec capacity is also installed and ready for usage here (Neuhaus & Özdemir, 2008).

CHAPTER 4

LABORATORY AND FIELD STUDIES

Assessing the stability of critical permanent slope in Çöllolar mine, detailed laboratory and field works were carried out. For geotechnical investigations 5 boreholes coded as SK-1, SK-3, SK-5, SK-6, SK-11 were drilled and logged. On the samples taken from boreholes, extensive soil mechanics tests were conducted. To handle the groundwater problem in the mining area water level measurements and pumping tests were conducted in 22 boreholes coded as TK-3, TK-5, TK-6, TK-7, A-35, A-36, OW-19, OW-20, S-24, S-32, S-154, S-343, S-344, S-345, S-346, S-347, S-348, S-349, S-350, S-352, S-353 and S-354.

4.1 Geotechnical Boreholes and Laboratory Tests

Five geotechnical boreholes coded SK-1, SK-3, SK-5, SK-6, SK-11 were drilled and logged. Geotechnical profile and lithology were assessed and determined from the borehole data. Undisturbed samples were sent to Soil Mechanics Laboratory in Civil Engineering Department, Middle East Technical University (METU). Laboratory results were reported by Karpuz et al. (2008). Location of these boreholes in the mine is given in Figure 4.1.

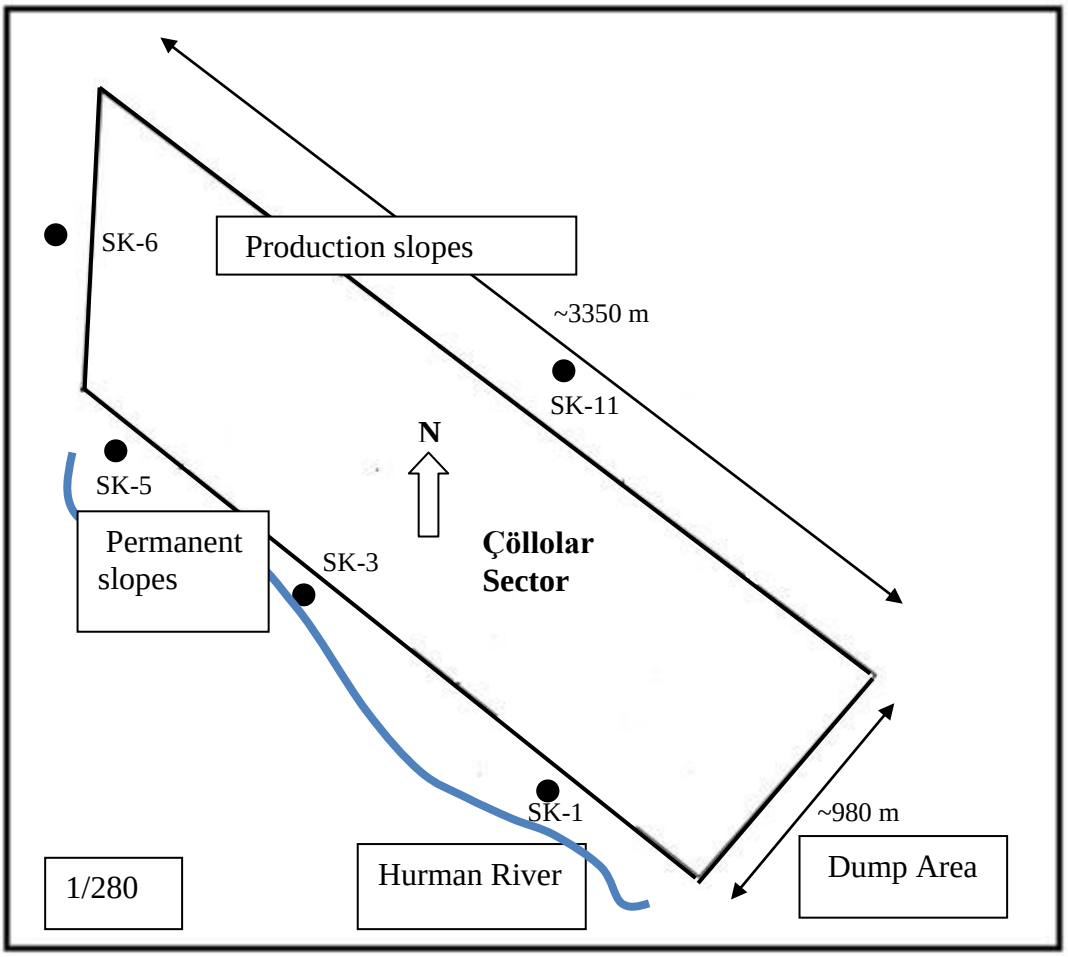

Figure 4.1 Locations of geotechnical research boreholes in Çöllolar Sector

About these boreholes Karpuz et al. (2008) provided the following information:

- SK-1 borehole is located at the side where the conveyors lie from pit to dump area.
- SK-3 borehole is located near to the Hurman River, on the middle of permanent slopes on the south-west side of the mine.
- SK-5 borehole is located at the west side; permanent south-west and north-west slopes junction.
- SK-6 borehole is located in the middle of the north-west permanent slope.
- SK-11 borehole is at the middle of temporary production slope, on the north-east side.

- SK-3 and SK-5 boreholes were drilled to sub-coal levels; the other three boreholes reach only up to coal levels.

Five geotechnical boreholes enabled soil mechanics testing by recovering undisturbed samples using Shelby Tubes. 51 sieve analysis, 53 hydrometer tests, 54 consolidated-drained direct shear tests, 11 unconfined compression tests, 57 water content tests, unit weight tests, 46 void ratio tests, 38 specific gravity tests, and Atterberg limits tests were conducted and reported. The summary of the results of laboratory experiments is given in Table 4.1.

Table 4.1 Summary of results of laboratory experiments (Karpuz et al., 2008)

Material	Water content w_n (%)	Unit Weight γ_n (kN/m^3)	Peak Cohesion c'_p (kPa)	Peak Internal Friction Angle φ'_p(^{o})	Residual Cohesion c'_r (kPa)	Residual Internal Friction Angle φ'_r(^{o})
Loam	36.0	18.66	56.00	15.00	48.0	11.00
Blue clay	31.3 (5.2)	18.06 (0.91)	34.30 (19.20)	26.30 (0.10)	21.5 (17.8)	21.00 (0.10)
Gyttja	78.0 (37.9)	15.06 (1.72)	59.00 (48.40)	31.80 (0.18)	41.3 (41.9)	28.33 (0.15)
Lignite	104.0 (45.0)	13.20 (2.32)	48.00 (19.44)	32.80 (7.28)	32.4 (17.9)	30.00 (9.64)
Black Clay	60.0	16.80	57.50	28.00	36.0	25.00
Green clay (Bottom clay)	47.0 (32.7)	16.74 (2.73)	32.83 (16.00)	23.17 (4.62)	15.5 (11.5)	16.00 (4.47)

(Standard deviation values are illustrated in the parentheses.)

4.2 Detection of the Confined Aquifer

Drilling operations were conducted in order to explore the karstic region in limestone formation. In borehole TK-3 at a depth of 108 m, bedrock (karstic limestone) was drilled through about 1 m and a sudden water rush of approximately 15-20 l/sec was observed out of the borehole at the surface.

Therefore in 30 different points geophysical investigations (e.g. electrical resistivity) were conducted aiming to investigate the distribution of the surface topography or contours of the bedrock (karstic limestone). This way bottom clay and limestone contact depth was determined. This was important, since the bedrock possibly contained a confined aquifer.

Groundwater level in TK-3 borehole was 3.25 m and in 1156.45 m elevation. A-35 and A-36 drill holes reaching limestone containing karstic aquifer indicated that there was a high quantity artesian leakage. This case point out the fact that there is an aquifer presence in this region and water rush reaches the surface. Although tests were intended to be conducted in TK-3 borehole for pump selection to be used in drainage of karstic aquifer, breakdown in the supply pipe prevented this study.

It is concluded that drainage operations should advance at least to 10-15 m in bottom clay and 3 groundwater wells should be opened to decrease groundwater level in the karstic formation. By this way, appropriate pump, amount of wells and spacing were determined. These boreholes are TK-5, TK-6 and TK-7 and their locations are shown in Figure 4.2.

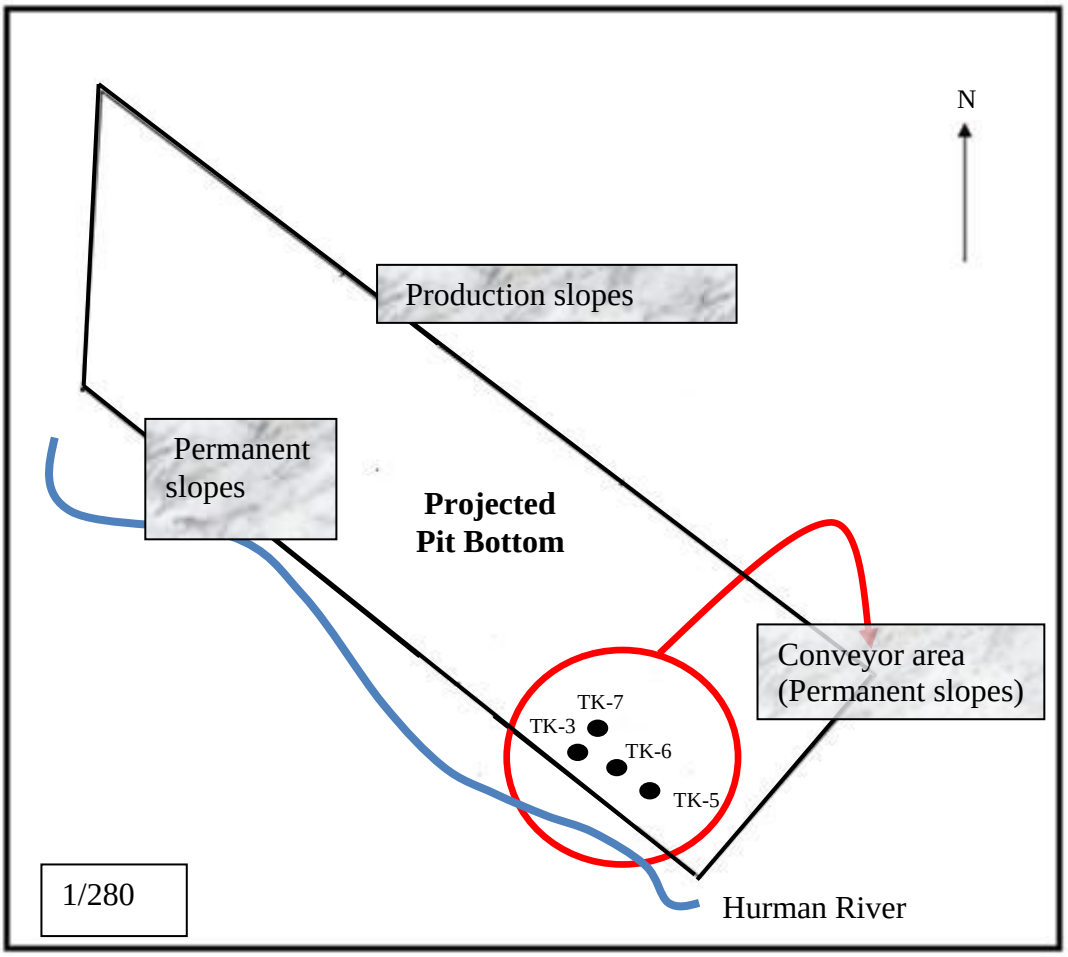

Figure 4.2 The locations of TK boreholes

From TK-5 51,840 m^3, from TK-6 92,880 m^3 and from TK-7 34,560 m^3 water were pumped out. Also TK-3 borehole was used as an observation well without installing a pump in it. Thickness of the bottom clay layer at the coal bottom lying over karstic aquifer is 80-90 m around the permanent slope region (at the Hurman side). 120-125 m thickness is predicted around the projected pit bottom according to the 5 year plans.

From borehole log of TK-3 a typical lithology in the region is summarized in Table 4.2. A detailed sample borehole log is presented in Appendix A.

Table 4.2 Typical lithology table of TK-3 borehole (Park Teknik, 2009)

Depth (m)	Detail
0-4	Filling material
4-5	Gravel
5-11	Blue Clay
11-13	Less hard rock
13-14	Gyttja
14-15	Calcareous
15-17	Gyttja
17-20	Calcareous
20-21	Gyttja
21-23	Calcareous
23-37	Gyttja with grey fossil
37-38	Lignite
38-49	Gyttja with grey fossil
49-50	Gyttja with lignite
50-53	Gyttja
53-54	Lignite
54-58	Gyttja
58-75	Lignite
75-76	Gyttja with less hard fossil
76-82	Lignite
82-91	Clay
91-94	Lignite with clay
94-96	Lignite
96-108	Clay
108-108.50	Limestone (Bed rock)

Critical information about boreholes are given below,

- Water rushed out through TK-3 as the surface elevation was 1156 m for this particular borehole. Limestone boundary was 108.5 m deep in this borehole the bottom clay-limestone contact elevation changes in the basin. Water pressure in the aquifer was assumed to be 1.2 MPa in the further modelling work, since aquifer water rushed out indicating that aquifer pressure is higher than the value predicted by the elevation difference of 108.5 m.
- Limestone was observed at 94 m depth in TK-5 borehole and drilling operation was carried out until 103 m depth was reached form surface. There was no water rush but a small amount of water leakage from the aquifer for this borehole. Limestone was observed at 109 m depth at TK-6 borehole and drilling operation was carried out until 126 m depth was reached from surface. Limestone was observed at 117 m depth at TK-7 borehole and drilling operation was carried out until 127 m depth was reached from surface. There was no water rush out of these two boreholes either, indicating that confined aquifer containing water under high pressure is only a local structure and it does not extend all along the pit bottom.

4.3 Field Dewatering Operations

- According to the available records, dewatering operations were started in September-October 2007. Up to now with reference to this groundwater level is assumed to be lowered down to 34 m depth from the surface.
- Water drainage reports were studied. Pump performances in wells pointed out that approximately 2-13 m^3/h or 0.6 -3.6 l/sec of water is drawn from the drainage boreholes. It is observed that drainage operation of pumps lowered the groundwater level by 2 to 4 m/month by studying October 2008 – December 2008 water level maps of Park Teknik. Comparatively lower levels were reached in some wells. These locations were requested to be

adjusted so that groundwater level is lowered 2 m/month in order to sustain safety for slope stability.

- In the Çöllolar mining area there is a delay in groundwater dewatering operations that should have been carried out simultaneously with the box-cut as it was planned. Pit bottom reached 40 m depth at the end of December 2008 and it is observed that dewatering operations cannot keep up with advance in depth at pit bottom so that an elevation difference of 5-10 m is present. However, dewatering still plays the major role maintaining the stability of slopes in the mine.
- Presence of local pressurized aquifers in the slopes is an outcome of the geological formation in the region, (Yörükoğlu, 1991). Lignite and the other formations above the coal may hold water in their structure and clay type local formations cover pressurized aquifers causing local problems in the excavation of slopes. Both in the drastic failure of Kışlaköy 2006, and in the other small scale failures, these pressurized local aquifers played major roles by pushing the sliding rock masses.
- Kışlaköy failure in 2006 affected an area of 200 m wide at the southern slope and 400 m wide in the northern part. It is supposed that the rock mass potentially tending to slide is affected by groundwater level, fault zones, presence of weak black clay unit and pressurized local aquifers. Therefore, considering this situation pumps in Çöllolar are placed with 100 m spacing in the dewatering project of Park Teknik constructing a sufficiently dense network. In the hydrogeology report of MBEG (2008) a water level depth of 100 m from the surface at the end of 5^{th} year is reported to be aimed. This pump network is predicted to be an effective precaution against pressurized local aquifers aiding the failure in upper clay and gyttja. The closely spaced pump network is assumed to restrict extension of any possible failures to 100 m.

CHAPTER 5

DESCRIPTION OF MODELING WORK AND INPUT PARAMETERS

For flooding scenarios and for analyzing the mechanical effects of a karstic aquifer on slopes Finite Element Method based software Phase^2 is used. Input parameters for soil units were assigned based on a previous project work (Karpuz et al., 2008) in which soil mechanics laboratory test results were provided in detail, and also shear strength properties were calibrated based on a back analysis of a landslide in Kışlaköy region.

5.1 Finite Element Software – Phase^2

Rocscience software Phase^2 based on Finite Element Method is used. In this software, Phase^2, numerical models can be developed for finite element analysis with plane strain deformation assumption and groundwater flow studies. Steady state groundwater flow, flow net in slopes and flow amounts are calculated by finite element method (Rocscience, 2008).

A plane strain model assumes that the excavations are of infinite length in the out-of-plane direction, and therefore the strain in the out-of-plane direction is zero. Using Phase^2 mechanical analysis of some geotechnical geometries (e.g. tunnels, earth dams, slope stabilities, etc.) can be done as well as groundwater analysis and seismic analysis. As it is menu driven and very user friendly program, various geometries can be formed and multiple boundaries can be added easily.

After defining all boundaries, the finite element mesh can be created. Phase^2 incorporates a state-of-the-art 2-D automatic finite element mesh generator, which can generate meshes based on either triangular or quadrilateral finite elements. To

give the user maximum flexibility in defining the mesh, the mesh generation procedure consists of two general steps; discretization and meshing. Before the mesh is generated the boundaries must first be discretized. This process subdivides the boundary line segments into discretization which will form the framework of the finite element mesh. After discretizing, the finite element mesh can be generated. The mesh is based on the discretization of the boundaries, and the mesh and element types selected. The user can choose between 4 different finite element types in the mesh setup dialog; 3 noded triangle, 6 noded triangle, 4 noded quadrilateral and 8 noded quadrilateral. Using 4-8 noded quadrilateral element type increases accuracy. However this greatly increases the size of the matrices used to solve the problem, and it will therefore increase solution time and memory requirements. In this study, meshes with 8 noded quadrilateral type elements are used.

Before computing, field stress, material properties, hydraulic properties, boundary conditions, hydraulic boundary conditions, and loading properties should be specified in the models. The following options are used to apply displacement boundary conditions to the model.

- Restrain XY (i.e. pinned)
- Restrain X (i.e. free to move in the Y direction only)
- Restrain Y (i.e. free to move in the X direction only)
- Free (i.e. free in both X and Y directions)

Phase^2 can also be used in groundwater analysis problems. Thus, groundwater analysis in Phase^2 has 3 options for entering groundwater level into the models; piezometric lines, water pressure grid (total head, pressure head, and pore pressure) and finite element analysis.

- If the piezometric lines option is selected, then a piezometric line will be assigned to each material. A piezometric line in Phase^2 can represent a water table.

- If the water pressure grid option is selected, then water pressure grids will be assigned to each material. The water pressure grid option allows the user to model the groundwater pore pressure distribution by defining the total head, pressure head or pore pressure at a grid of discrete x, y locations.
- If the finite element analysis option is selected, then Phase^2 will conduct a steady-state finite element seepage analysis to determine the pore pressure distribution, based on the groundwater boundary conditions defined for the model. In this option, the saturated and unsaturated permeability characteristics will be defined to each material as well. With the finite element seepage analysis option, the seepage analysis can be used to calculate pore pressures for an effective stress analysis, just as with the piezometric lines or water pressure grid options.

After selecting the groundwater analysis type then hydraulic boundary conditions should be added. The following options are used to apply hydraulic boundary conditions to the model

- Total Head (H)
- Zero Pressure (P=0)
- Unknown (P=0 or Q=0)
- None / Remove Boundary Condition

Additionally, the set linearly varied total head option allows the user to define total head boundary conditions which vary linearly along a boundary. Lastly a discharge section should be determined. Because a discharge section in Phase^2 is a user-defined line segment or polyline, through which the steady state, volumetric flow rate, normal to the line segments, will be calculated during a groundwater seepage analysis.

5.2 Cross Sections Used in Models

A-A', B-B', and C-C' cross sections intersecting the pit geometry from West to East in Figure 5.1 are used in constructing the finite element modelling frames.

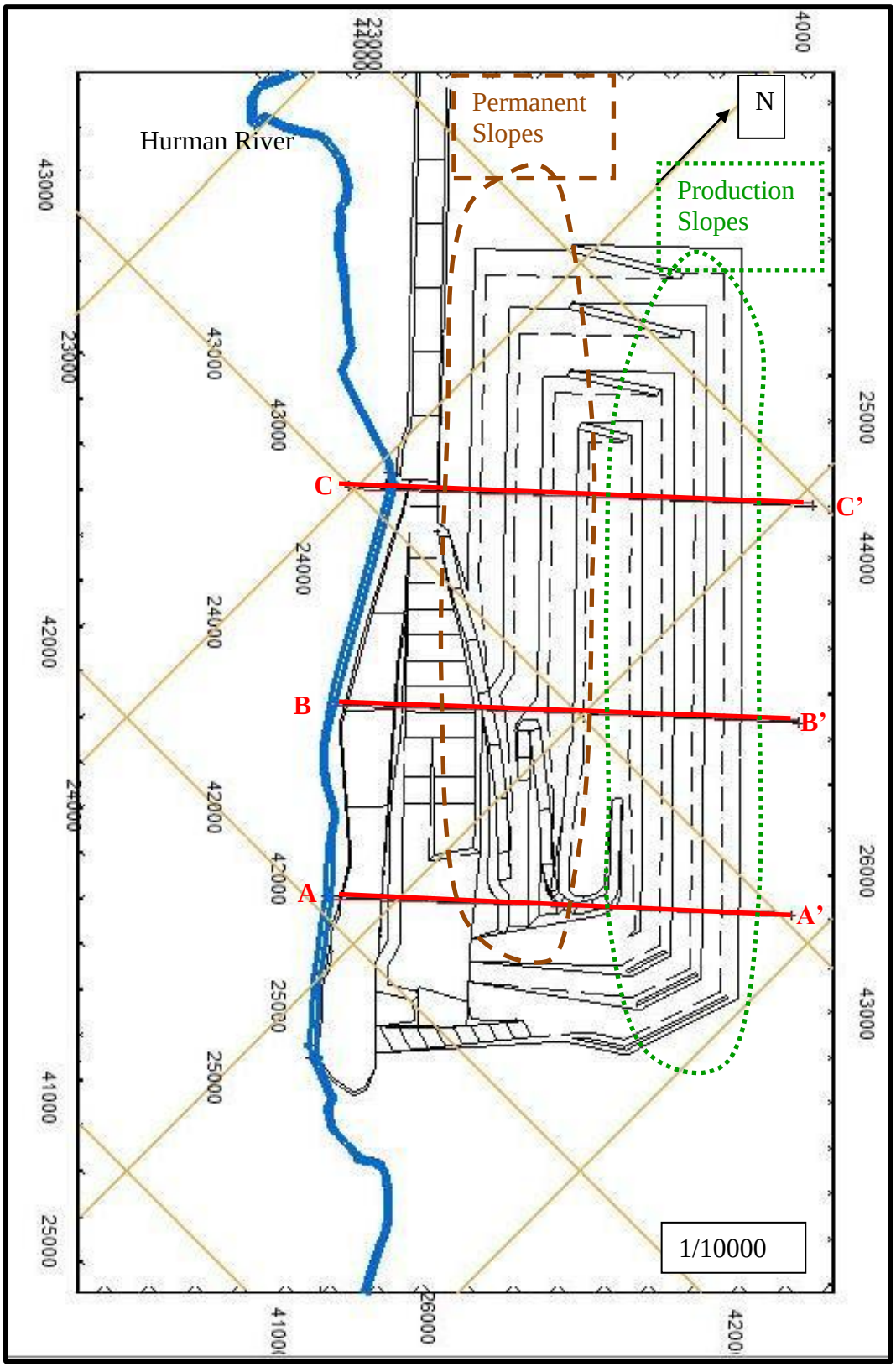

Figure 5.1 Future mining plan of the Elbistan-Çöllolar area and location of sections (Park Teknik, 2009)

These sections satisfactorily represent the typical mine sections showing the critical permanent slopes clearly and crossing the whole mine area. Among these sections, it was decided that the most representative and critical section was section A-A'. This section was used in the most of the modelling work. The other two sections were used only for checking some results. The reason for choice of A-A' section as the representative section was that, according to the future mine plans, pit depths for the other two sections will be less compared to section A-A'. As a result, the highest permanent slope is going to be excavated along this section.

Probable slope failures are analyzed conformable with scheduled pit plan of 3rd and 5th year periods. Pit geometry for the 5th year production phase is prepared by extending the bottom bench in the 3rd year plan towards the coal bottom. According to this geometry, slope under consideration for 3rd year period will reach 128 m height and pit bottom is expected to be at 1032 m elevation. For this case, projected overall permanent slope angle represented in A-A' cross section will be approximately 24^{o}. Slope height at 5 year plan is about 142 m and pit bottom is at 1020 m elevation. Ultimate pit slope angle given in A-A' cross section is assumed to reach 25^{o}. Pit models to be used in Phase^{2} analyses are produced from A-A' cross section according to 3rd and 5th year projections and they are given in Figure 5.2 and Figure 5.3. 3rd and 5th year pit models of B-B' and C-C' cross-sections are given in Appendix B.

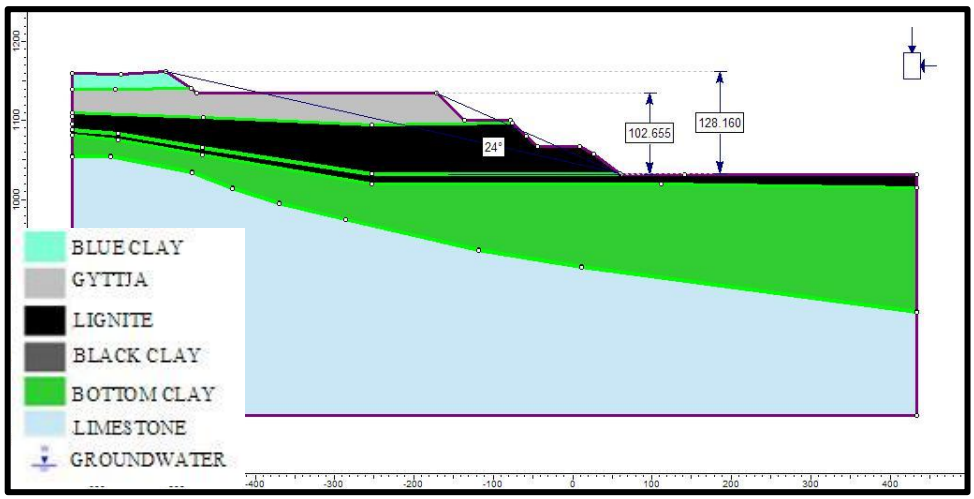

Figure 5.2 A-A' section 3rd year pit geometry

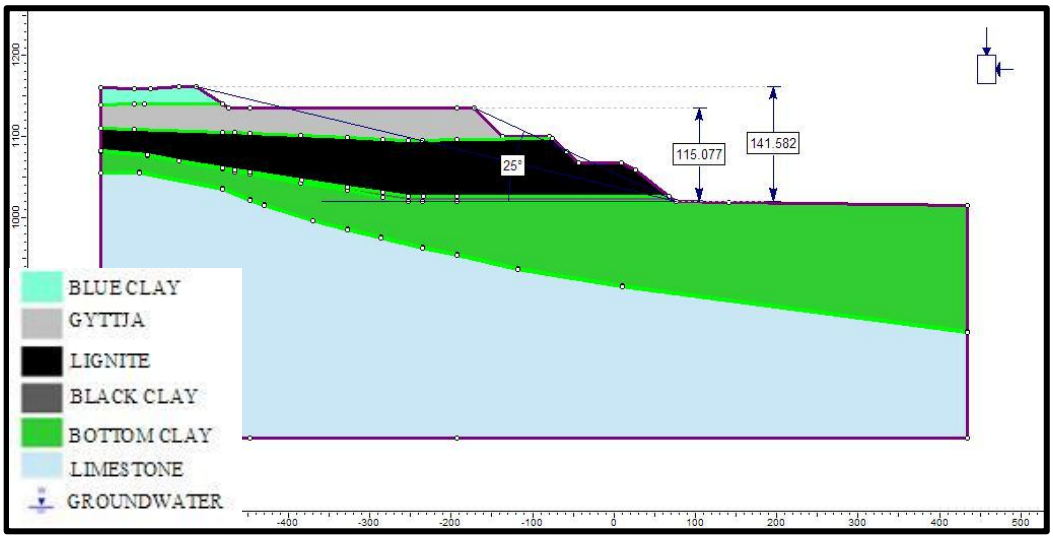

Figure 5.3 A-A' section 5th year pit geometry

5.3 Input Parameters for Modelling Work

Parameters used in numerical analysis are obtained from the report by Karpuz et al. (2008) where permanent and production slopes were designed considering possible variations in groundwater table levels. In addition to laboratory testing, back analysis of a previous major slide in Kışlaköy sector was conducted and effective shear parameters were evaluated and adjusted combining both laboratory and back analysis results.

According to the borehole logs occurrence of a weak clay layer (black clay layer) at the bottom or top of the lignite zone in Çöllolar is not as severe as in Kışlaköy. This weak layer appears rarely and disappears in most of the boreholes. However, to be on the safe side, a weak clay layer of thickness 1 m is always located right under the lignite zone in the models. For the weakest clay formation which is black clay layer and exists as thin bands on the bottom and top of the lignite with thicknesses ranging from a few centimetres to a few meters, shear strength parameters that were obtained by following a back analysis of a landslide in Kışlaköy sector were used.

Hydrostatic water pressure coefficient, H_u value in Phase^2 software, is used to define pore water pressure saturation degree in soil units under groundwater level. The H_u value is simply a factor between 0 and 1, by which the vertical distance from a point (in the soil or rock), to a Water Surface (i.e. Piezometric Line) is multiplied to obtain the pressure head. The H_u value is used to calculate pore pressure as seen in Equation 5.1.

$$u = \gamma_w h H_u \tag{5.1}$$

where:

u = pore pressure

γ_w = the pore fluid unit weight

h = the vertical distance from a point to a piezometric line

H_u = the H_u value for the material

For example, H_u value is assigned as "1" in case pore water pressure is applied totally and the material under groundwater table is fully saturated whereas "0" is used for cases where no pore water pressure is present and the material is dry. According to the efficiency of dewatering operations in a site, H_u value is predefined between "zero" and "one". In this study, H_u values are chosen according to the natural water content of the undisturbed samples collected from the Çöllolar mine site. Water contents found in laboratory testing represent the cases where no dewatering operation is carried out. As there is still an intensive dewatering work ongoing in Çöllolar, H_u values in the models are assumed to be decreased by 50% for upper units above the lignite zone and these values are referred as "reduced H_u values" for a more realistic pore water pressure saturation condition in the dewatering zones. Present dewatering process is not expected to penetrate into the

bottom clay under the lignite zone; H_u value is set to 1 to represent full saturation in the bottom clay unit.

Laboratory experiments and results of back-analysis were used for determining the design parameters to be used in models. Unit weight and water content parameters were taken to be average of the laboratory results. For loam, residual strength parameter results of only one available experiment were used. The lowest c_p' and φ_p' values were selected as input parameters for blue clay to be on the safe side.

Laboratory tests on undisturbed samples taken from the Çöllolar sector were carried out at the Soil Mechanics laboratory of the civil Engineering Department of METU. The shear strength parameters of the dominant units were as: c_p'=59 kPa and φ_p'=31.8^o for gyttja, c_p'=48 kPa and φ_p'=32.8^o for lignite, c_p'=57.5 kPa and φ_p'=28^o for black clay.

The failure occurred at the Kışlaköy sector in 2006 was analyzed with 2-D and 3-D back analyses in Karpuz et al. (2008). Shear strength parameters of a weak black clay layer obtained from back-analysis were quite lower than laboratory results while the other units had compatible values. After 2-D and 3-D analyses of the landslide, parameters were found as c'=54 kPa and φ'=32^o for gyttja, c'=54 kPa and φ'=32^o for lignite, c'=8 kPa and φ'=9^o for weak black clay. At the bottom of the lignite zone average values of laboratory testing were used for green clay shear strength parameter. For the thick bottom clay formation under lignite zone average values of laboratory shear strength parameters were used.

Engineering parameters used as input in Phase^2 finite element models are given in Table 5.1.

Table 5.1 Engineering parameters used for numerical models (Karpuz et al., 2009)

Material	Unit Weight γ_n (kN/m^3)	Internal Friction Angle $\varphi'(^o)$	Cohesion c' (kPa)	Water content w_n (%)	H_u Value	Reduced H_u Value
Loam	18.66	11	48	36	0.36	0.18
Blue clay	18.06	18	13	31	0.32	0.16
Gyttja	15.06	32	54	78	0.78	0.39
Lignite	13.20	32	54	104	1.00	0.50
Black clay	14.50	9	8	60	0.60	0.30
Green clay (bottom clay)	16.74	23	33	47	0.47	0.47
Transition zone	20.00	23	33	100	1.00	0.50
Limestone	20.00	35	10000	100	1.00	0.50

5.4 Modelling Work for Flooding

The parameter used to simulate the aquifer is the total pressure head that means confined aquifer pressure. Water pressure value is based on the total pressure head obtained from the karst aquifer observation well TK-3 in which total pressure head was believed to correspond to about 1156 m head. Ground water flow analyses are based on total pressure and pressure head values.

In the program, groundwater analysis can either be conducted using water inflow Q (m^3/sec) or total pressure head as an input value. In the models here, total head is taken as 1156 m to be used as input in the models. This means that approximate aquifer pressure is about 1.2 MPa as predicted from the water rush out of borehole TK-3 in the pit bottom linearly varied total head is used.

Aquifer water pressure value 1.2 MPa was applied to a 1 m thick transition zone shown in Figure 5.4. Between the limestone and bottom clay, aquifer water pressure was not directly applied to the contact. A transition zone with permeability between the permeability values of clay and limestone was necessary, since model instabilities occurred and flow did not move towards the mine surface boundary, instead it moved down towards the bottom boundary of the model frame due to the extreme difference between the permeability of clay and limestone. In fact assigning such a zone is realistic from geological point of view. Instead of a sudden transition it is expected to have a lower limestone zone where fractured parts of the limestone filled with the bottom clay penetration and some transitional clay bands exist in the limestone forming a geological unit between clay and limestone.

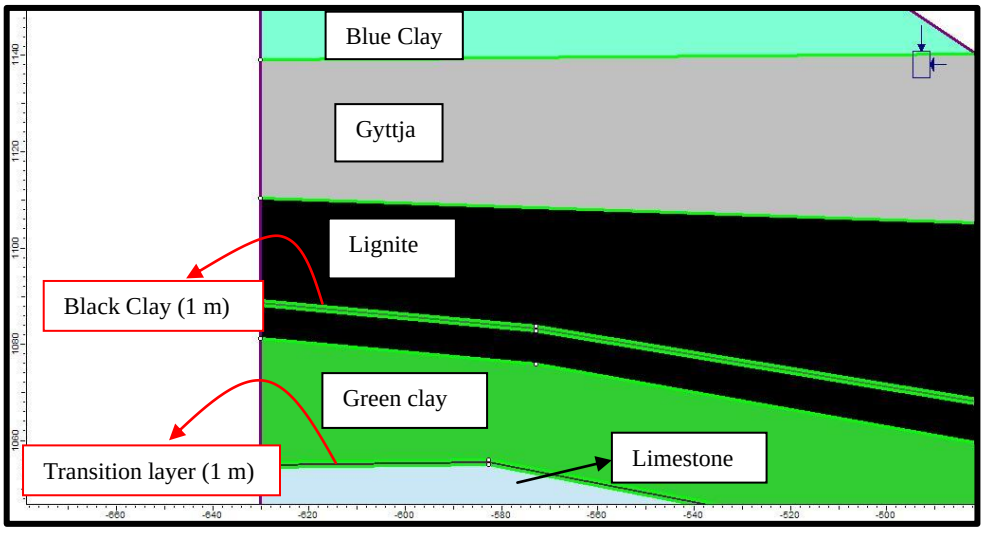

Figure 5.4 Used materials in the models

Program gives the water flow velocity as an output along specified model regions with length L_v. In these parts which are called discharge sections water flow velocities along specified points can be determined. Following equation (5.1) gives the area A of the zone at the pit bottom where a flooding can be possible due to a confined aquifer:

$$A = L_v \times t_d \qquad (5.1)$$

In equation 5.1, L_v is flooding area extension length and t_d is thickness of discharge section. L_v was taken to be 50 m in models here. Since the program is a plane strain program dimension perpendicular to the cross section is taken as automatically 1 m (t_d = 1 m). As a result a 50 m^2 area is assumed to be subjected to a sudden water rush from confined aquifer. A head of the permanent slope at the pit bottom discharge sections checked during analysis of flooding possibilities are shown in Figure 5.5.

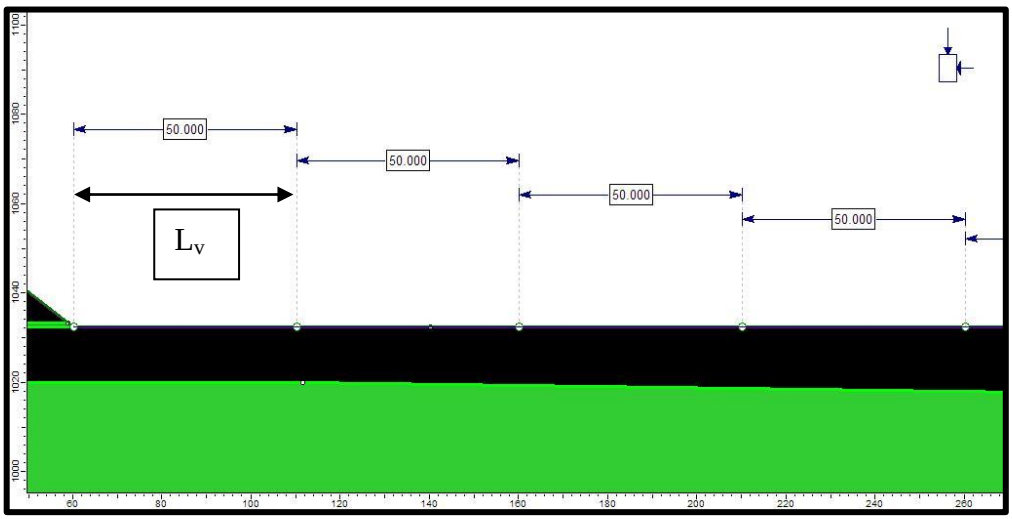

Figure 5.5 Position of the discharge sections where flooding can possible

CHAPTER 6

MODELING STUDIES FOR POSSIBLE FLOODING INTO THE PIT BOTTOM FROM CONFINED AQUIFER

Karstic confined aquifer containing pressurized water within the limestone bedrock may cause flooding to the pit bottom by water rushing through the bottom clay. In this section critical bottom clay thicknesses and permeability values for flooding are investigated by numerical models. Possibility of massive flooding situation towards pit bottom must be evaluated in order to prevent any kind of delay in production.

Following the excavation process, weight reduction on the unyielding, undisturbed bottom green clay is can cause difficulties. The confined aquifer enclosing water under 1.0-1.2 MPa pressure may lead the bottom clay layer to be displaced and cause a failure increasing its permeability by cracking. Concurrently, possible flooding at pit bottom induced by displaced bottom layer might negatively affect mining activities.

With numerical modeling first flooding scenarios due to the seepage through the bottom clay were studied. These analyses included only fluid flow through porous media modeling work. In these analyses, mechanical effects were not implemented, only steady state ground water flow analyses were included.

In the second part of the modeling work mechanical and structural responses of the bottom clay and the slopes were taken into account and mechanical effects of the pressurized aquifer were reflected onto the slope and pit bottom deformation response models. The results related to this work are presented in the next section.

Bottom clay layer permeability coefficient was determined in laboratory work by Karpuz et al. (2008) and permeability values of geologic units in the basin are given in Table 6.1. In order to investigate the worst case scenarios, permeability values for all geologic units in the models were applied as the highest laboratory value (the possible most permeable value) to be on the safe side considering the limited number of samples for some geologic units tested in the laboratory.

Cross sections A-A', B-B' and C-C' taken from 5 year pit plan as given before in the previous chapter were used in the hydrological analyses.

Table 6.1 Laboratory permeability coefficients used in the models (Karpuz et al., 2008)

Material	Permeability Constant k (m/sec)
Loam	$1.00x10^{-7}$
Blue Clay	$5.27x10^{-8}$
Gyttja	$8.66x10^{-9}$
Lignite	$5.66x10^{-9}$
Black Clay	$1.41x10^{-9}$
Green Clay (Bottom Clay)	$3.07x10^{-8}$
Transition zone	$1.00x10^{-10}$
Limestone	$1.00x10^{-19}$

6.1 Investigation of Permeability Parameter of Bottom Clay

Soil Mechanics Laboratory test results might show great variability due to the heterogeneous nature of soil and variable characteristics of samples taken from small boreholes trying to represent the whole soil mass. For those reasons,

sensitivity analyses for variable permeability of bottom clay were carried out during the modeling work. Extreme limits of permeability values of bottom clay were tried in the models.

Rocscience Phase^2 software was used to model cases where permeability of bottom clay layer increased as a result of tension cracks that can be formed due to pressure induced by karstic aquifer and flooding occurs through these cracks by a massive water flow towards the pit bottom.

In the models and analyses permeability constant value of green bottom clay is changed between $3.07x10^{-5}$ m/sec and $3.07x10^{-10}$ m/sec whereas its laboratory value is $3.07x10^{-8}$ m/sec. For different permeability values groundwater flow from the aquifer to the pit bottom is calculated. In literature the permeability constants consolidated clay like bottom clay is not more than around 10^{-7} m/sec.

A transition zone between the limestone bedrock and bottom clay was used as indicated before. For the transition zone, thickness was set to 1 m and its permeability was set to $1x10^{-10}$ m/sec for all analyses in this work.

In Phase^2 software to calculate the flow rate Q, a flow monitoring area where flooding is expected is to be defined in the models. Thus Phase^2 makes the necessary flow rate computations for that flow monitoring area.

In the flooding analyses here 4 different parts with an area 50 m^2 on the pit bottom were defined as shown in Figure 6.1. The groundwater flow amounts from these parts were calculated with flow models. Flow monitoring sections are zoomed and shown in Figure 6.2.

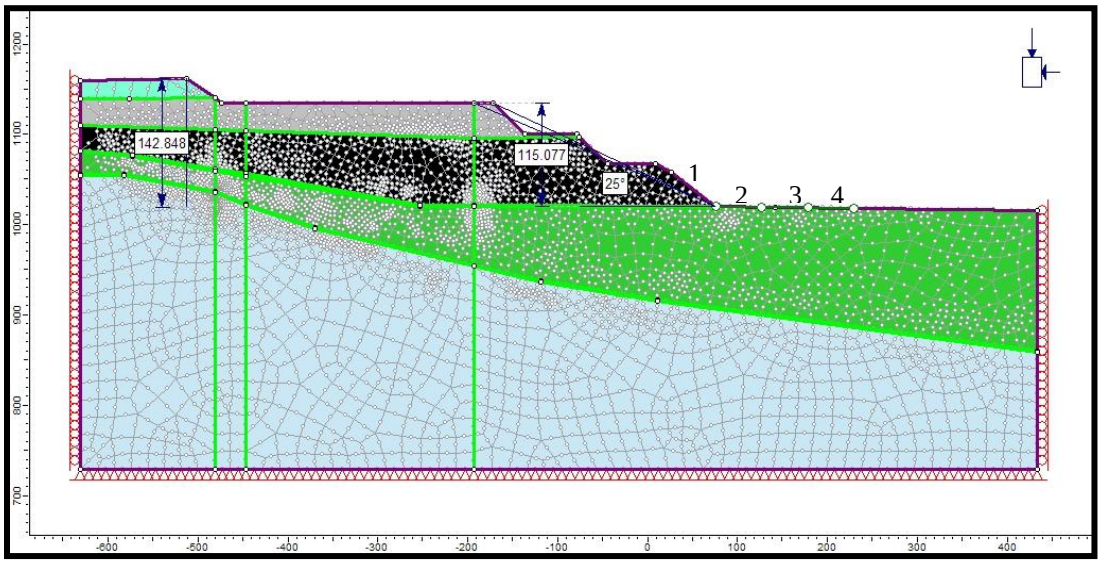

Figure 6.1 A-A' section according to 5th year pit plan with flow monitoring points

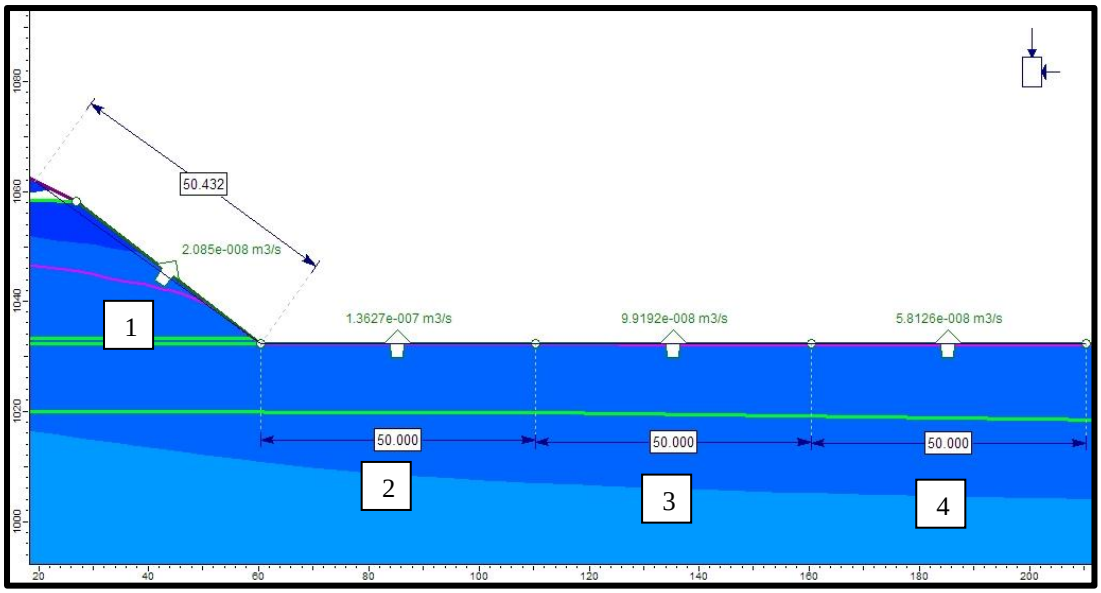

Figure 6.2 Zoomed model with flow monitoring sections and their dimensions

Analyzing 4 different flow monitoring sections, it was understood that water flow quantity from the flow monitoring section number 2 had always the highest value.

As a result of this, in the numerical modeling work the rest of the flow analysis concentrated only on flow monitoring section number 2.

In flow models, a typical flooding threshold value above which flooding was assumed to occur was to be set as the risk limit. There was no reliable data to do this. There were pumps that reached the confined aquifer and carried out pumping, and lowered the ground water. Therefore, capacities of the pumps reaching karstic aquifer and temporarily lowering aquifer water level were considered in the assumptions. 25 l/sec capacities of these pumps and their approximate 100 m spacing (around an area of 100 x 100 =10^4 m^2) were taken to be the basis for the flooding scenario assumptions.

As indicated above flow monitoring discharge sections were assigned with 50 m widths and unit thicknesses covering an area of 50 m^2 on the pit bottom. The flooding threshold value becomes 0.125 l/sec or 1.25 x 10^{-4} m^3/sec considering a 50 m^2 area of a discharge section. Thus, the flooding threshold value in these flooding analyses is taken as 1.25 x 10^{-4} m^3/sec. This amount was taken to be basis, since this amount of pumping rate succeeded to lower the water level of the confined aquifer temporarily.

According to this assumption, the sensitivity analyses of A-A', B-B' and C-C' sections for 3rd and 5th year s projected pit geometries are conducted using the flow rate from the flow monitoring discharge section number 2 for variable green clay permeability constants and thicknesses.

Results of the sensitivity analysis for A-A' section for 3rd and 5th year projected pit plans are given in Table 6.2 in terms of flow rate values for changing permeabilities of bottom clay layer..

Table 6.2 Green bottom clay permeability sensitivity analysis according to the A-A' section 3rd year and 5th year pit plans

Permeability constant k of green clay (m/s)	Flow rate (m^3/s)	
	A-A' (3rd year)	A-A' (5th year)
$3.07x10^{-05}$	$9.82x10^{-07}$	$2.30x10^{-04}$
$3.07x10^{-06}$	$9.36x10^{-07}$	$2.43x10^{-05}$
$3.07x10^{-07}$	$8.00x10^{-07}$	$3.70x10^{-06}$
$3.07x10^{-08}$	$5.98x10^{-07}$	$1.14x10^{-06}$
$3.07x10^{-09}$	$1.84x10^{-07}$	$2.16x10^{-07}$
$3.07x10^{-10}$	$3.81x10^{-08}$	$2.41x10^{-08}$

For A-A' section, results of the sensitivity analysis are presented in the graph of Figure 6.3 which is flow rate vs. permeability constant of green bottom clay. Flooding threshold flow rate value is marked as reference value in the figures following.

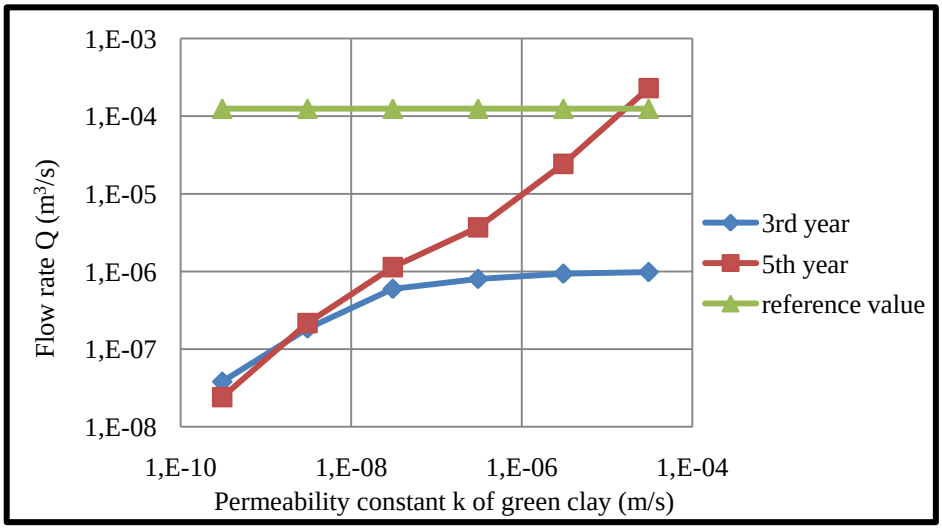

Figure 6.3 Green bottom clay permeability sensitivity graph according to the A-A' section 3rd year and 5th year pit plan

Similar results for 3rd and 5th year B-B' sections are given in Table 6.3.

Table 6.3 Green bottom clay permeability sensitivity analyses according to the B-B' section 3rd year and 5th year pit plans

Permeability constant k of green clay (m/s)	Flow rate (m^3/s)	
	B-B' (3rd year)	B-B' (5th year)
$3.07x10^{-05}$	$8.15x10^{-07}$	$4.37x10^{-04}$
$3.07x10^{-06}$	$7.89x10^{-07}$	$4.48x10^{-05}$
$3.07x10^{-07}$	$7.02x10^{-07}$	$5.51x10^{-06}$
$3.07x10^{-08}$	$5.39x10^{-07}$	$1.23x10^{-06}$
$3.07x10^{-09}$	$1.85x10^{-07}$	$2.25x10^{-07}$
$3.07x10^{-10}$	$4.22x10^{-08}$	$2.47x10^{-08}$

The B-B' sensitivity analysis graph which is flow rate vs. permeability constant of green clay graph is shown in Figure 6.4.

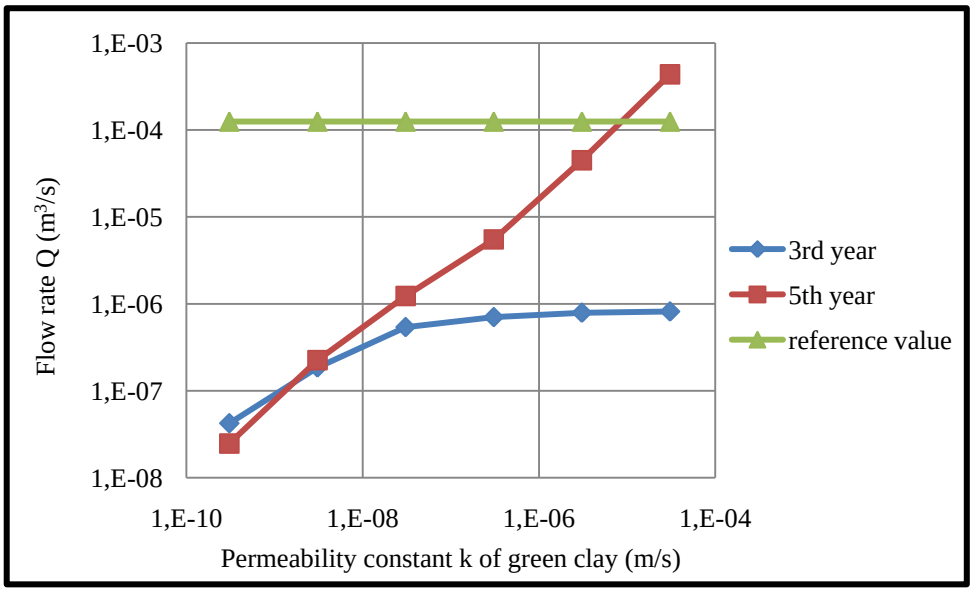

Figure 6.4 Green clay permeability sensitivity graphs according to the B-B' section 3rd year and 5th year pit plan

Sensitivity analysis results of C-C' section on 3rd and 5th year pit plan geometry data are given in Table 6.4.

Table 6.4 Green clay permeability sensitivity analyses according to the C-C' section 3rd year and 5th year pit plans

Permeability constant k of green clay (m/s)	Flow rate (m^3/s)	
	C-C' (3rd year)	C-C' (5th year)
$3.07x10^{-05}$	$1.03x10^{-06}$	$4.09x10^{-04}$
$3.07x10^{-06}$	$9.95x10^{-07}$	$4.17x10^{-05}$
$3.07x10^{-07}$	$8.51x10^{-07}$	$4.91x10^{-06}$
$3.07x10^{-08}$	$5.65x10^{-07}$	$9.46x10^{-07}$
$3.07x10^{-09}$	$1.58x10^{-07}$	$1.50x10^{-07}$
$3.07x10^{-10}$	$3.54x10^{-08}$	$1.56x10^{-08}$

C-C' section sensitivity analysis graph which is flow rate vs. permeability constant of green clay graph is shown in Figure 6.5.

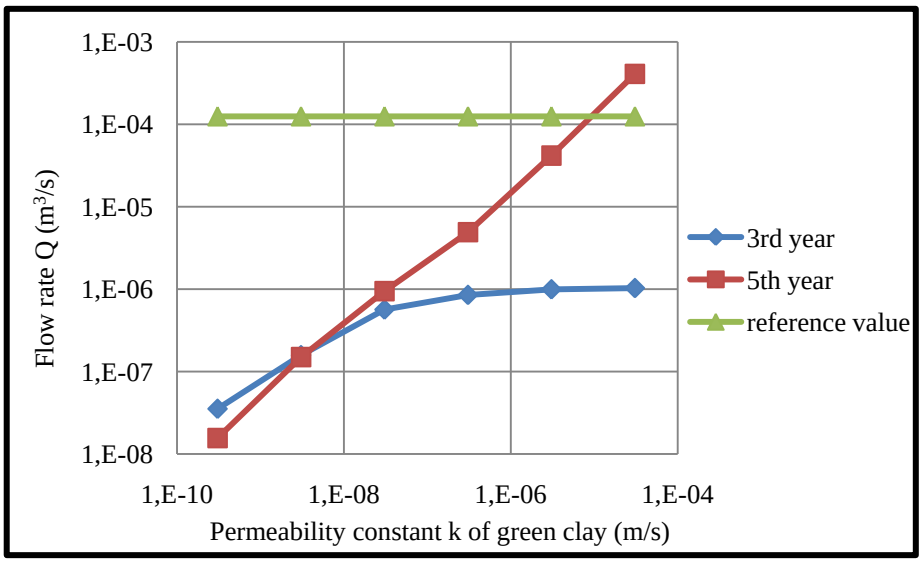

Figure 6.5 Green clay permeability sensitivity graphs according to the C-C' section 3rd year and 5th year pit plan

It is found out that after a bottom clay permeability value of 10^{-5} m/sec flooding threshold value or reference value is exceeded. For values lower than this value, such as 10^{-6} m/sec flow rate was ten times less (an order of magnitude less) than the accepted flooding threshold value. For clay type soil materials permeability values never go down to these levels. These levels are generally observed for sandy or silty formations. Clay deposit at the bottom of the pit is highly consolidated. Therefore, permeability value of this clay is not expected to go lower than 10^{-10} m/sec, or even if the lowest laboratory value found is considered, it will be around 10^{-8} m/sec levels.

In summary, permeability coefficient of bottom green clay was varied in the range between $3.07x10^{-5}$ – $3.07x10^{-10}$ m/sec in cross-sections A-A', B-B', C-C' considering 3rd and 5th year pit geometries projected in plans. According to the analyses conducted, in the models prepared for cross sections A-A', B-B' and C-C' for the end of 5^{th} year, flooding threshold value was exceeded in case permeability coefficient was more than $3.07x10^{-5}$ m/sec. However, this value is not common for a soil material that contains clay. As a result of these analyses, it is predicted that there is no risk of massive water overflow from the karstic confined aquifer to the projected pit bottom.

6.2 Variability in Bottom Green Clay Thicknesses

Risk analyses for flooding possibilities were carried out considering the uncertainities in results of geotechnical investigations for the green bottom clay thickness. Following these analyses, first a graph of flow rate vs. green clay thickness was generated, and shown in Figure 6.6. For the flow modelling here permeability of the bottom clay was taken to be $3.071x10^{-8}$ m/sec as found in soil mechanics tests.

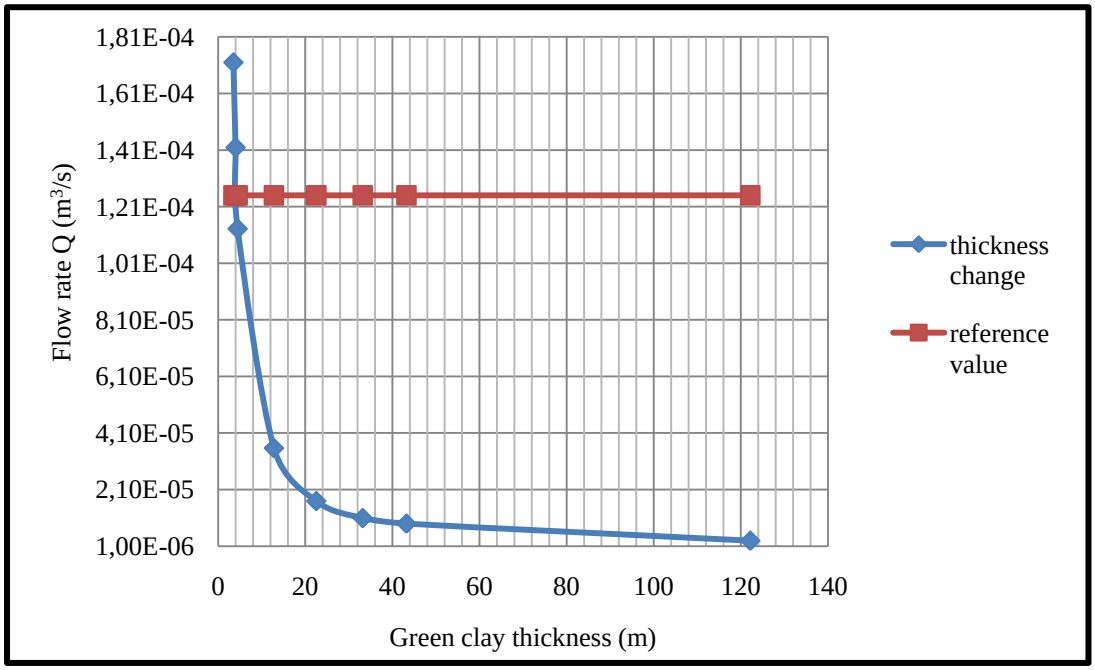

Figure 6.6 Green bottom clay thickness change sensitivity analysis

According to Figure 6.6 it is concluded that when green clay thickness is less than 20 m, there is a sharp increase in flow rate from the confined aquifer to the projected pit bottom. If the thickness is less than 5 m flow rate value will be greater than the flooding threshold value ($1.25x10^{-4}$ m^3/sec) which can generate negative results.

Results of these analyses suggested that the green clay (clay layer under the coal layer) acts as a barrier to block up water flow. The sensitivity studies were carried out by varying the thickness of the clay barrier. It is found that unless clay thickness takes values lower than 20 m levels; there is no risk of flooding from the karstic aquifer to the projected pit bottom. According to 5^{th} year plans, flow rate from confined aquifer to the pit bottom abruptly increases as clay layer thickness decreases to 5 m levels and flooding becomes highly possible. The aim of these thickness variation efforts was to check the limits of the software used in groundwater flow modeling for verification purposes. It was concluded that models produced expected water flooding results as the clay layer gets thinner and thinner.

In the point of a possible flooding case by a confined aquifer, it is seen that for the 5^{th} year plan, green clay thickness of 120 m has no negative influence on mining activities. For a bottom clay thickness about 120 m, water inflow rate is $2.9x10^{-6}$ m^3/s, so the reference value of $1.25\ x10^{-4}$ m^3/s is not reached. In case, clay layer thickness is reduced by 50%, this value becomes $8.6\ x10^{-6}$ m^3/s. It is clearly seen in Figure 6.6 that critical bottom clay thickness is approximately 20 m. In fact, this thickness should reach 3-5 m in order to cause a water overflow to the pit bottom as a result of the analyses. These values are calculated as $1.13x10^{-4}$ m^3/s for 4 m bottom clay thickness and $1.72\ x10^{-4}$ m^3/s for 3.5 m bottom clay thickness. When bottom clay layer thickness at the pit bottom becomes less than 20 m, risk of flooding starts.

Since the important issue is the advancement of stripping excavation and deepening of mine towards pit bottom and the confined aquifer, and thus increase in depth H of the pit and slope heights, results were plotted in a normalized way against flow rate by considering a variable which is bottom clay layer thickness/pit depth or slope height (t/H). The values listed in Table 6.5 were used to produce the plot in Figure 6.7.

Table 6.5 Flow rate values vs. t/H ratio

Green clay thickness t (m)	Flow rate Q (m^3/s)	Slope height H (m)	t/H
3.50	$1.72x10^{-04}$	115.53	0.0303
4.00	$1.42x10^{-04}$	115.53	0.0346
4.47	$1.13x10^{-04}$	115.53	0.0387
12.80	$3.56x10^{-05}$	115.53	0.1108
22.53	$1.69x10^{-05}$	115.53	0.1950
33.19	$1.09x10^{-05}$	115.53	0.2873
43.22	$8.95x10^{-06}$	115.53	0.3741
122.19	$2.90x10^{-06}$	115.53	1.0577

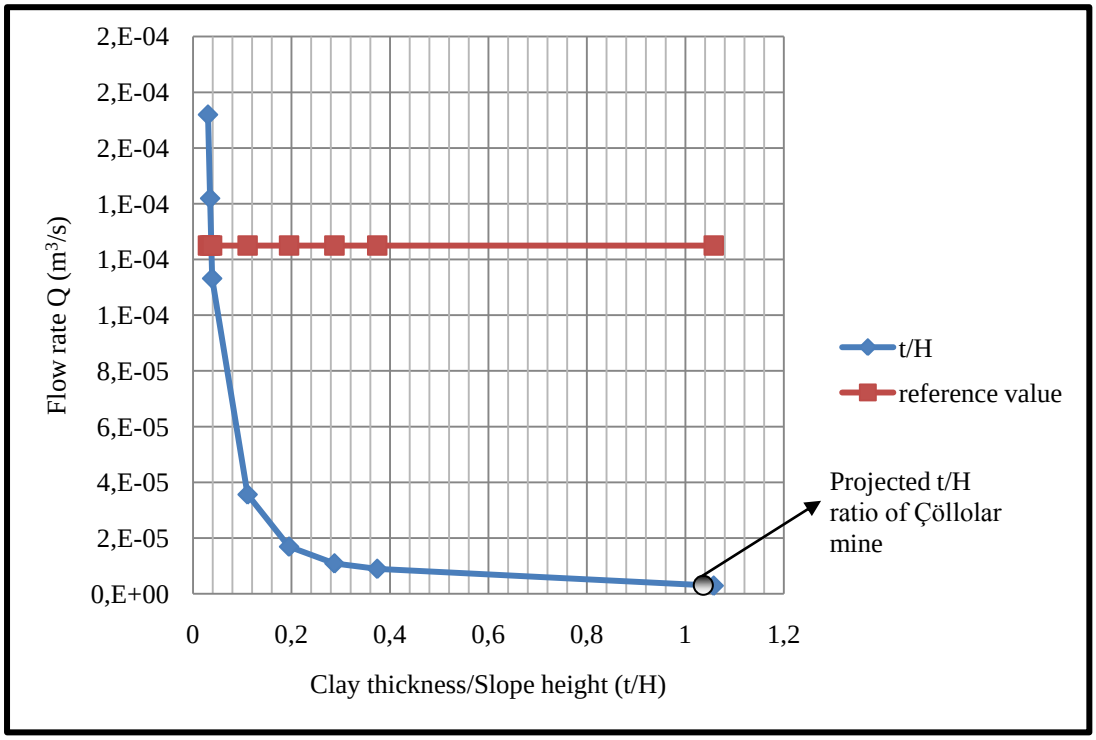

Figure 6.7 Sensitivity analysis graph of flow rate vs. t/H ratio

This graph shows that as the mine or excavation depth and thus slope height increases and the ratio t/H reaches around 0.2 risk of flooding increases. This is due to the depth of the overburden material removed which was covering the bottom clay before the excavation. When this cover is removed there will be a relaxation in bottom clay. Amount of this relaxation will be proportional to the depth H of the cover removed. The higher the pit depth the more relaxation to which bottom clay is subjected and the higher possibility of cracking in the bottom clay layer. As the mine or excavation depth becomes about 5 times the bottom clay layer thickness (t/H=0.2) tendency of the flow rate towards the flooding reference value starts. However, according to the projected pit depth which will be around 115 m, t/H for this mine will stay around 1.07 and no flooding is expected to occur due to overburden removal and load relaxation. Phase^2 model geometries related to this are given in Appendix C.

In Figure 6.8 a plot of flow versus bottom clay thickness is presented for different bottom clay layer permeability constants. Data related with this figure are listed in Appendix C. For the projected pit depth and bottom clay layer thickness at the end of the 5th year, flooding can occur if the bottom clay layer permeability exceeds an order of magnitude of 10^{-5} m/s as found before.

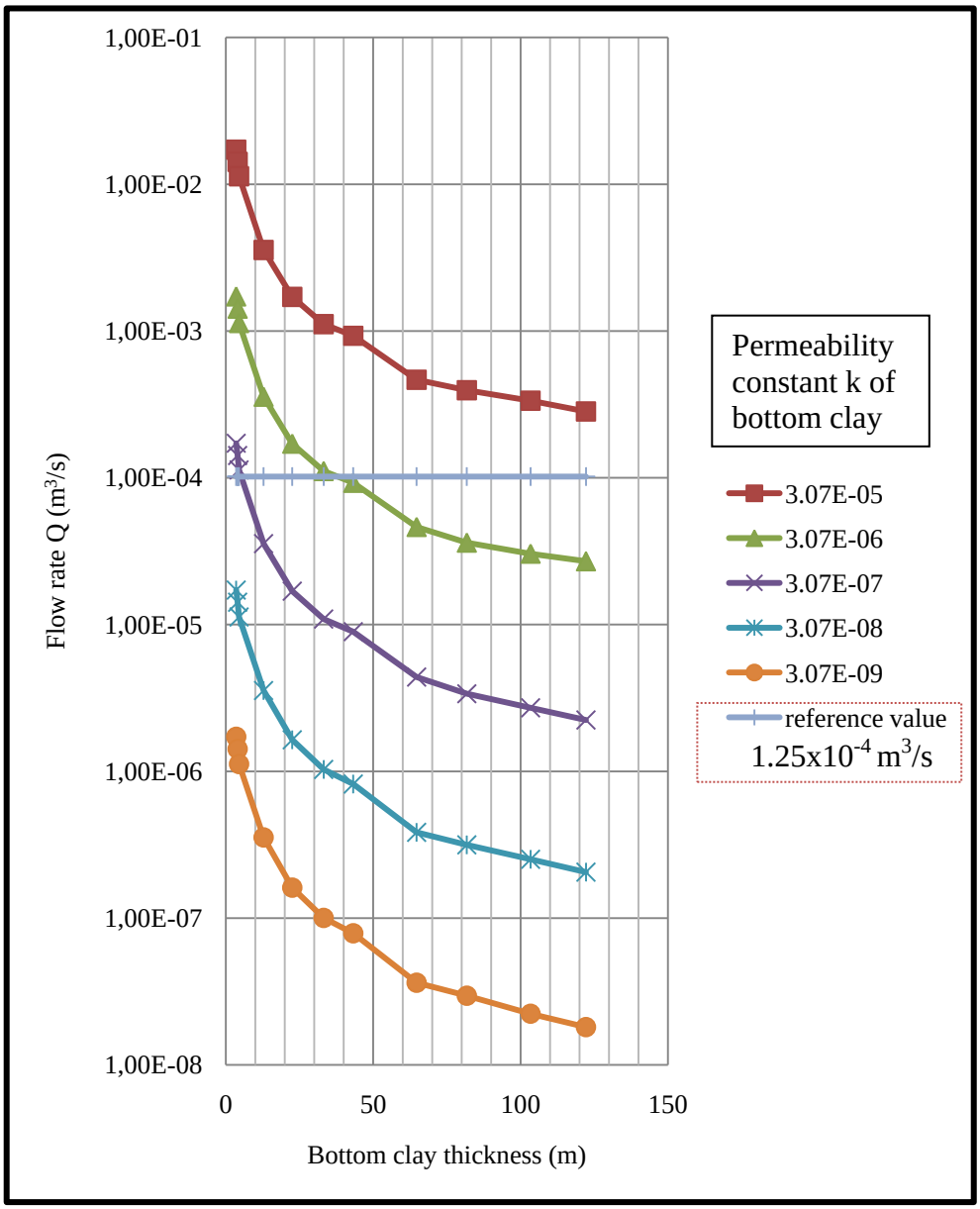

Figure 6.8 Flow rate values for variable permeability constants and thicknesses of bottom green clay

As seen in Figure 6.8 flow rate Q is affected by both clay layer permeability k and thickness. To generalize the results and estimate Q for different impermeable clay layer thickness and different clay permeabilities a 3-D plot is generated by TableCurve 3D software (Figure 6.9).

TableCurve 3D is the first and only program that combines a powerful surface fitter with the ability to find the ideal equation to describe three dimensional empirical data. TableCurve 3D was acquired by Systat Software Inc. from the US-based scientific software development company, AISN Software Inc. These tools together form a unique suite of products for automated data fitting of 2-D, 3-D and peak data (www.sigmaplot.com, last visited on 31.11.2009).

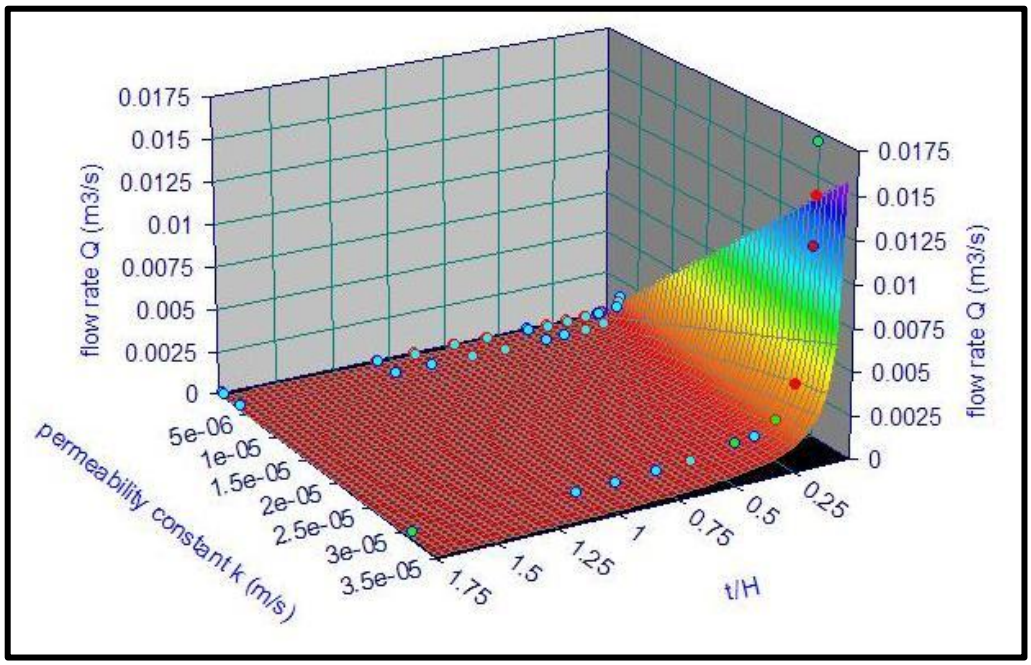

Figure 6.9 Flow rate values for variable permeability constants and thicknesses of bottom green clay in 3-D plot

Figure 6.9 shows that flow rate increases with decreasing clay layer thickness, increasing pit depth or slope height and increasing permeability. An equation was

fit to the surface in the figure with r^2=0.999 correlation. According to this graph Q in m^3/s can be estimated as:

$$lnQ = 2.05 - 1.22 \ln\left(\frac{t}{H}\right) + \ln(k) \tag{6.1}$$

or

$$Q = e^{2.05 - 1.22 \ln\left(\frac{t}{H}\right) + \ln(k)} \tag{6.2}$$

This expression (Equations 6.1 and 6.2) can be used to estimate flooding possibilities around a surface excavation due to the presence of a karstic aquifer and a clay layer with varying permeability k between the ground surface and limestone bedrock containing the aquifer. Excavation depth or slope height (H) is implemented into the expression with the term t/H where t is the thickness of the clay layer.

Sometimes it might be necessary to estimate the thickness of the confining clay layer which becomes risky for flooding. In this case, assuming that a flooding threshold value was set and permeability value of clay layer was determined equation above can be used in a different way as follows. This way a critical thickness for the confining layer can be determined.

$$\ln\left(\frac{t}{H}\right) = \frac{2.05 + \ln(k) - lnQ_c}{1.22} \quad \text{or} \tag{6.3}$$

$$\frac{t}{H} = e^{\frac{2.05 + \ln(k) - lnQ_c}{1.22}} \tag{6.4}$$

In equations 6.3 and 6.4, Q_c is critical flooding flow rate value or reference value.

Another way of treating the results is to generate plots of normalized variable $i = \frac{Q}{Ak}$ vs. normalized clay layer thickness ($\frac{t}{H}$). This plot can be seen in Figure 6.10.

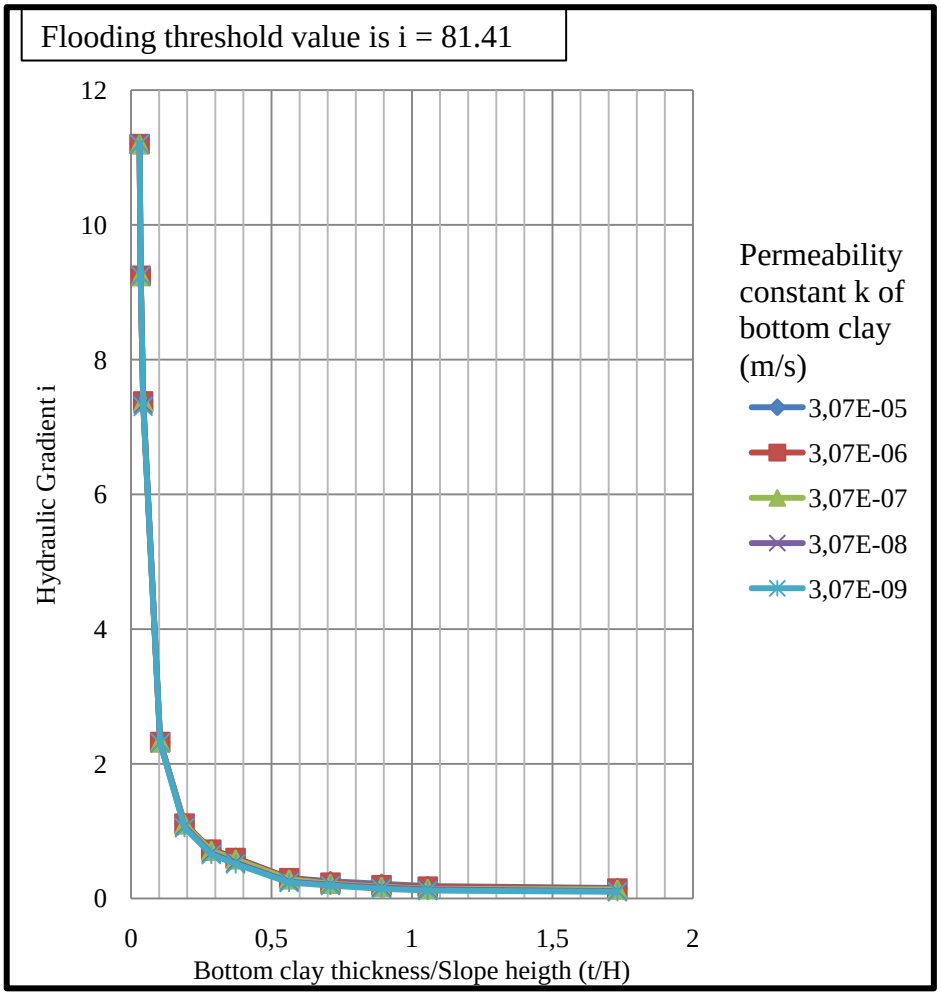

Figure 6.10 Hydraulic gradient vs. normalized clay layer thickness (t/H) plot

Hydraulic gradient i is calculated by Darcy's Law where flow rate Q and permeability constant k are derived from the graph above. Area of discharge section A is taken as 50 m^2 in these computations.

$$i_c = \frac{Q}{Ak} \tag{6.5}$$

To calculate i_c critical threshold gradient or reference gradient discharge area A is used as 50 m^2 as indicated before, Q was taken to be equal to the reference value $Q_c = 1.25 \times 10^{-4}$ m^3/s, and k permeability of clay was $k = 3.07 \times 10^{-8}$ m/s which was the laboratory value for this unit.

Figure 6.10 show that hydraulic gradient increases abruptly after a t/H ratio of 0.2. After this point hydraulic gradient moves very fast towards the flooding threshold value. To see the detailed behavior of hydraulic gradient for different clay layer permeabilities a detailed view is produced around the critical turning point of the plot, (Figure 6.11).

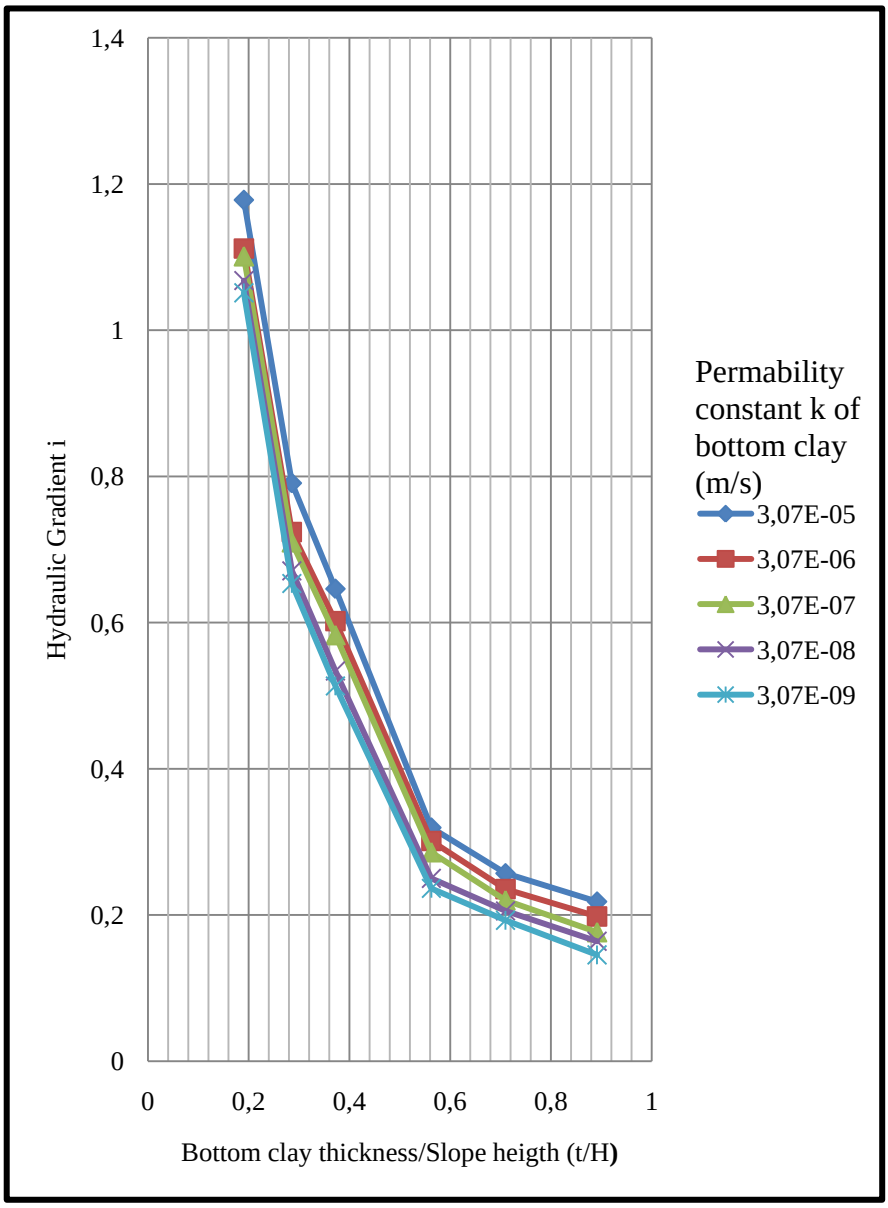

Figure 6.11 Detailed view of hydraulic gradient (i) vs. clay layer thickness/excavation depth (t/H) plot

Hydraulic gradient slightly increases with increasing permeability and decreases with t/H ratio. However, effect of permeability on hydraulic gradient is not so strong. To see this condition more clearly again a 3-D plot of hydraulic gradient i, permeability constant k, and t/H ratio was generated with TableCurve3D software as seen in Figure 6.12. Again an equation was fit.

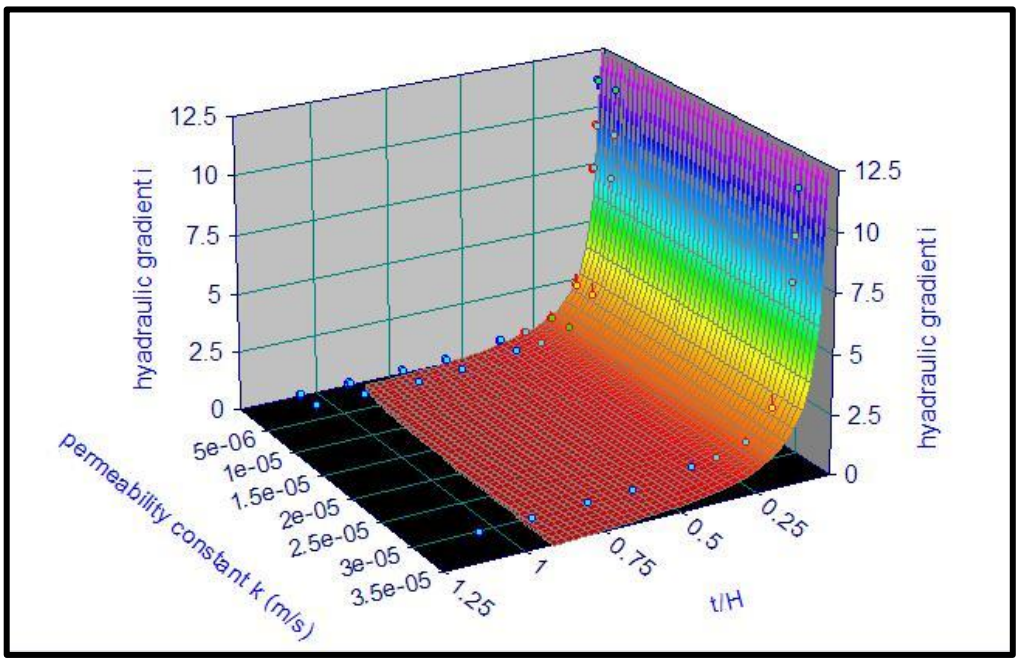

Figure 6.12 Hydraulic gradient values for variable permeability constants and thicknesses of bottom green clay in 3-D view

Fitting with r^2= 0.996 a typical equation was found as follows.

$$i = -029 + \frac{0.34}{(\frac{t}{H})} + 0.007lnk \qquad (6.6)$$

In the surface fit operation permeability variable constant is very low (0.007) as seen in this equation. This shows that its effect on the hydraulic gradient is not significant. This equation can be used to find the hydraulic gradient value for a

certain clay layer thickness t and pit depth. Then this value can be compared to the flooding threshold hydraulic gradient value set specifically for that site.

This equation can be modified to produce critical clay layer thickness/slope height or pit depth (t/H) relationship as follows:

$$\frac{t}{H} = \frac{0.34}{i+0.29-0.007lnk} \tag{6.7}$$

If a flooding critical hydraulic gradient value $i = i_c$ is excepted corresponding to the reference flow rate value $Q = Q_c$ for a particular region, critical clay layer thickness or critical excavation depth or slope height can be found from the equations above.

Data related to these plots are listed in Appendix D.

6.3 Change in Aquifer Pressure

As mentioned before groundwater level in TK-3 boreholes is in 1156.45 m altitude so aquifer total pressure head is taken as 1156 m. However, 5th year pit geometries by changing the aquifer pressure between 1050 MPa and 1450 MPa a sensitivity analysis was conducted. In this analysis clay thickness was used as 120 m which was determined from the geotechnical and geophysical work in the pit site and clay layer permeability was taken to be 3.071×10^{-8} m/sec as determined from the laboratory work. The graph on which aquifer pressure used in this work is marked is shown in Figure 6.13.

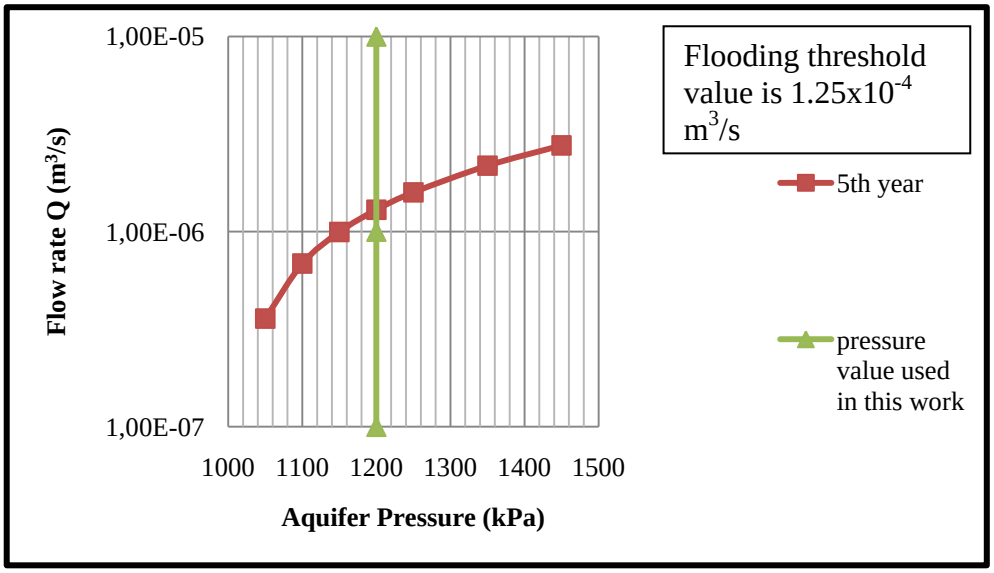

Figure 6.13 Aquifer pressure sensitivity analysis (5th year pit plan)

According to this figure it is concluded that if aquifer pressure is rising then the flow rate is also rising. However, as it is observed from the graph, variation in aquifer pressure does not force the flow rate to approach to the threshold value which proves the fact that there is no risk of flooding considering the uncertainties associated with the aquifer water pressure.

CHAPTER 7

FINITE ELEMENT ANALYSIS OF THE MECHANICAL EFFECTS OF CONFINED AQUIFER

Possible mechanical effects of the confined aquifer include instabilities of permanent slope failure and fracturing of bottom clay layer leading to permeability increases. A significant effect may be observed on the stability of permanent slope as the bottom clay layer thickness decreases and its permeability increases. In these cases, displacements on the slope and at the surface of pit bottom may be excessive in the orders of magnitudes of meters indicating possible failure states. Another check for the mechanical effects of aquifer on the stability of permanent slope can be in terms of slope safety factors generated by the Phase^2 software for different overall permanent slope angles and bottom clay thicknesses.

Permanent slope at the southwestern part and location where the coal haulage systems and belt conveyors pass through are of major importance so that risk caused by the aquifer should be investigated in detail. Mechanical effects of an aquifer pressure on permanent slope and pit bottom are analyzed by using A-A' section for 5th year pit geometry. Permanent slope in A-A' section is very important because of the conveyors and related stations that will be settled on this slope for the life of the mine. There is a limestone bedrock portion with a considerable thickness and a bottom clay layer above it that the water under pressure must yield and penetrate through this layer first before reaching the pit bottom.

According to TK-3 borehole data, a thickness of 1 m limestone rock mass was drilled and after that water rush through the borehole was observed. Then, 1.2 MPa stress is possibly not directly applied onto the bottom clay boundary. There is a considerable reduction of the stress transmitted onto the clay layer due to the

presence of a limestone layer first before the contact of aquifer water with bottom clay bound. Nonetheless, to be on the safe side, in the numerical models aquifer pressure is directly applied onto the bottom boundary of the clay layer.

1.2 MPa aquifer water pressure was applied on the overall bottom boundary of the bottom clay to study mechanical effects of the aquifer for the worst case scenarios. Thereafter, more realistic cases were investigated where local confined aquifers of different sizes and positions along the bottom clay boundary with 1.2 MPa pressure were simulated. In order to point out the impact of 1.2 MPa pressure on models in a more realistic way, application zone was selected as boundary between bottom clay and limestone.

The most critical cross-section A-A' derived from the 5^{th} year pit plan in permanent slope region was the basis of analyses and displacements of critical points are presented and checked in the graphs. Slope stability was first evaluated by studying total displacements of critical points on the surfaces of slopes and pit bottom.

7.1 Current Situation of the Mine

According to Park Teknik data groundwater level is assumed to be lowered to 50 m by dewatering operations and parameters used were left unchanged. Permeability constant of green clay is used as laboratory value 3.071×10^{-8} m^3/s, thickness of green clay is around 120 m, mechanical parameters of other formations is same as listed in Table 5.1 and Table 6.1. Groundwater level in the pit bottom is assumed right at the pit bottom surface.

7.2 Aquifer Water Pressure Along The Whole Upper Contact Boundary

Model geometries, points for displacement monitoring and change in displacement as graphs are represented for each scenario. The case where no confined aquifer pressure was present is studied with a model in order to represent the extreme case with no dewatering operation. A-A' section 5th year pit geometry is given in figure 7.1 to summarize the state where 1.2 MPa pressure is not applied (no confined aquifer) on the boundary between bottom clay and limestone.

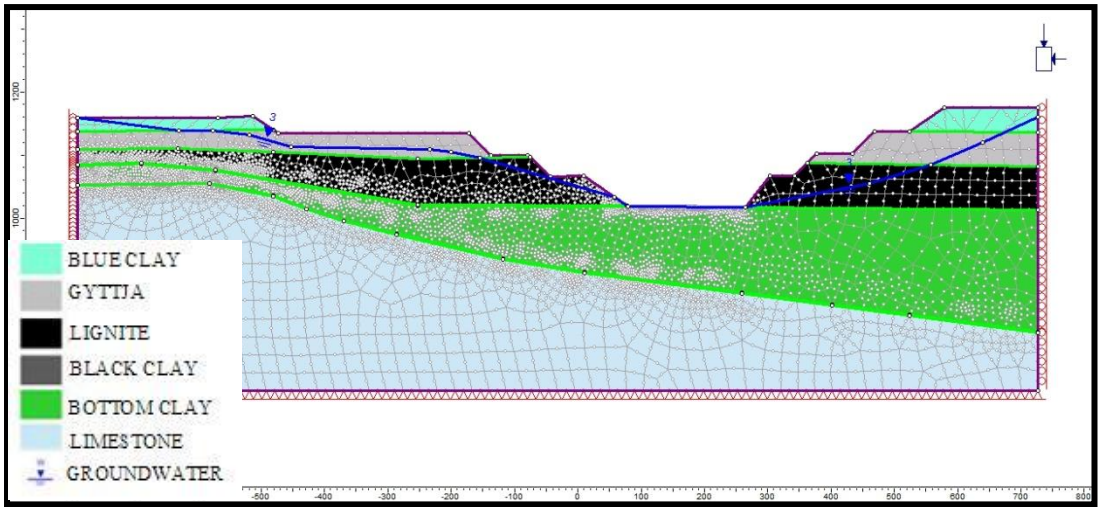

Figure 7.1 A-A' section of 5th year open pit plan without 1.2 MPa aquifer water pressure

A-A' 5th year pit geometry in figure 7.2 represents the state where 1.2 MPa pressure is applied all along to the bottom clay – limestone boundary. As stated before, a transition zone of thickness 1 m is used in between bottom clay boundary and limestone bedrock and aquifer to the transition zone element nodes for a stable not sudden flow transition from an aquifer condition to relatively impermeable clay layer. To be able to see the real effect of the aquifer pressure, 1.2 MPa pressure is applied along the whole green clay-limestone boundary. Transition zone and pressure application area can be seen in detail from the Figure 7.3.

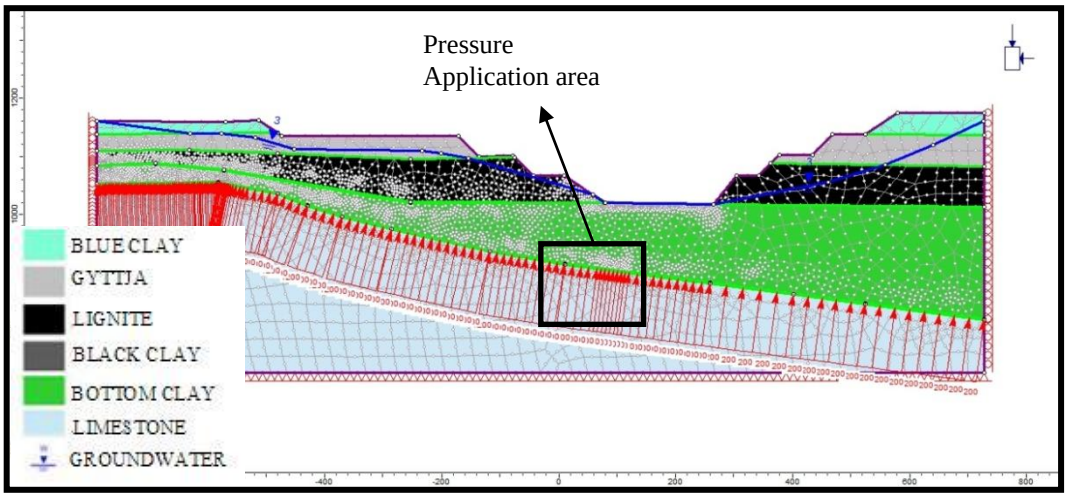

Figure 7.2 Model geometry with an aquifer water pressure of 1.2 MPa pressure applied all along the limestone-bottom clay boundary

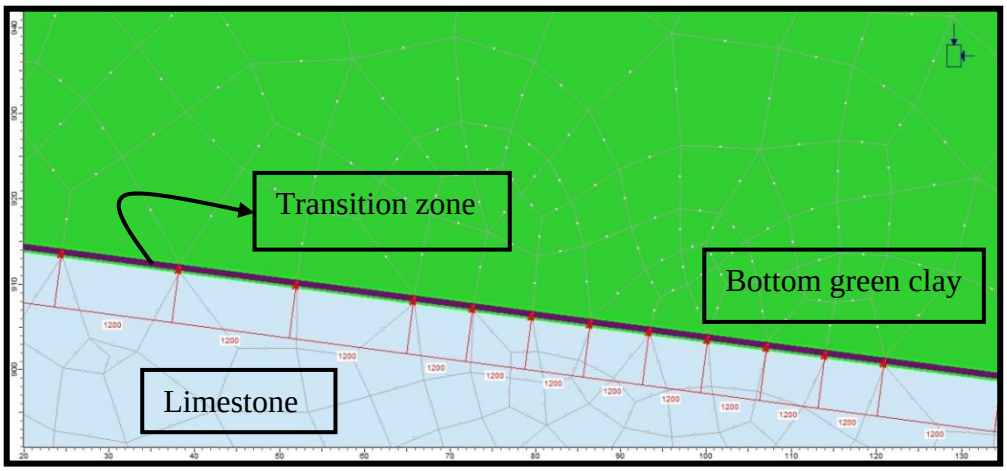

Figure 7.3 1.2 MPa aquifer pressure application nodes in detail

A-A' section 5th year pit plan (without 1.2 MPa) with displacement monitoring point and displacement contours is shown in Figure 7.4.

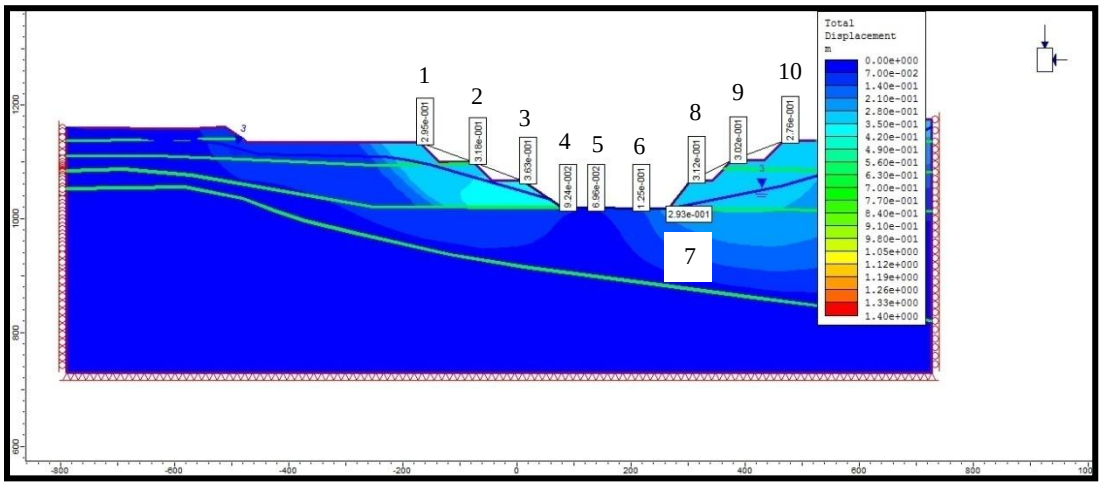

Figure 7.4 Displacements of monitoring points and displacement contours of the model geometry without aquifer pressure

The same section but this time with an aquifer pressure of 1.2 MPa is shown in Figure 7.5.

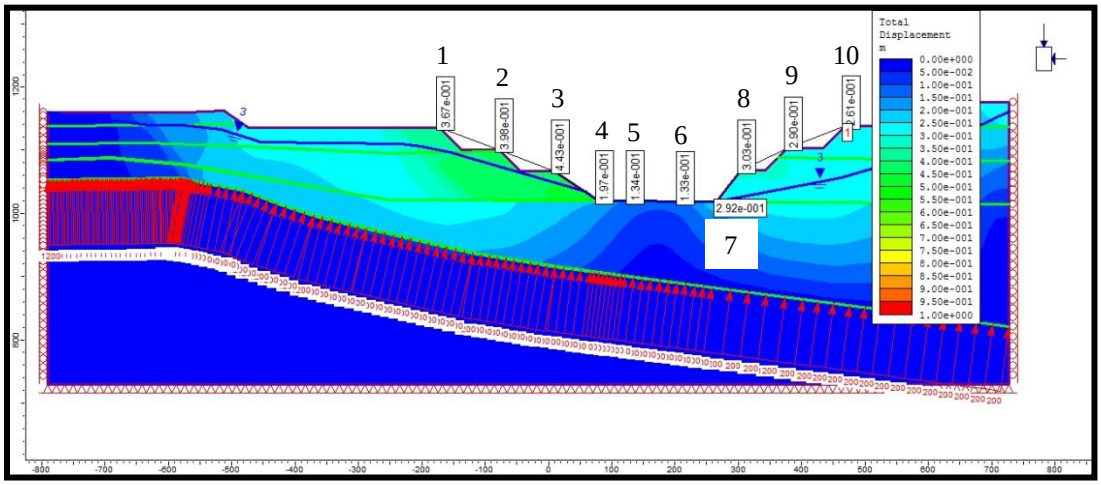

Figure 7.5 Displacements of monitoring points and displacement contours of the model geometry with aquifer pressure

Effect of 1.2 MPa confined aquifer pressure is represented by the graph prepared for two different displacement monitoring cases taken from the same monitoring points in Figure 7.6.

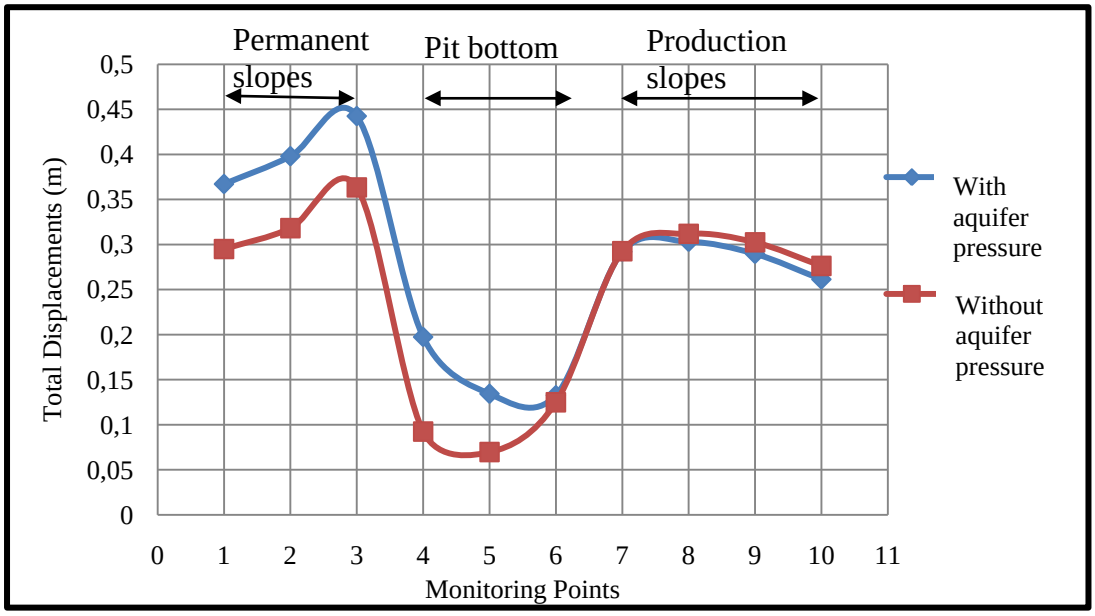

Figure 7.6 Total displacement graph of monitoring points

Aquifer water pressure applied on bottom green clay causes a certain amount of increase in displacements on the slope faces and pit bottom. Impact of the confined aquifer on the model is reflected as a change in displacement in “cm” ranges, so that it is not expected to affect slope stability significantly. As a landslide that will affect the slope is only possible in case displacements are in “meters” range at critical points on slope such as points 2 and 3 on the slope face.

Points 4, 5 and 6 are assigned to monitor the effects of confined aquifer on the bottom clay layer stability. As it is seen in figure, swelling of bottom clay is observed in the range of 8-10 cm due to the confined aquifer pressure. These displacements are again low as the slope displacements so that no risk of failure of bottom clay is expected to occur with removal of the overburden material above it.

7.3 Smaller Local Aquifers in Upper Contact Boundary

1.2 MPa aquifer water pressure is applied all along the karstic limestone to the transition layer attached to the clay boundary to simulate the worst case scenarios.

Such a case is not expected in practice. Therefore, 1.2 MPa aquifer water pressure is applied on bottom green clay locally with smaller finite dimensions aquifers with different positions. Local aquifers where only along some finite distances water exerts pressure on the bottom boundary of transition layer and bottom green clay zone are more realistic in practice. Karstic aquifer water usually penetrates into caves, joints, fractures and similar paths in the limestone bedrock and this applies pressure to the relatively impermeable confining clay layers. These aquifer combinations with different dimensions and locations along the limestone-bottom clay layer are named as Local Aquifer-A, Local Aquifer-B and Local Aquifer-C respectively. Again displacements of monitoring points were plotted and analyzed in terms of order of magnitudes against any potential instability of slopes and pit bottom.

7.3.1 Local Aquifer-A

In the Local Aquifer-A model the dimension of aquifer is decreased and aquifer is positioned to a specific location which is forcing the bottom clay against the permanent slope. Local aquifer dimension is 297 m in length and shown in figure 7.7

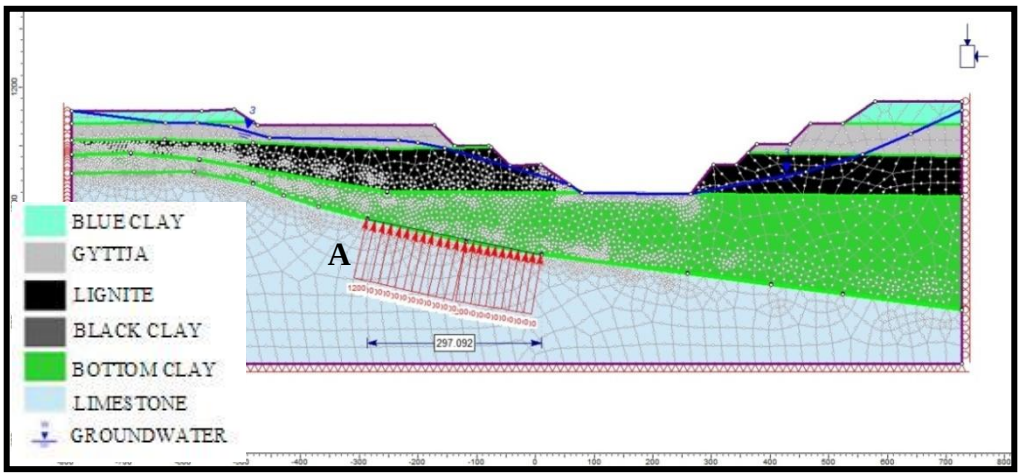

Figure 7.7 Dimension and position of Local Aquifer-A

To make comparisons total displacement values of the permanent slope and pit bottom surfaces due to the Local Aquifer-A are compared to the case where no aquifer water pressure is applied to the transition zone-bottom clay boundary. This is represented in Figure 7.8.

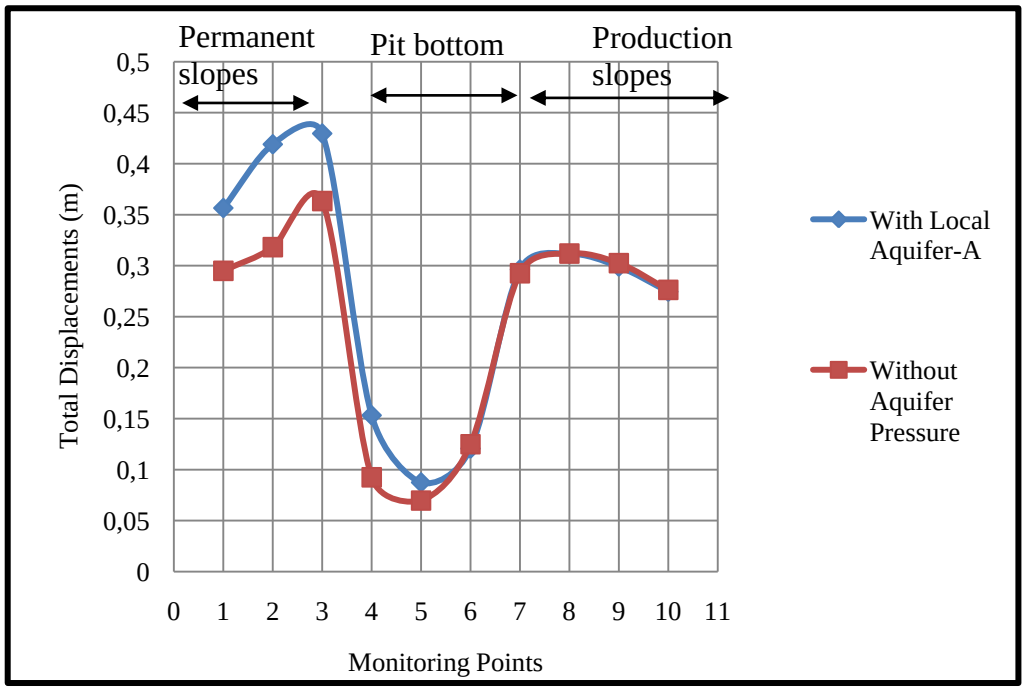

Figure 7.8 Comparison graph of total displacement values with and without Local Aquifer-A

7.3.2 Local Aquifer- B

In the local aquifer-B model case the dimension of the aquifer is decreased to 239 m and it is positioned under the slope front and pit bottom. The model is shown in Figure 7.9.

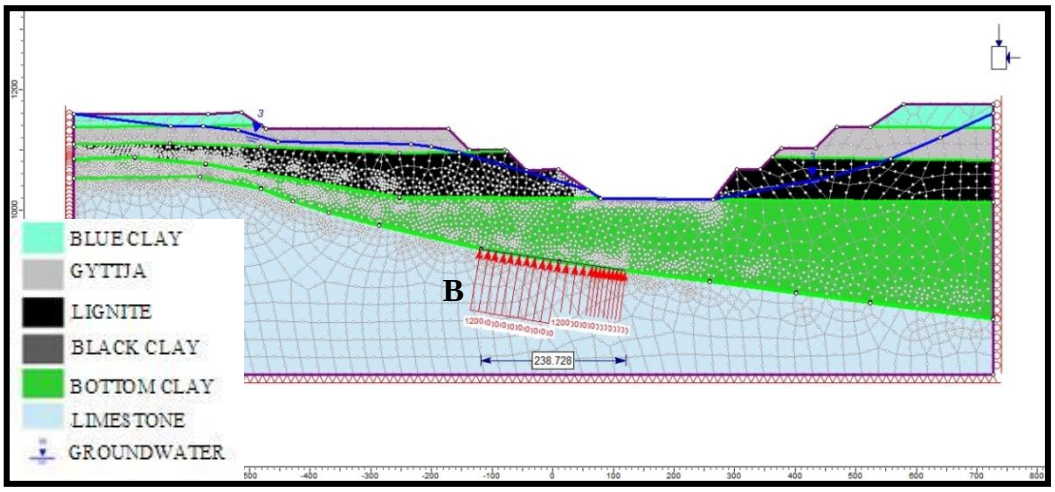

Figure 7.9 Dimension and position of Local Aquifer-B

Total displacements comparison graph is shown in figure 7.10 for with and without aquifer cases.

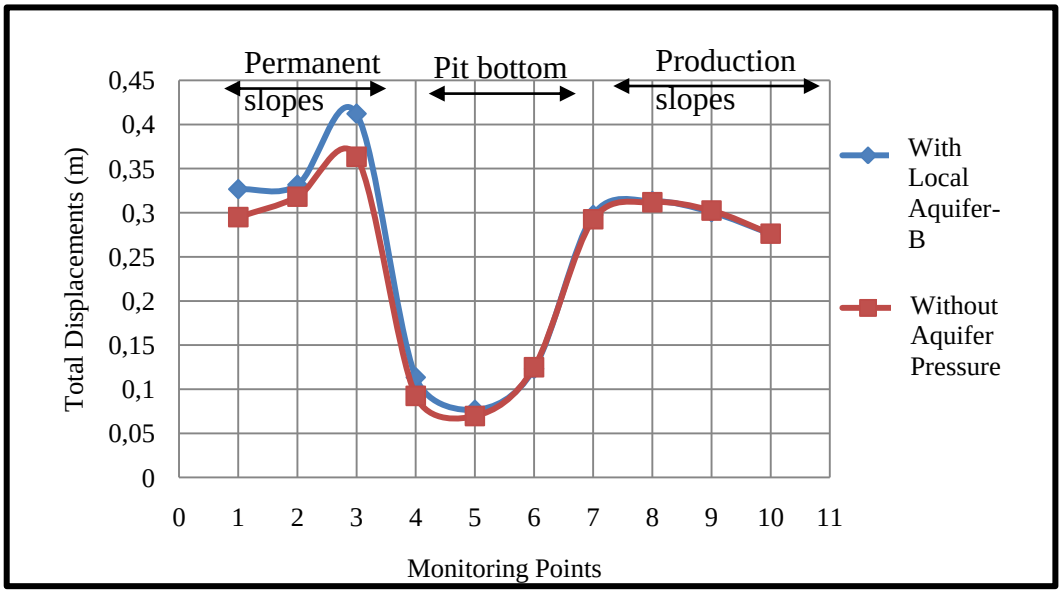

Figure 7.10 Comparison graph of total displacement values with and without Local Aquifer-B

7.2.3 Local Aquifer-C

For the last local aquifer model pressure application region length is around 108 m and this region by being moved more towards the pit bottom is positioned directly under the intersection of slope front and pit bottom. Similar to all local aquifer models the aquifer water pressure is used as 1.2 MPa. The details related to the location and dimension of the Local Aquifer-C are shown in Figure 7.11. Total displacement values can be seen from the comparison graph in Figure 7.12.

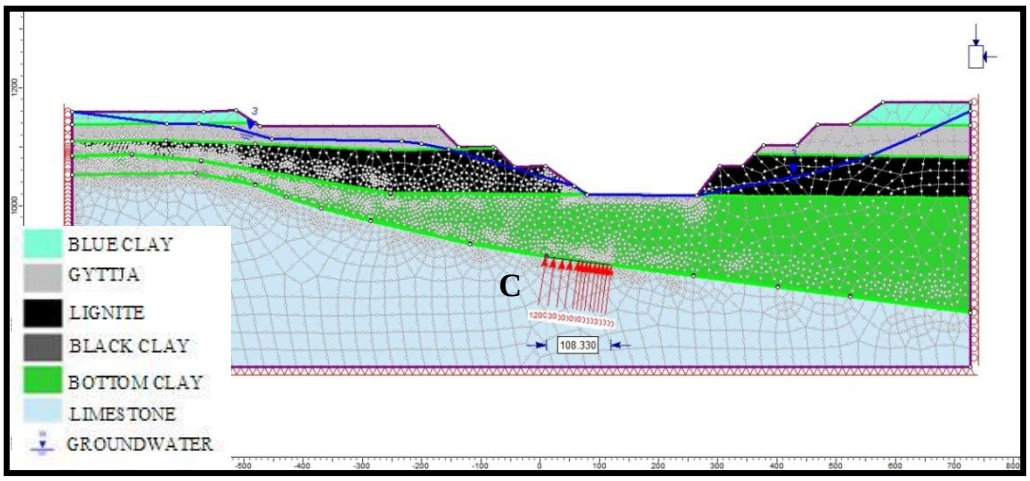

Figure 7.11 Dimension and position of Local Aquifer-C

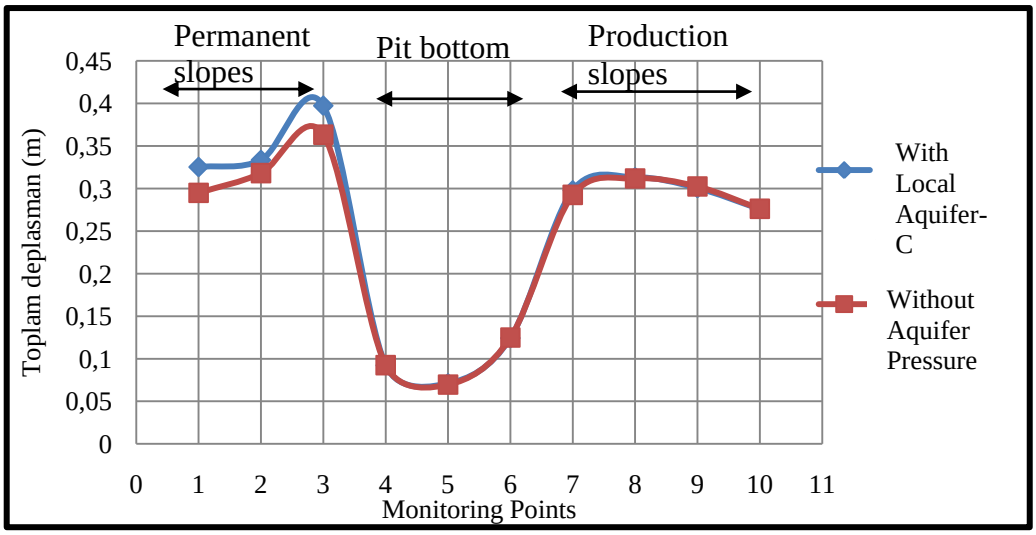

Figure 7.12 Comparison graph of total displacement values with and without Local Aquifer-C

7.4 Effect of Different Aquifer Models on Stabilities of Permanent Slope and Pit Bottom In Terms of Displacements

To make a general comparison the total displacement values of different aquifer cases for the monitoring point 5 for all five aquifer models are summarized graphically in Figure 7.13 below. Monitoring point 5 is located in the middle of the pit bottom. Aquifer model names are specified on the graph.

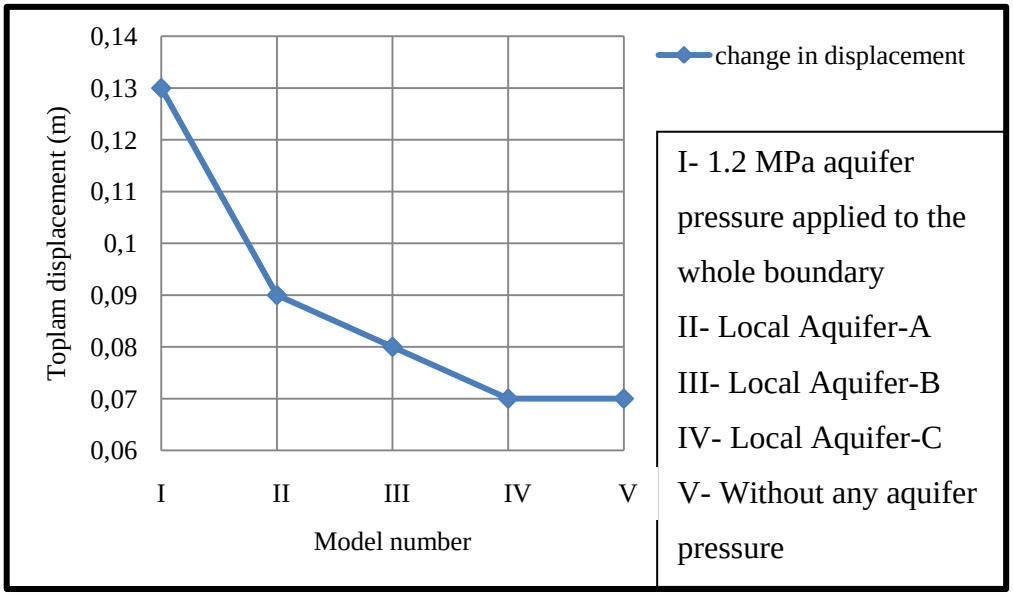

Figure 7.13 Total displacement data of monitoring points #5

From aquifer model I to V length of the aquifer pressure application area decreases. It is seen that if the length of aquifer decreases, the effect on the displacements decreases. The lowest displacement value is obtained from Model V which is the case without 1.2 MPa aquifer pressure. Also the displacement values are in orders of cm levels as before so these types of local aquifers does not have considerable negative effects on permanent slope and pit bottom.

7.5 Mechanical Effects of Changes in Green Clay Thickness

In this part mechanical and structural responses of the bottom clay and the slopes were taken into account and mechanical effects of the confined aquifer were reflected onto the slope and pit bottom deformation response models. Structural analysis involves two stages. Models started with an unexcavated state as seen on Figure 7.14. In the first stage the whole area is modeled without excavation and then in the second stage excavation was completed and coal was removed.

So that pit bottom was completely exposed to any flooding or structural instability situations. Then excavation of overburden and coal was completed and pit bottom and slopes were exposed to any possible structural instability due to the presence of 1.2 MPa aquifer pressure in the limestone bottom clay contact. The excavated model and monitoring points A, B and C are shown in Figure 7.15. Original geological cross section was used and a complete stress due to the aquifer water pressure 1.2 MPa is applied to the entire bottom clay lowest boundary. Bottom clay layer thicknesses were changed, and breakage of the bottom clay layer was investigated by checking the heaving kind of displacements.

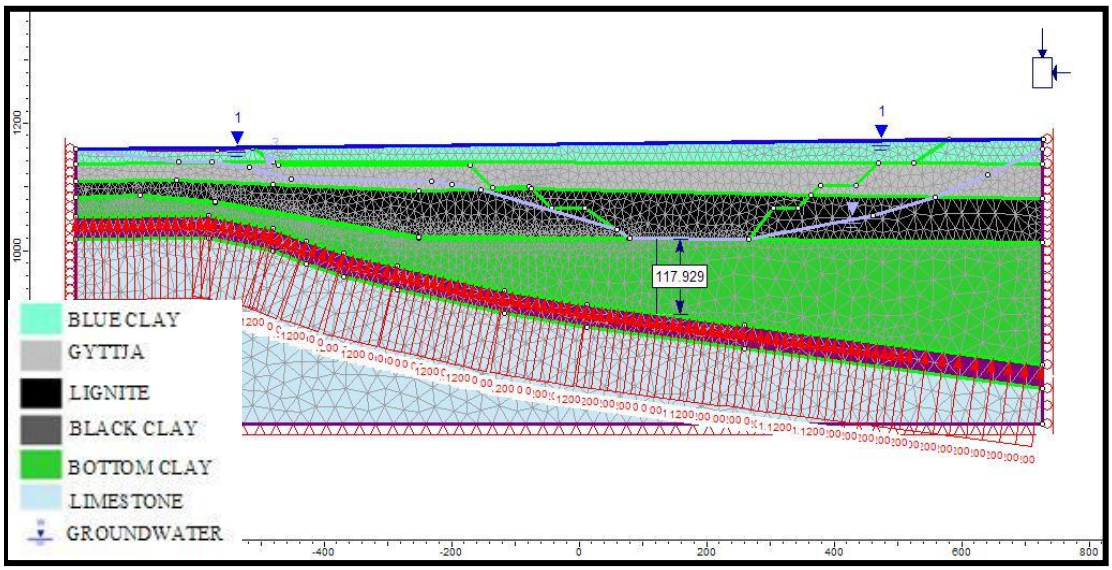

Figure 7.14 The unexcavated model of permanent and temporary pit slopes

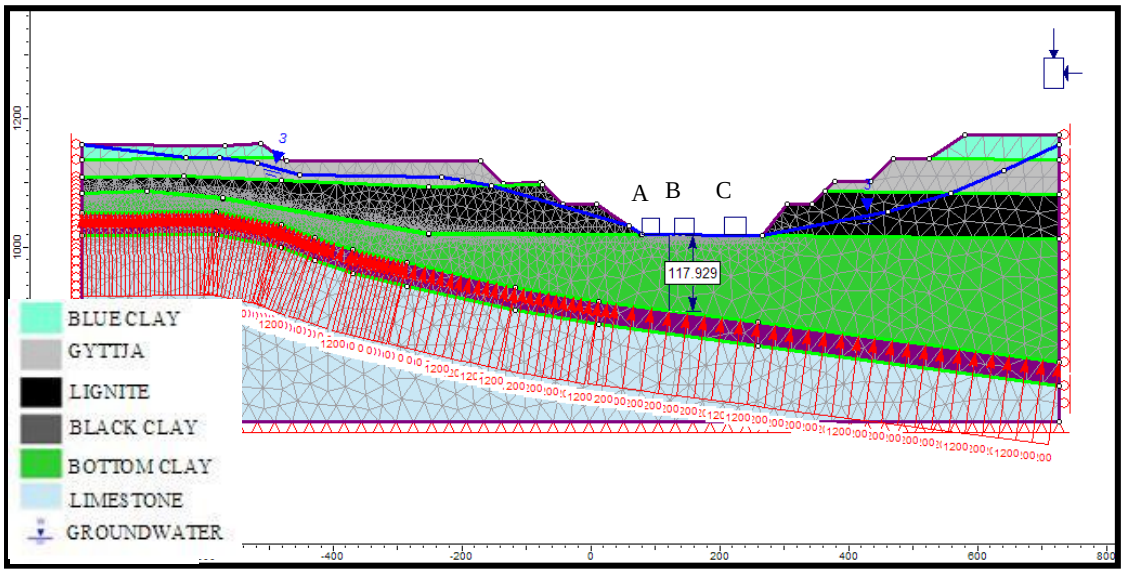

Figure 7.15 Excavated pit bottom with the locations of displacement monitoring points

Total displacement values of monitoring points A, B and C are shown in Figure 7.16.

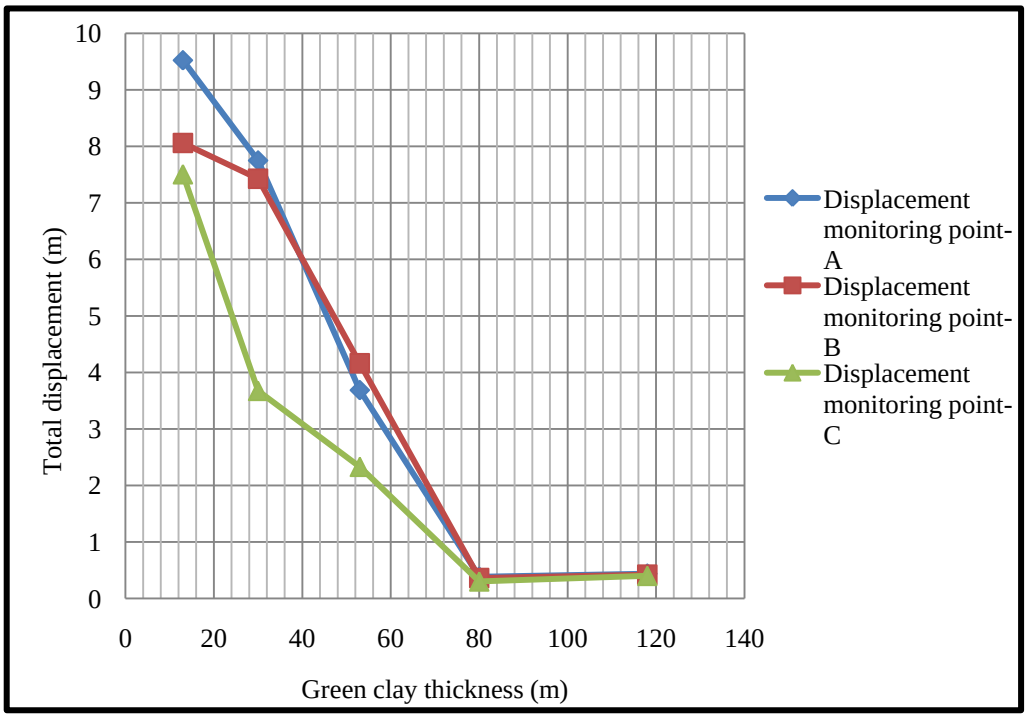

Figure 7.16 Green bottom clay thickness vs. total displacements graph

These displacements were in orders of magnitudes of centimeters up to bottom clay layer thicknesses of 70-75 m, shown in Figure 7.16. After these thickness levels such as the 50-60 m levels displacements suddenly increase to meter levels indicating that clay might crack and break leading to increased clay permeability that might result in pit bottom flooding.

Whether confined aquifer pressure leads the bottom clay layer to fail and crack with the current known thickness is investigated here. According to the technical information provided so far, the bottom clay layer is concluded to be on the safe side and its permeability is not affected in any case.

To complete the mechanical analyses related with the green clay thickness safety factors of the permanent slope should be checked. According to these analyses green clay thicknesses were lowered and factor of safety values of the permanent slope were determined. 25^{o} slope angle of the permanent slope as planned by the mine management was not changed in these analyses. In Table 7.1 the calculated factor of safety values are shown.

Table 7.1 Safety Factor values vs. Green clay thickness

Green clay thickness (m)	**Safety factor**
120	1.2
82	1.2
72	1.1
53	1.0

The safety factor vs. Green clay thickness graph can be seen in Figure 7.17.

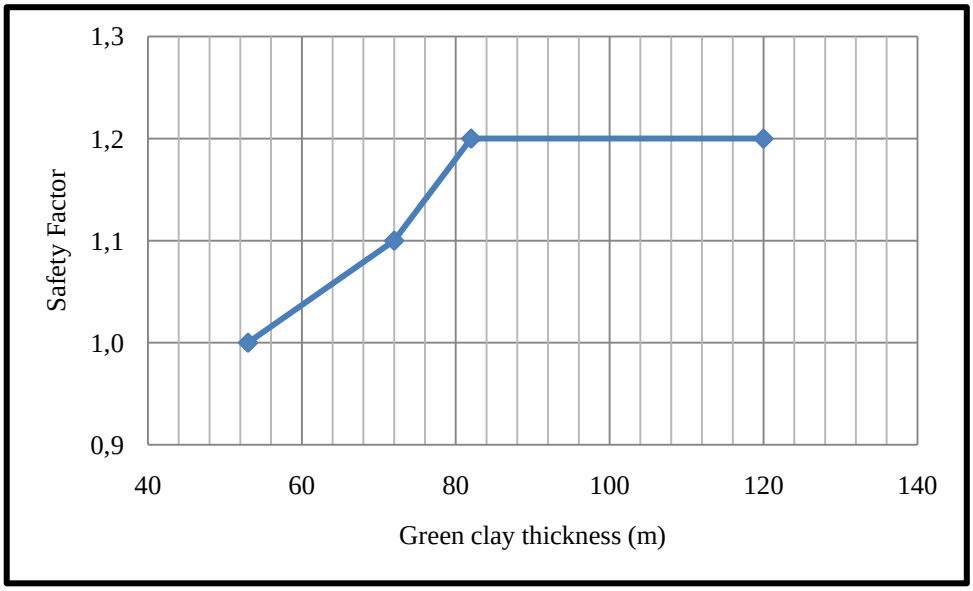

Figure 7.17 Safety Factor vs. Green clay thickness graph

As it is seen from the Figure 7.17 there is a risk of failure when the green clay thickness is less than 50-60 m. In general, the condition that factor of safety equals to one or greater is accepted as a safe condition. However, to be on the safe side safety factor should be tried to be kept over 1.1 for such critical slopes. Therefore, if bottom clay thickness becomes less than 50-60 m there might be stability risk for the permanent slope, however reported thickness of bottom clay formation is around 120 m here and there should not be any potential risks under the circumstances.

7.6 Determination of an Overall Slope Angle for the Permanent Slope

In order to determine a safe overall slope angle for the permanent slope of Elbistan-Çöllolar open cast mine new models were generated by changing the slope angles while keeping the clay layer thickness and permeability at 120 m and 3.071×10^{-8} m/s as determined before. In the new models the bench heights and widths were homogeneously adjusted as the slope angles were changed. Overall slope angles were changed and according to these new slope angles safety factors were

determined for the permanent slope. The Phase^2 outputs of new models are given in the Appendix E in detail. The results of these analyses are summarized in Table 7.2.

Table 7.2 Overall slope angle vs. Safety factor

Overall slope angle (^{o})	**Safety factor**
25	1.2
28	1.1
32	1.0
35	0.9

To express the results better the graph of overall slope angle vs. safety factor is shown in Figure 7.18.

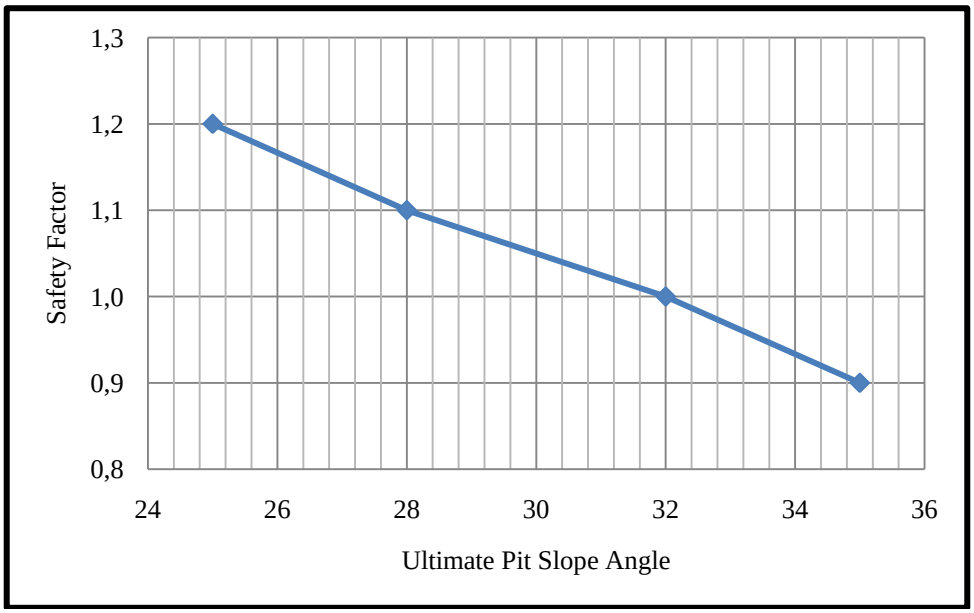

Figure 7.18 Overall slope angles vs. Safety factor graph

According to the current practice by the mine management the overall slope angle is 25^o and current factor of safety for the permanent slope is 1.2 bottom clay with its current thickness prevents any harmful effects of the confined aquifer on permanent slope. Up to 32^o the slope is in safe condition. However, when the overall slope angle is higher than 32^o, then there is a risk of failure. This 32^o value can be adopted for production slopes.

7.7 Solution Recommendations

For recommending some solution alternatives for handling confined aquifer problems following remarks from a various references are summarized below.

Karstic formation is a term defined for units originated from sink holes or hidden caves formed by dissolution. Transmissivity and permeability of dissolved limestone might be high and dewatering process is hard to achieve as water amount to be pumped out is great. Dewatering in karstic formations leads to increase in sink hole activity. Groundwater activity increases dissolution in rocks. Lowering of groundwater level (drainage of karstic aquifer) might lead to sinkhole formation by increased effective tension (Drumm et al., 2008).

In its natural equilibrium state, the hydraulic pressure of groundwater in the pore spaces of the aquifer and the aquitard supports some of the weight of the overlying sediments. When groundwater is removed from aquifers by excessive pumping, pore pressures in the aquifer drop and compression of the aquifer may occur. This compression may be partially recoverable if pressures rebound, but much of it is not. When the aquifer gets compressed it may cause land subsidence, a drop in the ground surface (Ford and Williams, 2007).

As a result pumping the water out of the aquifer is no recommended, since aquifer water pressure is not expected to cause any stability problems on the pit bottom and the permanent slope.

CHAPTER 8

CONCLUSIONS AND RECOMMENDATIONS

This study was aimed to assess the flooding possibilities and slope stability problems due to a confined aquifer in the Elbistan-Çöllolar open cast mine. As a conclusion, with current conditions of 25^{o} permanent slope angle and 120 m bottom clay thickness no serious problems are expected to occur in the mine. Affects of a confined aquifer on mining activities and slope stability were studied in this area and results are given as follows:

1. Based on the actual 5^{th} year pit geometry, bottom clay thickness is predicted to be approximately 120 m. Under the circumstances it is concluded that there is no need for preventive action for flooding possibility. Water flooding to pit bottom is likely to occur only if bottom clay (green clay) thickness is 20 m or less.

2. Analysis show that flow rate increases both with clay layer thickness and permeability. Hydraulic gradient slightly increases with increasing permeability and decreases with clay thickness/ excavation depth (t/H) ratio. However, effect of permeability on hydraulic gradient is not so strong.

3. Mechanical models were used to study case where confined aquifer pressure of (1.2 MPa) causes bottom clay to fail and cracks lead to increase in permeability. It is found that bottom clay layer strength is on the safe side and there is no possible crack formation in this layer, so that permeability of this layer is not significantly effected.

4. Effect of confined aquifer pressure on permanent slope stability is studied. The displacements were in orders of magnitudes of centimeters up to bottom clay layer thicknesses of 70-75 m. After these thickness levels, such as the 50-60 m levels, displacements suddenly increase to meter levels indicating that clay might crack and break leading to increased clay permeability that might result in pit bottom flooding. Even though the aquifer water pressure creates displacements in cm range, permanent slope still preserves its safe condition. Whereas 50-60 m green clay thickness is critical for cracking, 20 m bottom clay thickness is critical for water rush.

5. Permanent slope factor of safety is not effected negatively from the aquifer unless bottom clay layer thickness goes below 70 m levels. For the permanent slope of Elbistan-Çöllolar open cast mine the overall slope angle can be maximum 32^{o}. Higher than this value there will be a risk of failure in permanent slope.

6. Back analyses results provide valuable information for determination of shear strength parameters of the formation in the basin. More data about local slope failures on gyttja and lignite formations should be collected. Dimensions of the slides should be recorded, slope geometries before and after the slides should be documented and reported.

7. In order to study similar problems easier in future, groundwater level and pump locations should be taken under record in a proper and more detailed way as a part of the documentation in the drainage report.

REFERENCES

Akbulut, İ., Aksoy, T., Çağlan, D., and Ölmez, T. (2007). *Afşin-Elbistan Kışlaköy Açık Kömür İşletmesi Şev Stabilitesi Çalışması*.

Akbulut, İ. (2006). *Kahramanmaraş-Afşin-Elbistan Kömür Sahası rezerv belirleme ve geliştirme projesi hidrojeoloji etüdü*. Ankara: Maden Tetkik Arama Genel. Müdürlüğü.

Bulut M. (2008, April). *EÜAŞ Termik santrallarında elektrik üretimi*. EÜAŞ Genel Müdürlüğü, Ankara.

Cech, T.V. (2009). *Principles of water resource: history, development, management, and policy*. 3rd Ed. USA: John Wiley & Sons. pp.116-119.

Cöllolar Open Cast Mine Afşin-Elbistan Coal Basin, *Hydro-geological model and dewatering concept*. (2008). MBEG.

Dirik K. (2006). Su döngüsü ve yeraltı suları. *Fiziksel Jeoloji II Ders notları*.

Doyuran, V. (2006). *Maden işletmeciliğinde yeraltısuyu sorunları ve hidrojeolojik yaklaşım*.

Drumm, E. C., Aktürk Ö., Akgün H., Tutluoğlu L. (2008). *Stability Charts for the Collapse of Residual Soil in Karst*. ASCE Journal of Geotechnical and Geoenvironmental Engineering.

Ford, D., and William P. (2007). *Karst Hydrogeology and Geomorphology*. USA: Wiley. pp.103-107.

Goodman, R.E. (1989). *Introduction to Rock Mechanics*. USA: Wiley & Sons. p.34.

Hiscock, K.M. (2005) *Hydrogeology principles and practice*. USA: Hackwell Publishing. p.28.

Karpuz C., Tutluoğlu L., Bakır S., Koçal A., and Öge F. (2008). *Elbistan-Çöllolar Sektörü Linyit Sahası Şev Duraylılığı Çalışması ve Laboratuvar Deneyleri*, ODTÜ, Ankara.

Karpuz C., Tutluoğlu L., Bakır S., Öge F., and Yoncacı S. (2009). *Afşin-Elbistan B sahasında akiferin ocak faaliyetlerine ve şevlere etkisinin ve Palplanş İstinat yapısı olanaklarının araştırılması*, ODTÜ, Ankara.

Kasenow M. (2000). *Applied groundwater hydrology and well Hydraulics*. USA: Water resources publications.

Koçak Ç., Kürkçü S.N., and Yilmaz S. (2003). *Afşin-Elbistan linyit havzasının değerlendirilmesi ve linyit kaynakları arasındaki yeri.*

Konikow L.F., and Reilly T.E. (2000). Groundwater modeling. In J.W. Delleur (Ed.). *The handbook of groundwater engineering*, p.662.

Lee, C.C., and Lin Shun Dar. (2000). *Handbook of environmental engineering calculations*, USA: McGraw-Hill. p.223.

Loofbourow, R.L. (1973). *Groundwater and groundwater control: SME Mining Engineering Handbook*. Vol.2. USA: New York. p.26.2-26.55,

Misstear, B., Banks, D., and Clark, L. (2006). *Water wells and boreholes*. England: Wiley and Sons. pp.7-29.

Neuhaus, D., and Özdemir, K. (2008). *Çöllolar kömür sahası 17. 250. 000 ton/yıl kömür üretim kapasiteli açık maden işletmesinin kurulması ve işletilmesi" işi çöllolar linyit işletmesi aralık 2008 ayı faaliyet raporu*. Park Teknik.

Obrer, C. (2006). *Permeability of stabilized clay*, Unpublished thesis. Finland: Helsinki University of Technology. pp.15-16.

Oge, F. (2008). *Slope stability analysis and design in Elbistan-Çöllolar Open cast mine*. Unpublished thesis. Ankara: ODTÜ.

Ozbek and Güçlüer. (1977). *Kahramanmaraş-Afşin-Elbistan Kömür Sahası rezerv belirleme ve geliştirme projesi hidrojeoloji etüdü*. p.2.

Painter S., Sun A., and Green R.T. (2006). *Enhanced characterization and representation of flow through karst aquifers*. Denver: IWA Publishing. pp.1-8.

Raghunath, H. M. (2007). *Groundwater*. New Delhi: New Age International Publishers. p.4.

Rocscience, (2008). *Phase^2 version 7.0 User's manual*.

Romanov D. (2003). *Evolution of Karst Aquifers in natural and manmade environments: a modeling approach*. Unpublished thesis. Germany: Bremen University. p.3.

Rushton K.R. (2003). *Groundwater hydrology conceptual and computational model*, England: Wiley and Sons. p.11.

TableCurve 3D Homepage, from
http:// http://www.sigmaplot.com/products/tablecurve3d/tablecurve3d.php

Thusyanthan, N.I. and Madabhushi, S.P.G. (2003). *Scaling of Seepage Flow Velocity in Centrifuge Models. CUED/D-SOILS/TR326.* United Kingdom. p.4.

Township of Langley website, *Introduction to Groudwater*, British Colombia Canada, http://www.tol.ca/index.php?option=com_content&view=article&id=1063&Itemid=901 (Last accessed date: 28.08.2009)

Usul, N. (2008) *Mühendislik Jeolojisi*. Ankara: ODTÜ Yayıncılık. pp. 337-343.

Yeraltı suyu ve jeofizik genel tanımlar. JF409 Ders notları. COMU Jeofizik Mühesiliği Bölümü.

Yörükoğlu, M. (1991) *Afşin-Elbistan Mining Project and Mining Activities at AELI Establishment of TKİ*. Madencilik dergisi. Sayı 3. Pp. 13-29.

Wang H.F., and Anderson M.P. (1982). *Introduction to groundwater modeling finite difference and finite element methods.* USA: Academic Press. pp.3-6.

White W.B. (2000). The handbook of groundwater engineering. In J.W. Delleur (Ed.). *Groundwater flow in karstic aquifer*. p.600.

APPENDIX A

SAMPLE LITHOLOGY OF BOREHOLE LOG

A detailed sample borehole log prepared by Park Teknik Inc. is presented in Figure A.1 and A.2.

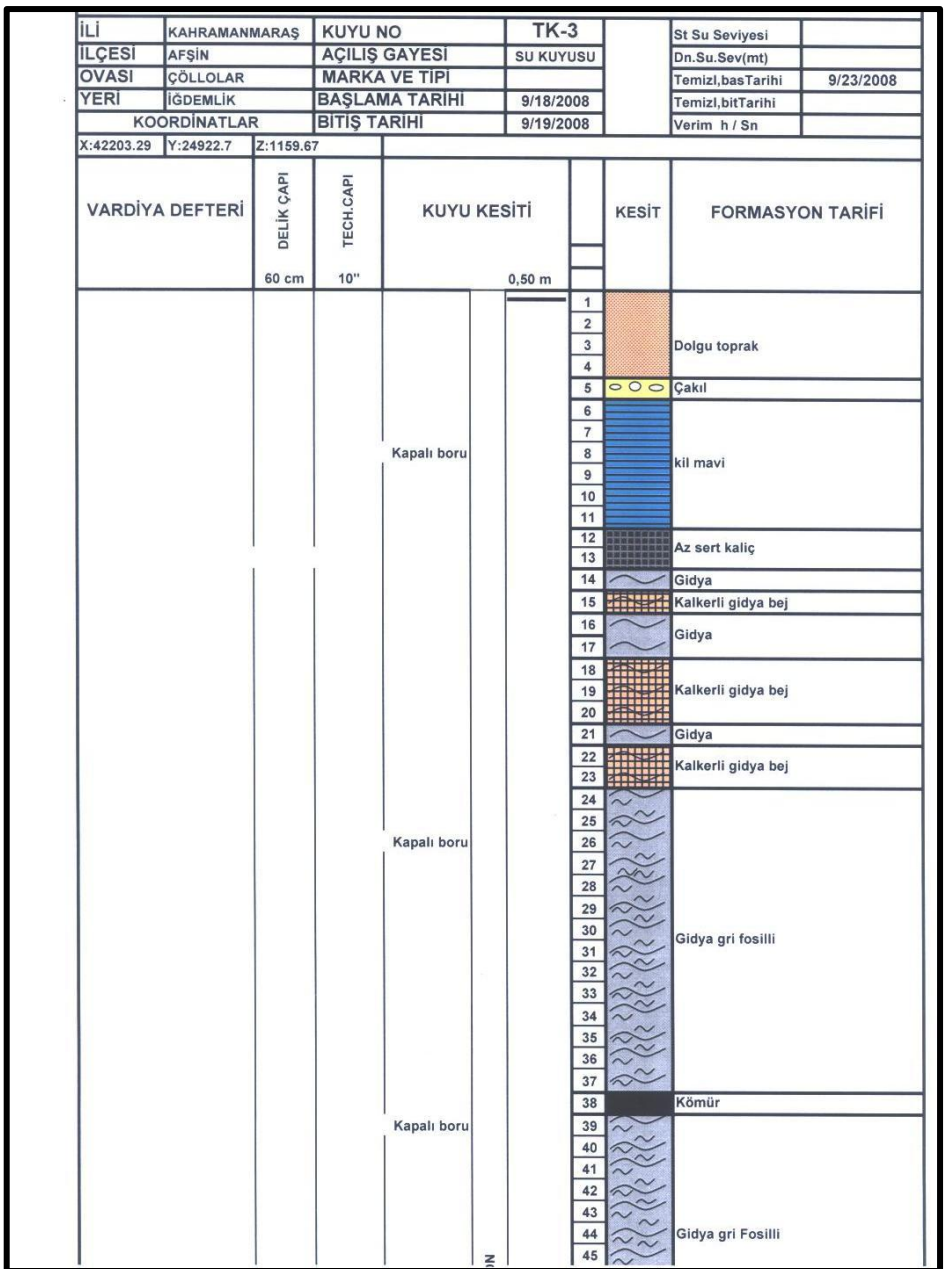

Figure A.1 TK-3 borehole log

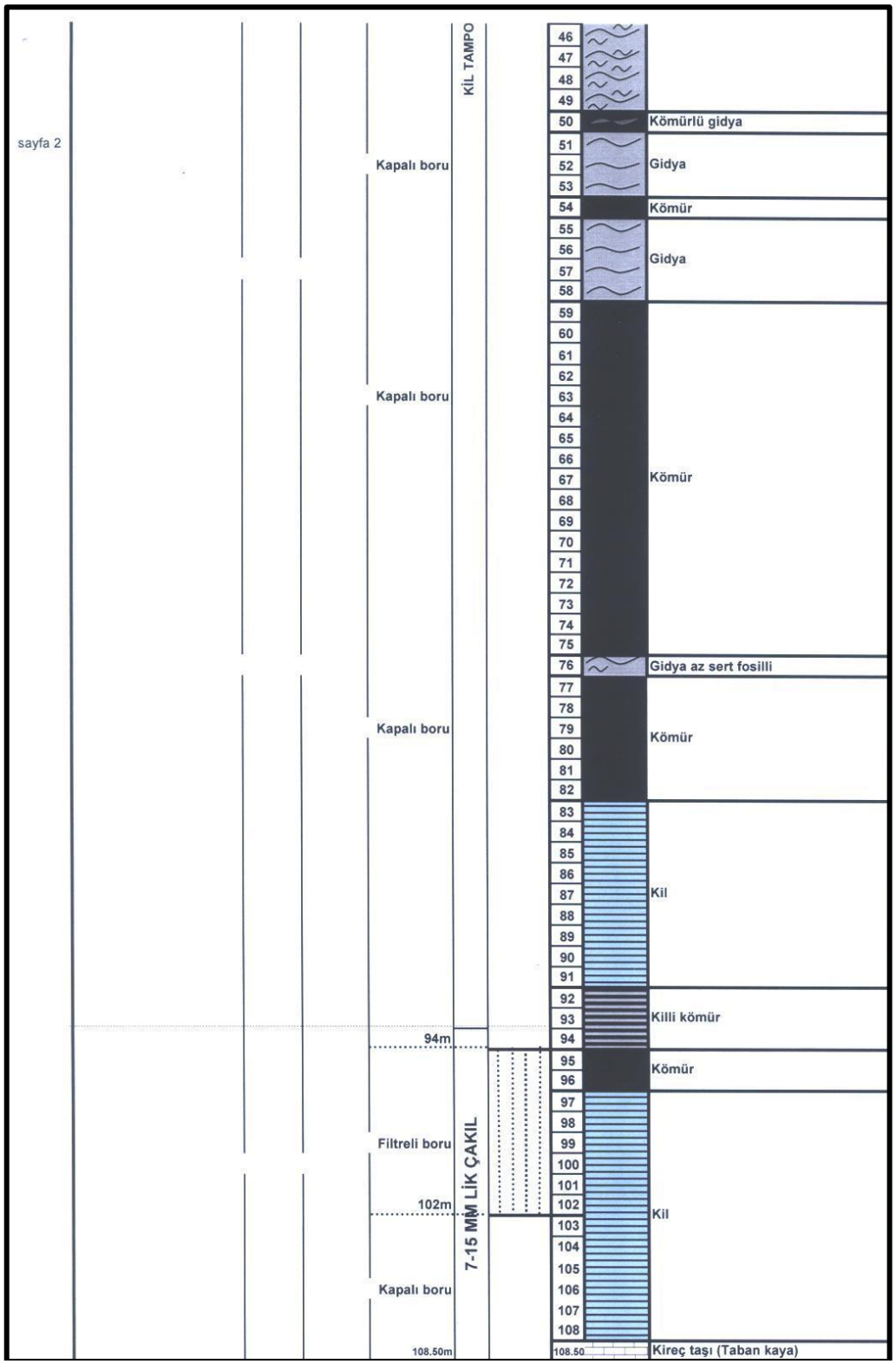

Figure A.2 TK-3 borehole log (cont'd)

APPENDIX B

CROSS SECTIONS OF USED MODELS

B.1 B-B' CROSS SECTION MODELS

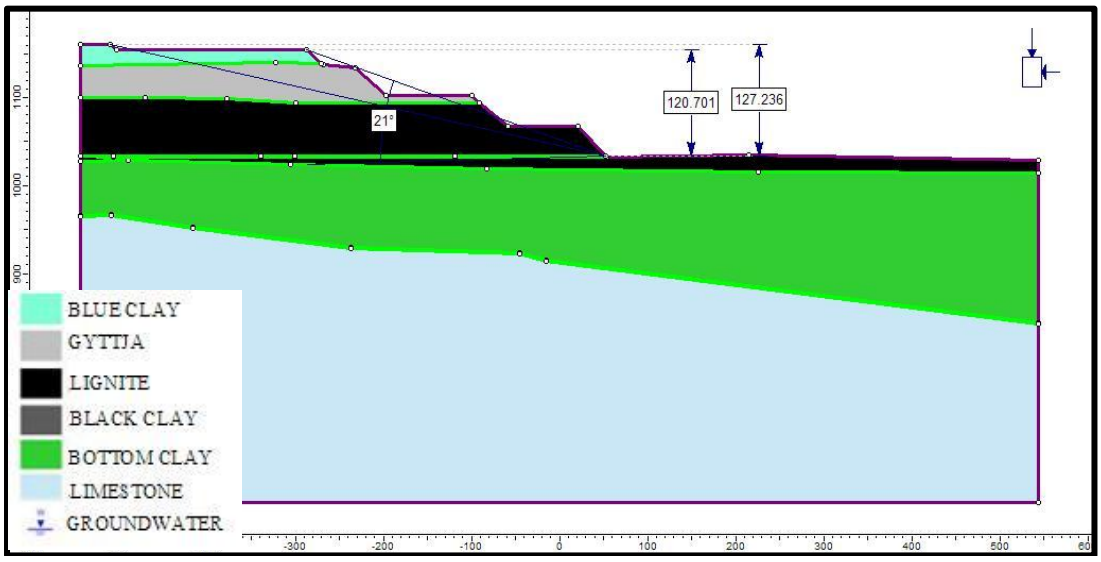

Figure B.1 B-B' section 3 year pit plan

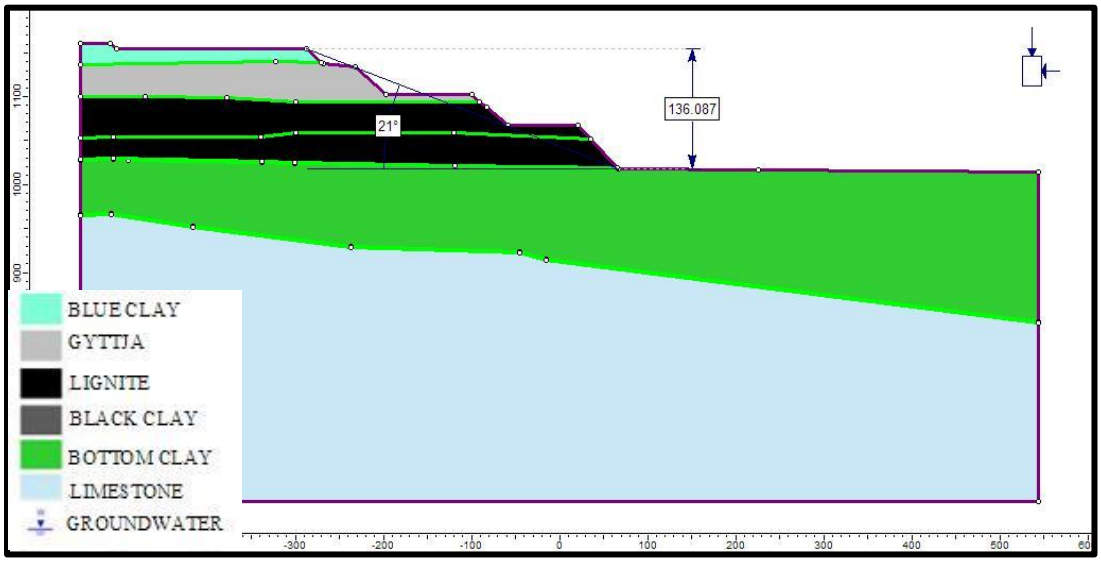

Figure B.2 B-B' section 5 year pit plan

B.2 C-C' CROSS SECTION MODELS

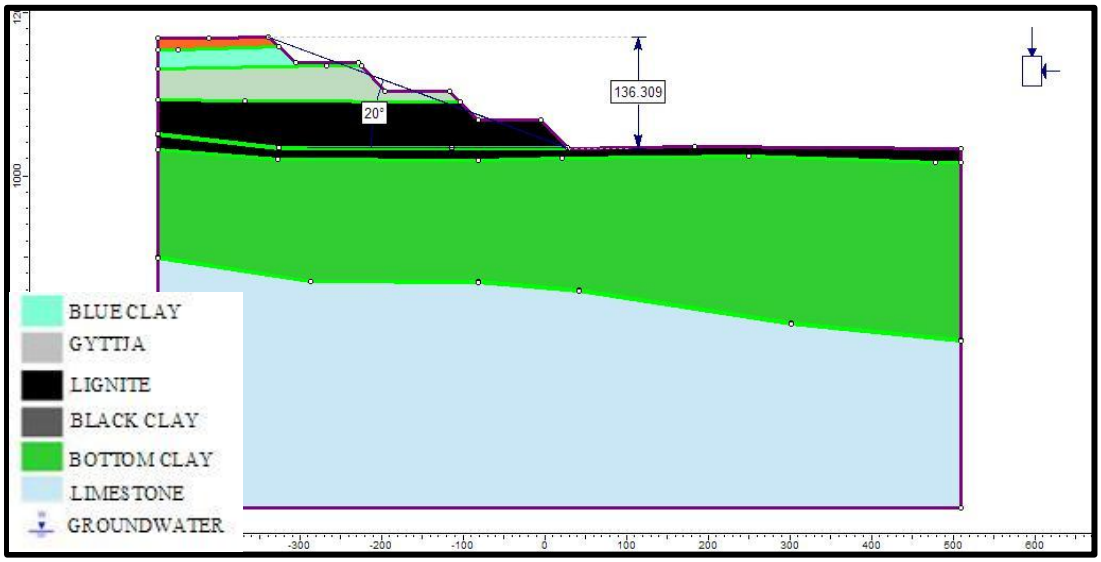

Figure B.3 C-C' section 3 year pit plan

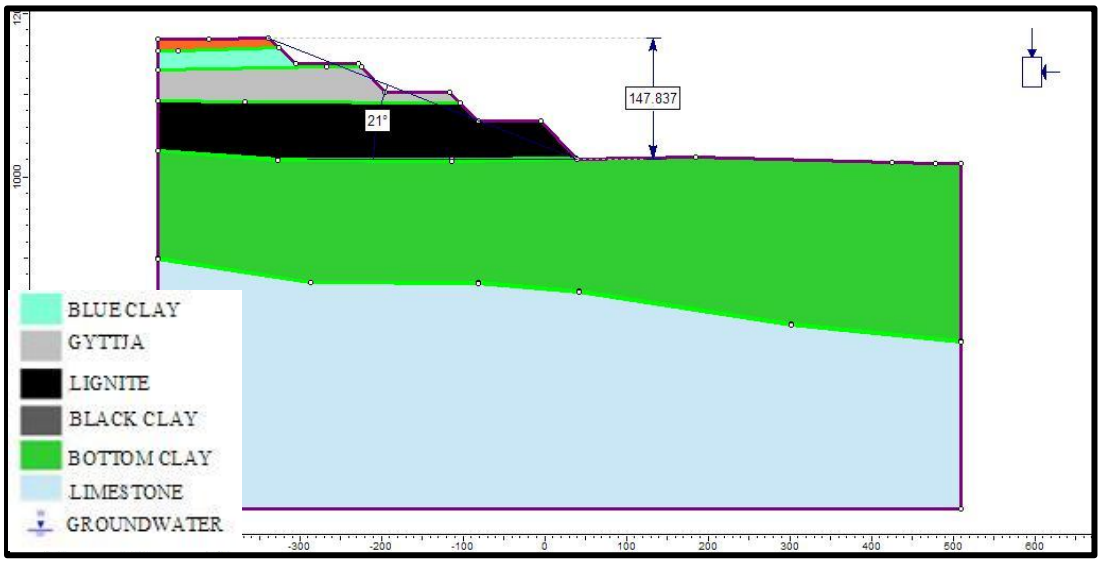

Figure B.4 C-C' section 5 year pit plan

APPENDIX C

HYDRAULIC GRADIENT ANALYSIS

Table C.1 Flow rate values changing thickness and permeability of green clay

	k (m/s)	**$3.07x10^{-05}$**	**$3.07x10^{-06}$**	**$3.07x10^{-07}$**	**$3.07x10^{-08}$**	**$3.07x10^{-09}$**
Flow rate Q (m^3/s)	**t=3.5 m**	$1.72x10^{-02}$	$1.72x10^{-03}$	$1.72x10^{-04}$	$1.72x10^{-05}$	$1.72x10^{-06}$
	t=4 m	$1.42x10^{-02}$	$1.42x10^{-03}$	$1.42x10^{-04}$	$1.42x10^{-05}$	$1.42x10^{-06}$
	t=5 m	$1.13x10^{-02}$	$1.13x10^{-03}$	$1.13x10^{-04}$	$1.13x10^{-05}$	$1.12x10^{-06}$
	t=12 m	$3.57x10^{-03}$	$3.57x10^{-04}$	$3.56x10^{-05}$	$3.55x10^{-06}$	$3.55x10^{-07}$
	t=22 m	$1.71x10^{-03}$	$1.71x10^{-04}$	$1.69x10^{-05}$	$1.64x10^{-06}$	$1.61x10^{-07}$
	t=33 m	$1.11x10^{-03}$	$1.11x10^{-04}$	$1.09x10^{-05}$	$1.03x10^{-06}$	$1.00x10^{-07}$
	t=43 m	$9.28x10^{-04}$	$9.24x10^{-05}$	$8.95x10^{-06}$	$8.20x10^{-07}$	$7.88x10^{-08}$
	t=65 m	$4.66x10^{-04}$	$4.63x10^{-05}$	$4.39x10^{-06}$	$3.84x10^{-07}$	$3.63x10^{-08}$
	t=82 m	$3.95x10^{-04}$	$3.62x10^{-05}$	$3.38x10^{-06}$	$3.16x10^{-07}$	$2.96x10^{-08}$
	t=103 m	$3.35x10^{-04}$	$3.04x10^{-05}$	$2.71x10^{-06}$	$2.52x10^{-07}$	$2.23x10^{-08}$
	t=122 m	$2.83x10^{-04}$	$2.70x10^{-05}$	$2.24x10^{-06}$	$2.06x10^{-07}$	$1.81x10^{-08}$
	t=200 m	$2.40x10^{-04}$	$2.28x10^{-05}$	$2.07x10^{-06}$	$1.68x10^{-07}$	$1.52x10^{-08}$

Table C.2 Hydraulic gradient values changing thickness and permeability of green clay

	k (m/s)	**$3.07x10^{-05}$**	**$3.07x10^{-06}$**	**$3.07x10^{-07}$**	**$3.07x10^{-08}$**	**$3.07x10^{-09}$**
Hydraulic Gradient	**t=3.5 m**	11.20026	11.20026	11.20026	11.20026	11.20026
	t=4 m	9.243894	9.243894	9.243894	9.243894	9.243894
	t=5 m	7.379355	7.378704	7.37154	7.337024	7.304461
	t=12 m	2.323022	2.322761	2.320742	2.313709	2.310062
	t=22 m	1.178183	1.111755	1.101075	1.067926	1.051254
	t=33 m	0.790817	0.723934	0.709866	0.670791	0.653468
	t=43 m	0.64618	0.602032	0.582859	0.533787	0.513357
	t=65 m	0.319551	0.301231	0.285887	0.250081	0.236379
	t=82 m	0.257069	0.235454	0.220098	0.205562	0.192752
	t=103 m	0.218339	0.198046	0.176509	0.164018	0.145438
	t=122 m	0.184305	0.175838	0.145881	0.134158	0.117877
	t=200 m	0.15619	0.148258	0.135083	0.109619	0.099251

APPENDIX D

GREEN CLAY THICKNESS GEOMETRIES

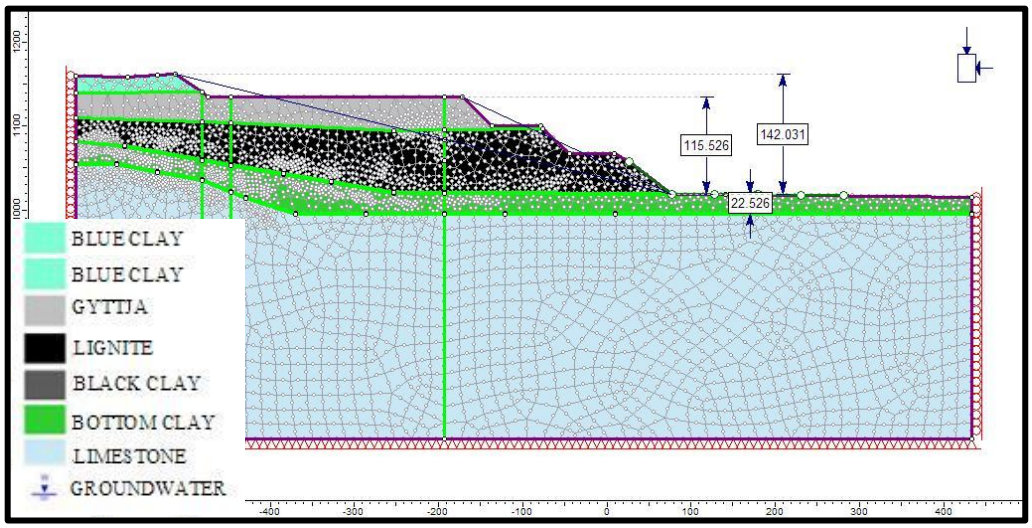

Figure D.1 Model of Green Clay thickness about 25 m

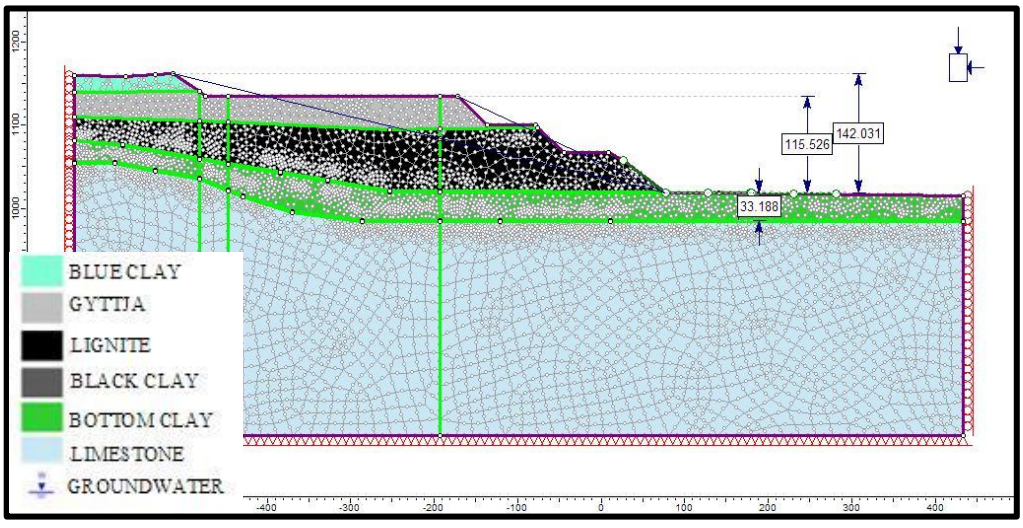

Figure D.2 Model of Green Clay thickness about 35 m

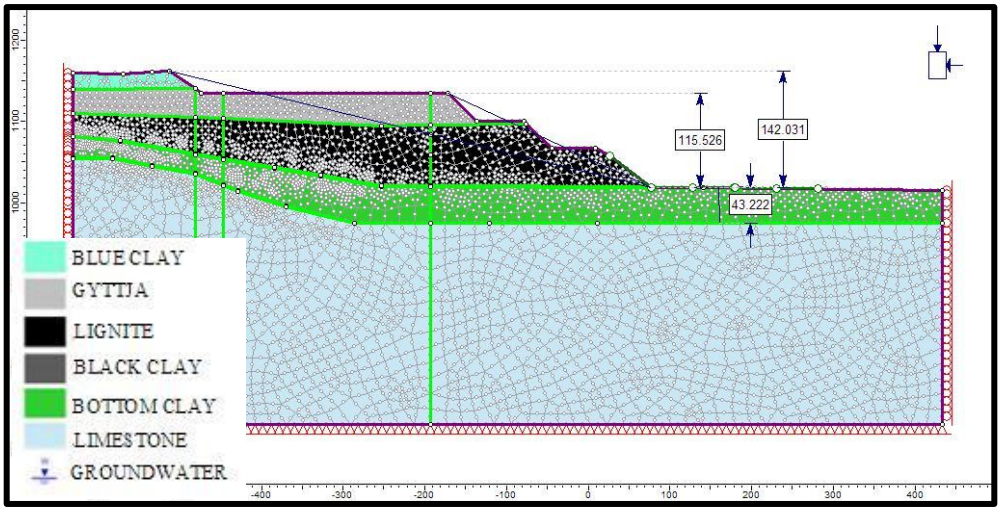

Figure D.3 Model of Green Clay thickness about 45 m

APPENDIX E

PHASE^2 OUTPUTS FOR OVERALL SLOPE ANGLE DETERMINATION

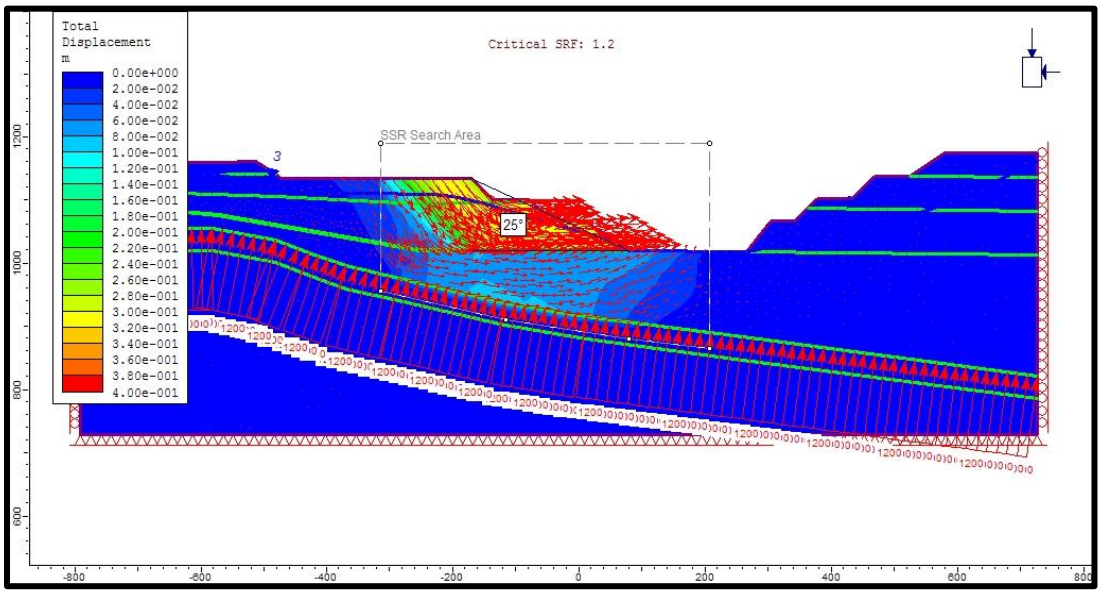

Figure E.1 Factor of safety values of 25^o overall slope angle

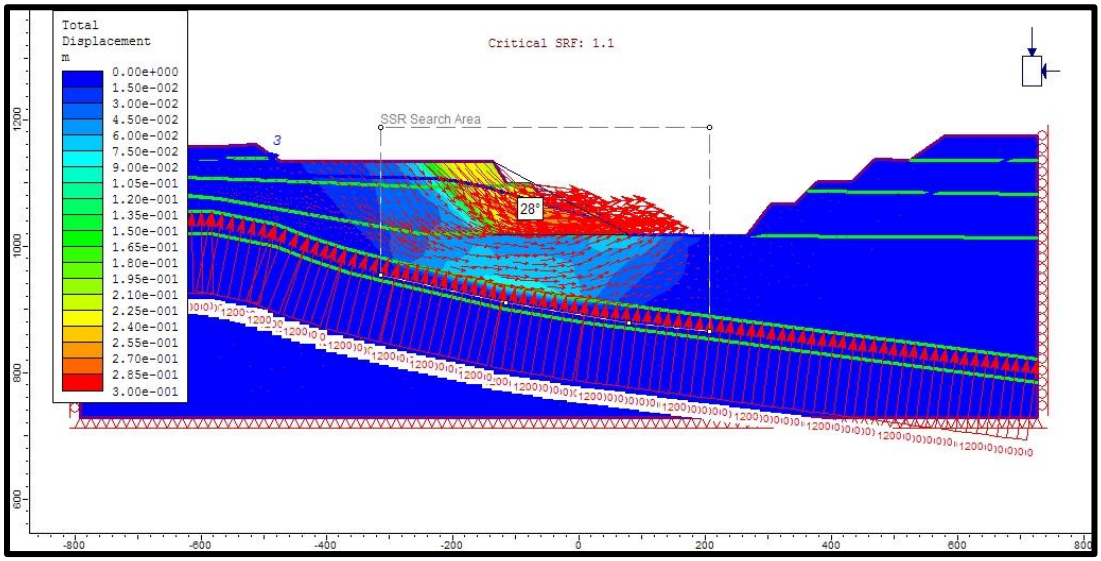

Figure E.2 Factor of safety values of 28^o overall slope angle

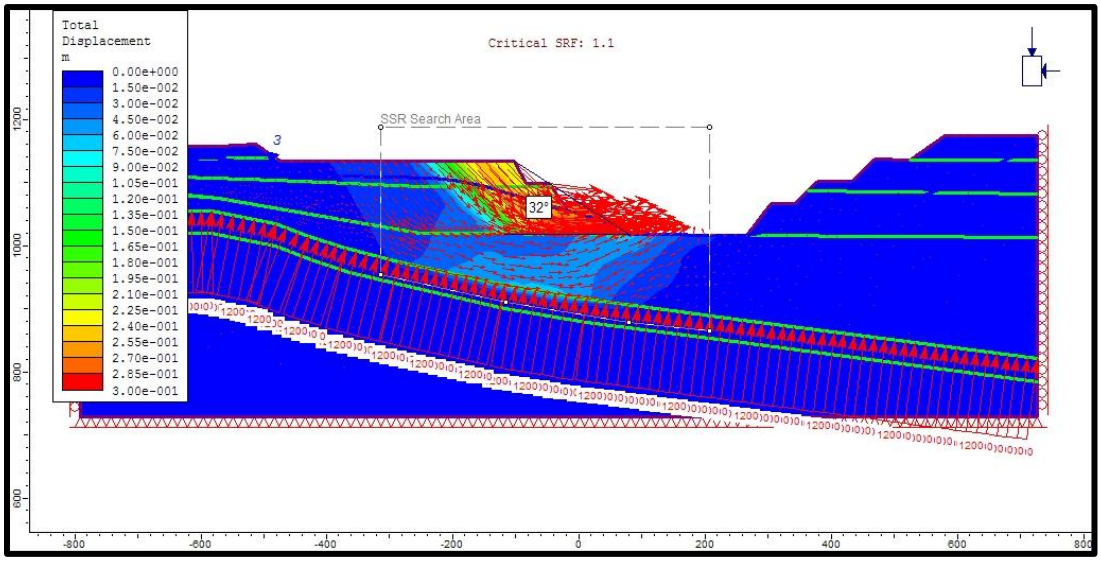

Figure E.3 Factor of safety values of 32^{o} overall slope angle

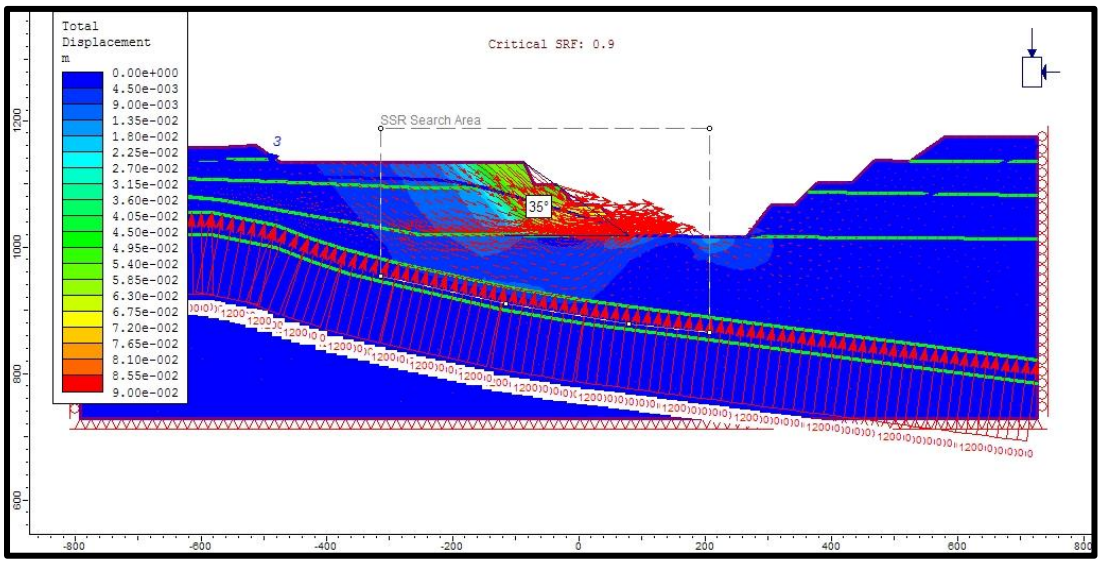

Figure E.4 Factor of safety values of 35^{o} overall slope angle